NASA Technical Memorandum 106858

Microgravity Combustion Science: 1995 Program Update

Prepared for the
3rd International Microgravity Combustion Workshop
sponsored by NASA Lewis Research Center
Cleveland, Ohio, April 11–13, 1995

National Aeronautics and
Space Administration

Microgravity Combustion Science: 1995 Program Update

The Microgravity Combustion Branch
National Aeronautics and Space Administration
Lewis Research Center
Cleveland, Ohio 44135

Summary

Microgravity greatly benefits the study of fundamental combustion processes. In this environment, buoyancy-induced flow is nearly eliminated, weak or normally obscured forces and flows can be isolated, gravitational settling or sedimentation is nearly eliminated, and temporal and spatial scales can be expanded. This document reviews the state of knowledge in microgravity combustion science, with the emphasis on NASA-sponsored developments in the current period of 1992 to early 1995. The scope includes basic research in gaseous premixed and diffusion-flame systems, flame structure and sooting, liquid droplets and pools, and solid-surface ignition and flame spread. Other subjects include applied research in combustion synthesis of ceramic-metal composites, advanced diagnostic instrumentation, and on-orbit fire safety. The review also describes the opportunities for Principal Investigator participation through the NASA Research Announcement program and the NASA Lewis Research Center ground-based facilities available to researchers. This review is compiled by the members and associates of the NASA Lewis Microgravity Combustion Branch.

Highlights of Changes and Key Accomplishments in Microgravity Combustion Science Since the Last Review (NASA TM–105410, April 1992)

Ground-Based (Drop Tower and Airplane) Experiments and Analyses

- Dilution-enhanced flammability ("flame-balls") was observed in certain premixed gaseous systems in microgravity at high-dilution levels where normally flames do not exist.
- Theories were developed to explain the stability of "flame-cylinders" and "flame-balls" in stationary, premixed flames.
- High-Lewis number ($k/C_p\rho D$), premixed, microgravity flames show pulsating and traveling-wave instabilities never before observed.
- Flame heights in microgravity gas-jet diffusion flames exceed those in normal gravity not only in the laminar regime (known previously) but also in transitional and fully turbulent conditions, at Froude numbers (U^2/gd) higher than 100. Blow-off extinction was observed at high Reynolds numbers (Ud/v) in microgravity.
- Measured soot-containing volumes in fuel-jet diffusion flames are broader in microgravity, and primary and aggregate soot-particle sizes are significantly larger.
- Limiting-oxygen indices for opposed-flow flame spread of thin solid fuels are lower (greater flammability) in partial gravity than in microgravity.
- Combustion synthesis of ceramic-metal composites in microgravity gives more uniform distribution of phases and porosity and improved microstructure, as compared to normal-gravity counterparts.

Spaceflight Experiments

- The *Solid Surface Combustion Experiment*, still in progress, completed eight successful missions on the Shuttle, five with ash-free filter-paper fuel and three with polymethylmethacrylate (PMMA). The latter tests provided the first reference data for heat transfer and combustion of thick solid fuels in a quiescent, microgravity environment.
- The first combustion experiment on a sounding rocket, *Spread Across Liquids*, completed its mission, demonstrating successful liquid-fuel experiment management and revealing significant differences in flame-spread behavior in microgravity.
- Three low-cost experiments (*Candle Flames in Microgravity*, *Smoldering Combustion in Microgravity*, and *Wire Insulation Flammability*) proceeded from inception to successful flight in a "Glovebox" facility on the Shuttle in less than three years. The experiments not only yielded interesting results but also demonstrated the practicality of the Glovebox accommodation for small-scale experiments on space laboratories.
- Three large-scale experiments (*Droplet Combustion Experiment*, *Laminar Soot Processes*, and *Structure of Flame Balls at Low Lewis Number*), two moderate-scale experiments (*Diffusive and Radiative Transport in Fires* and *Microgravity Smoldering Combustion*), and five Glovebox experiments (*Candle Flames in Microgravity*,

Comparative Soot Diagnostics, *Fiber-Supported Droplet Combustion*, *Forced Flow Flamespreading Test*, and *Radiative Ignition and Transition to Spread*) were authorized to proceed to flight development for near-future missions.
- An archive for imaging and digital data and publications was established at the NASA Lewis Research Center to provide a central repository of spaceflight combustion-science information.

Microgravity Combustion Diagnostics and Technology

- A new method, based on light extinction of a single laser beam, was developed for soot volume-fraction measurements over a two-dimensional field.
- A variety of advanced diagnostic techniques, including infrared and ultraviolet imaging, two-dimensional light extinction, particle-image velocimetry, two-wave-length soot pyrometry, and spectral and broadband radiometry, performed successfully on sounding rockets and demonstrated their feasibility for the Shuttle.
- A reliable technology to deploy nearly-motionless fuel droplets without tethered supports in microgravity is now in practice in ground-based drop towers.

Spacecraft Fire Safety

- An experiment that evaluates, for the first time, the response of the Shuttle and Space Station smoke detectors to model fires in microgravity is approved for a Shuttle flight in 1996.

Ground-Based Facilities

- The NASA Lewis Research Center drop-tower facilities are at an all-time high utilization. For experimenters, the 2.2-Sec Drop Tower is available on an extended-hour operation basis, and the 5.2-Sec Zero Gravity Facility is available for two drops per day.
- The NASA Lewis 2.2-Sec Drop Tower has been extensively renovated. The major improvement is an air-bag decelerator, which reduces the landing loads to levels of 15 to 25 g (previous loads could approach deceleration levels of 100 g) and permits the use of more delicate instrumentation and equipment.
- The new Space Experiments Laboratory at NASA Lewis provides eight advanced combustion-science laboratories, several spaceflight hardware assembly and integration laboratories, and high-bay and clean-room areas for facility-level hardware.
- NASA Lewis also has a state-of-the-art image-processing and object-tracking workstation available to on-site and visiting investigators for analysis of microgravity-experiment data.
- A new airplane laboratory, a DC-9 aircraft based at NASA Lewis, will be available for low-gravity experiments early in 1995.

Program Management and International Collaboration

- The NASA Lewis Research Center was designated the Agency Center of Excellence for Microgravity Combustion Science.
- Open, competitive solicitations for microgravity combustion-science investigations are now planned by NASA Headquarters every two years. Upon award, approval is granted for nominal four-year investigations.
- The number of NASA-supported projects in microgravity combustion science has more than doubled to over 40.
- New subjects for microgravity combustion research (turbulent combustion, metal combustion, combustion synthesis of materials, and advanced diagnostics) were established as a result of successful proposals to a NASA Research Announcement in 1993.
- An agreement on the mutual use of low-gravity facilities by investigators from each country was established between the NASA Microgravity Science and Applications Division and the Japan NEDO; a similar agreement for use of the NASA low-gravity aircraft and the Canadian vibration-isolation technology was established with the Canadian Space Agency.
- An agreement to conduct collaborative science investigations was established between NASA and the Russian Space Agency.

Introduction

The purpose of this document is to provide a review of the field of NASA-sponsored microgravity combustion research through descriptions of current research and findings, participants and their projects, and available low-gravity facilities.

The study of fundamental combustion processes in a microgravity environment is a relatively new scientific endeavor. As stated in previous reviews, the influence of gravity "is so ubiquitous that we tend not to recognize the enormous negative impact that it has had on the rational development of combustion science" (G.M. Faeth, 1991). Microgravity leads combustion science to a new range of experiments that take advantage of the following characteristics of the environment.

- *Buoyancy-induced flow is nearly eliminated.* Due to the hot, less dense products of combustion, buoyancy-induced flows tend to develop in normal-gravity experiments, promoting turbulence and instabilities. Microgravity reduces these flows and their complicating influences, thus fur-

thering the understanding of low-gravity behavior and, by comparison, related normal-gravity processes.

- *Normally obscured forces and flows may be isolated.* Buoyancy-induced flows frequently obscure those of weaker forces, such as electrostatics, thermocapillarity, diffusion, and low-velocity forced flows, that may be particularly important in weak flames. By removing buoyancy, one may observe and analyze the roles of these forces and flows.
- *Gravitational settling is nearly eliminated.* Free suspensions of fuel droplets or particles may be created and sustained in a quiescent environment, eliminating the need for mechanical supports, levitators, or stirring devices and enabling a high degree of symmetry to be achieved in a quiescent environment.
- *Expanded experimental time or length scales become feasible.* The size or duration of tests in normal gravity is often constrained by the development of buoyancy-driven disturbances. Microgravity permits larger-scale experiments, which can allow more detailed diagnostic observations and new tests of similitude.

Low-gravity combustion experiments are conducted in ground-based drop towers and aircraft and in space on sounding rockets and the Shuttle. These microgravity facilities provide opportunities for scientists and engineers to pursue fresh insights into the physics and chemistry of combustion. Unexpected phenomena have been observed—with surprising frequency—in these experiments, spawning the reexamination of classical theories and the vigorous pursuit of new hypotheses.

Microgravity combustion research also has direct practical applications. The most obvious is in spacecraft fire safety. Fire protection for the Shuttle and its international laboratories is based on adaptation of terrestrial systems. Experience demonstrates that current fire safety is adequate to respond to expected fire-threatening incidents. Nevertheless, there is a recognized need for fundamental research and technology with the long-term objective of improving the safety and efficiency of spacecraft fire protection. Other microgravity combustion applications are in the improvement of combustion synthesis of ceramic-metal composites and in innovations in combustion diagnostics, effluent sampling, and combustion-system design.

This document updates two previous overviews of microgravity combustion science (NASA TM–101424 and TM–105410, which appeared six and three years ago, respectively). The present review describes NASA sponsored basic research on microgravity flame structure and combustion in gaseous, liquid, solid, and mixed phases and applied research in combustion synthesis of ceramic-metal composites, advanced diagnostic instrumentation, and on-orbit fire safety. While recent findings are emphasized, some background information is retained from the prior overviews to make this review a "stand-alone" reference.

An additional purpose of this document is the encouragement of the participation of new Principal Investigators in analytical and experimental microgravity combustion research through the frequent opportunities offered by open competitive solicitations, i.e., the NASA Research Announcements. A description of the NASA Lewis low-gravity test facilities and the spacecraft experiment hardware and accommodations available to researchers is in Appendix A. Current NRA-awarded participants are listed in Appendix B, and a selected bibliography of recent publications is in Appendix C.

This review has been compiled by members and associates of the NASA Lewis Research Center Microgravity Combustion Branch. Lewis is the recognized NASA Center of Excellence in this field.

Note that color plates are in back and may not be in sequence.

NASA Lewis Research Center Low-Gravity Facilities

The low-gravity research facilities at the NASA Lewis Research Center are unduplicated in total anywhere in the world. These facilities are available to Principal Investigators collaborating with NASA in microgravity combustion-science projects.

The new Space Experiments Laboratory at NASA Lewis provides eight advanced combustion-science laboratories, several spaceflight hardware assembly and integration laboratories, and high-bay and clean-room areas for facility-level hard-ware. A separate state-of-the-art image-processing and object-tracking workstation aids the analysis of data from microgravity experiments.

Short-duration microgravity testing is conducted in two drop-tower facilities. The newly renovated 2.2-Sec Drop Tower is an ambient-pressure, drag-shield facility, offering the advantage of quick turnaround, with schedules of eight or more drops daily. The 5.2-Sec Zero Gravity Facility is a large-scale, evacuated facility with schedules of two drops daily.

Longer-duration testing at the expense of residual gravity levels is conducted in airplane facilities, which can fly multiple parabolic (Keplerian) trajectories in daily missions. The newest airplane is a large-capacity DC-9, based at NASA Lewis, to be placed in service early in 1995. Previous airplane experiments were conducted in a Learjet 25 and a KC-135A.

A detailed description of the NASA Lewis ground-based facilities and NASA space accommodations is in Appendix A.

Candle Flames

The candle flame serves as the example to introduce the subject of microgravity combustion and to illustrate phenomena affected by the various low-gravity environments. In micro-

gravity, the candle may exhibit a nearly steady-state, non-propagating, non-convective diffusion flame over a relatively long test time. (Prior to the tests described here, this behavior was unknown.)

Fig. 1 (color) illustrates a candle flame in normal gravity, low gravity (of the order of 10^{-2} g) in an airplane-based experiment, and microgravity (10^{-4} g or less) in a drop tower and the Shuttle. (The reference acceleration, 1 g, is that of Earth sea-level, 9.8 m/s^2.) The visible flame in microgravity is different from that in normal gravity in a number of aspects: shape, size, color, and structure. Microgravity (Shuttle) candle flames clearly stand off from the wick, with typical distances of the order of 5 to 7 mm, compared to 1 to 2 mm for normal-gravity candle flames (at the base region). This longer flame stand off implies a weaker heat feedback from the flame and a low fuel-consumption rate. The nearly spherical shape of the microgravity flame implies that all of the flame provides heat feedback to the wick. This differs from the normal-gravity behavior in which only a portion of the vaporized fuel burns in the vicinity of the wick; the rest of the fuel vapor is swept downstream by buoyant convection and reacts in the plume region. In low gravity (airplane environment), the flame is distorted by the buoyant flow induced by the residual gravity; yet even here the flame appearance is clearly different from that in normal gravity.

An obvious question is why the microgravity candle flame color is blue while the corresponding normal-gravity and low-gravity candle flames are yellow (a result of soot radiation in the flame zone). There are three possible reasons for the lack of soot:

(1) The temperature throughout the flame zone is so low that soot is not formed.

(2) Soot exists; but the temperature is low, and the particles are not luminous.

(3) The flame is partially premixed because oxygen can leak through the quenched base.

Of these three reasons, the most likely is the first: the lack of soot is due to the low diffusion-flame temperature. A supporting evidence for this hypothesis is in the similar appearance to a low-pressure candle flame, which has a measured maximum temperature near 1530 K, a level below the soot-formation-threshold temperature stated in the literature.

Premixed Gas Combustion

Flammability Limits

It is well known that combustible gas mixtures will not burn if sufficiently diluted with excess fuel, oxidant, or inert gas. The compositions delineating flammable from non-flammable mixtures are called the flammability limits. Studies of flammability limits are important for assessment of fire safety in many environments and for estimation of the operating limits of combustion engines.

Despite many years of study, much is unknown about the mechanisms of flammability limits, including the effects of hydrodynamic strain and flame-front curvature (collectively called "flame stretch"), preferential diffusive, conductive, and radiative heat losses, and flame chemistry. In practice, many of these factors are present simultaneously and may interact, making the isolation and evaluation of the influence of an individual factor difficult.

Flammability limits differ for upward and downward propagation of a flame in a cylindrical tube, if the tube is large enough that heat losses to the tube walls are not the dominant extinction mechanism. It can be shown that the characteristic heat-loss times for upward-propagating flames in tubes (t_{up}), downward-propagating flames in tubes (t_{down}), radiation (t_{rad}), and conduction to tube walls (t_{cond}) scale as $(d/g)^{1/2}$, $(\alpha/g^2)^{1/3}$, $\rho C_p T/L$, and d^2/α, respectively, where d is the tube diameter, g the gravitational acceleration, α the thermal diffusivity, ρ the density, C_p the constant-pressure specific heat, T the flame temperature, and L the radiative heat loss rate per unit volume. Comparison of these time scales shows that, for a representative normal-gravity gas mixture, pressure, and tube diameter, t_{rad} is much greater than t_{up} or t_{down}; thus, radiative losses are insignificant compared to buoyancy-induced heat-loss effects.

Experiments have shown, however, that the flammability-limit compositions in microgravity differ from those of either upward or downward propagation in normal gravity and t_{up} and t_{down} can be very large. Comparisons of theoretical predictions to experimental measurements, such as those of the propagation rate at the limit and the thermal-decay rate in the burned gases, indicate that radiative heat loss from the combustion products is probably the dominant process leading to flame extinction at microgravity. Still, in order to observe radiative-loss effects and establish $t_{rad} < t_{cond}$, experiments in large-diameter tubes are necessary.

Radiative influences in microgravity may couple to other phenomena in interesting ways. For example, it is known that, for mixtures in which the Lewis number (Le, defined as the ratio of thermal diffusivity of the mixture to the mass diffusivity of the stoichiometrically deficient reactant) is small, flame-front curvature that is concave with respect to the burned gases, as in a spherically expanding flame, increases the flame-propagation rate. Under conditions where the radiative losses are strong enough to extinguish the planar flame, the curved, spherically expanding flame may be able to survive until it reaches some critical radius for extinguishment. Such behavior, termed "self-extinguishing flames," has been observed in a variety of low-Le mixtures.

The effects of gravity on flammability limits were studied in microgravity and normal-gravity upward- and downward-

propagating hydrogen/air flames in a two-dimensional channel of a standard flammability-limit tube. In the tests, the hydrogen concentration was decreased systematically from 15 to 7.5 percent. Results indicated that, for mixtures with 12 percent or more hydrogen, the stability and structure of the flame are controlled primarily by the thermal-diffusive instability mechanism. In leaner hydrogen/air mixtures, gravity effects become more important. Upward-propagating flames are highly curved, and they evolve into a bubble rising in the tube. Their extinction is thought to be caused by flame stretch acting at the tip of the rising bubble-shaped flame. Downward-propagating flames are flat, or they oscillate between concave and convex curvatures. Their extinction is thought to be caused by the formation of a cooling layer of burned gas descending near the tube walls that overtakes the flame front and extinguishes it, if the propagation rate is too low. The microgravity flame shows only cellular structures, which can be suppressed by the effect of buoyancy for mixtures leaner than 11 percent hydrogen. These observations have been explained on the basis of an interaction between the processes leading to buoyancy-induced Rayleigh-Taylor instability and the thermal-diffusive instability.

Modeling of downward propagation of flames indicates that buoyancy and heat losses to the walls are simultaneously required to cause the observed extinguishment. The actual mechanism of extinguishment has been identified as the dilution of the unburnt mixture by the products of combustion, caused by the recirculating flow near the walls induced by buoyant forces. Near the limit, the flame is quenched at the walls, and tongues of colder gases, comprised mainly of combustion products, flow down the sides. At the same time, there is an upward motion in the gases at the center of the channel, causing the flame to rise into the products.

Intrinsic Flammability Limits

Intrinsic flammability limits are limiting compositions that are defined purely by internal characteristics of the flame and not by external factors, such as heat losses to the burner or to confining walls and dispersion of heat through the gas. Intrinsic flammability limits are difficult, if not impossible, to study at normal-gravity conditions because the external influences of non-uniform, buoyancy-induced convective flows are difficult to exclude. Internal factors are also difficult to eliminate in microgravity, since the burner and confinement effects are not thereby eliminated for conventional flames.

A class of stationary premixed spherical flames, or "flame-balls," observed uniquely in microgravity is controlled exclusively by reaction, diffusion, and radiation: i.e., there is no convection because the mass-averaged velocity vanishes everywhere. The lack of buoyant convection preserves the spherical symmetry of these flames. Because all three factors controlling their behavior are exclusively intrinsic, flame-balls provide a suitable configuration for the study of intrinsic flammability limits.

Flame-balls are stable only if the effective Lewis number is small, and thus they are observed only in such mixtures as lean hydrogen and air. Theoretical analyses have identified the circumstances under which stable flame-balls can be expected to occur and also the nature of the instabilities that exist when these conditions are not met. Detailed numerical simulations for hydrogen/air mixtures are based on the assumption that the flame-ball is optically thin, so there is negligible reabsorption of the radiation from the water generated by the reactions. This is certainly valid in the neighborhood of the lean and rich flammability limits, where the flame-ball is small. Analyses show that only the limited domain near the lean limit corresponds to stable solutions, and experiments confirm that only this flame condition has physical significance. In the experiments, non-absorbed radiation is lost to the chamber walls, an external factor. In the numerical simulations, all emitted radiation is lost at "infinity." A theoretical treatment in which all radiation is absorbed in the surrounding gas, however, shows that, if the scale on which absorption occurs is large compared to the flame-ball diameter, the flammability limits remain unchanged.

Stability Limits

It is known that buoyant convection has an important effect on the stability of premixed gas flames, just as it does on flammability limits. For example, some flame structures that are unstable in normal gravity may not exist in microgravity, while others may have unique characteristics. In mixtures with low Le, thermal-diffusive instabilities may cause spatial perturbations to grow, thereby rendering planar flames into wrinkled shapes. While such wrinkling is suppressed by buoyant convection for downward-propagating flames because this configuration is Rayleigh-Taylor stable (the less dense burned gas is on top), flame wrinkling is observed in microgravity.

The stability of a planar flame front steadily propagating in the absence of forced or natural (buoyancy-induced) convection will depend on:

(1) the rate at which the heat generated by the flame diffuses into the unburned reactants versus the rate at which the stoichiometrically scarce reactant diffuses into the flame (i.e., thermal-diffusive mechanism) and

(2) the ratio of the heat lost to the heat generated by the flame.

The first of these two effects can be characterized by the Lewis number of the mixture. Linear and nonlinear stability analyses are particularly useful in that they predict cellular flames at Lewis numbers sufficiently less than unity and pulsating or traveling flame-wave instabilities at Lewis numbers sufficiently greater than unity.

The low-Le (cellular flame) instability, which was first observed a century ago, has been the subject of extensive experimental and theoretical studies. In contrast, the high-Le instability has received considerably less attention. Although the thermal-diffusive models suggest that the Lewis number has to be sufficiently large for a pulsating or traveling-wave instability to manifest itself, periodic and chaotic flames have been stabilized on a porous-plug burner for methane-air and propane-air mixtures. The nature of these flames is attributed to the thermal-diffusive mechanism, since the instabilities occur only in mixtures with the Lewis number slightly greater than unity. The frequencies of the observed oscillations are generally much lower, however, than those predicted by the thermal-diffusive theory. In fact, they are closer to those predicted by a buoyancy-driven mechanism. Furthermore, the flame behavior is sensitive to the flow rate of the mixture through the porous plug, a result that cannot be interpreted solely in the context of the thermal-diffusive mechanism. Consequently, a study of freely-propagating flames in tubes was recently initiated at NASA Lewis to demonstrate or refute the existence of the high-Le pulsating or traveling-wave instability. Freely-propagating flames were selected to eliminate the complexities of heat loss to the porous plug and the restrictions on the flow-field and flame-shape characteristics of burner-stabilized flames. Comparative tests were conducted at both normal gravity and microgravity to eliminate the possibility that any observed instabilities might be buoyancy-induced.

For lean mixtures of butane and oxygen diluted with helium (Le ≈ 3.0), two intrinsically unstable modes of flame propagation were observed:

(1) a pure radial pulsation and
(2) a combined radial-pulsation and traveling-wave instability.

The radial pulsation was observed in both normal gravity and microgravity. It is illustrated in Fig. 2 by multiple views of the expanding radial rings made visible by high-speed intensified video imaging. The traveling-wave instability assumed the form of a rotating spiral wave at normal gravity and a rotating multi-headed spinning wave at microgravity (Fig. 3). Although the frequencies of the pulsation and rotation rates of the spinning waves are relatively high (~100 Hz), they are lower than the fundamental acoustic resonant frequencies of the tubes, which suggests that the instabilities are not acoustically induced. Moreover, the frequencies of the pulsation rates scale to the square of the mean axial flame-propagation speed, in accordance with the thermal-diffusive models.

One of the striking features of these high-Le instabilities is that the resultant spatial-temporal patterns rival those observed in other excitable media. Specifically, this premixed gas-phase reaction exhibits many of the same features and analogous dynamical behavior as the well-studied liquid-phase, weakly exothermic, Belousov-Zhabotinskii reaction. Both reactions have chemical fronts that progress from single or multiple pacemaker sites into circular ring waves or rotating spiral waves. Moreover, both reactions are reactive-diffusive systems; i.e., they exist due to the balance between chemical reaction and diffusion. The premixed gas flame, however, is different from previously observed oscillators, because it has a reaction rate that is exponentially sensitive to temperature and because both heat and mass diffusion are important.

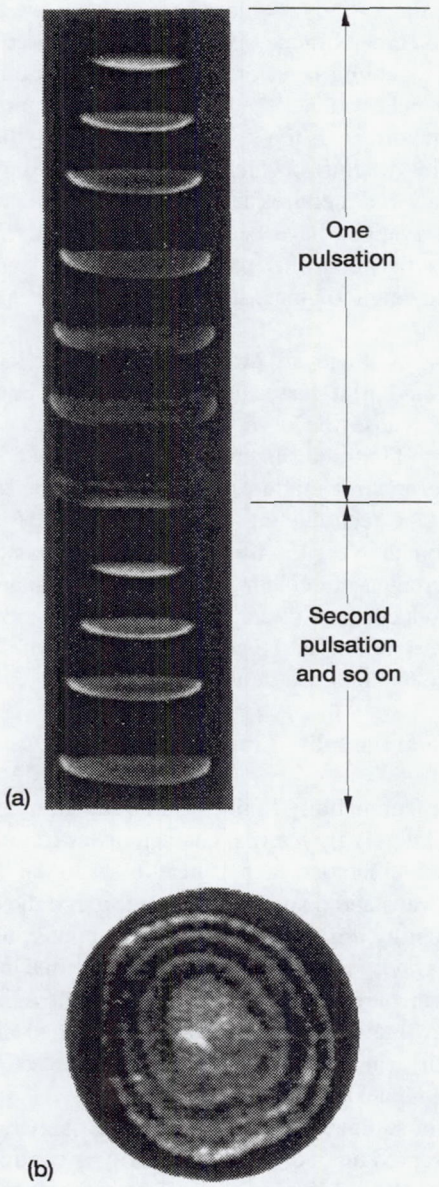

Figure 2.—Multiple consecutive images, 2 ms apart, of propagating radial pulsation waves for 1.3% butane/21% oxygen/helium flames in a 14.3-cm-diam tube burning downward in normal gravity. (a) Axial cross-section. (b) Radial cross-section.

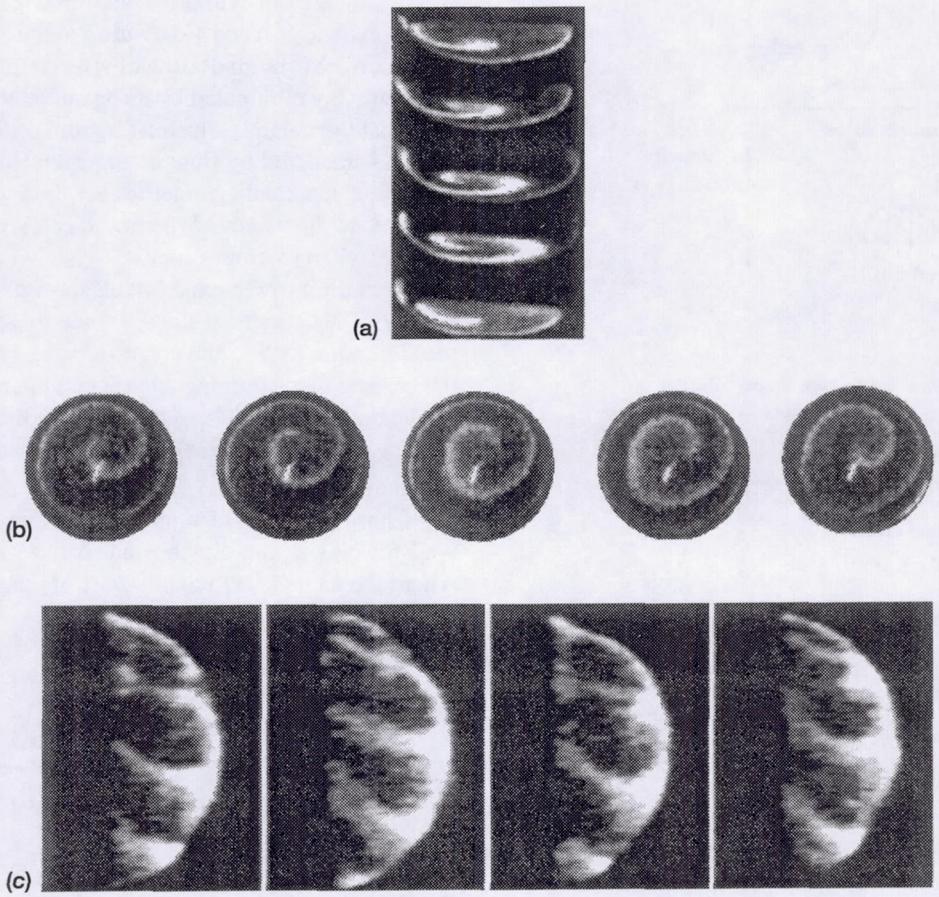

Figure 3.—Multiple consecutive images of traveling-wave instabilities for 1.3% butane/21% oxygen/helium flames in a 14.3-cm-diam tube. (a) Rotating spiral wave in downward normal gravity, 2 ms between images; axial cross-section. (b) Rotating spiral wave in downward normal gravity, 2 ms between images; radial cross-section. (c) Multiheaded spinning wave in microgravity, 5 ms between images; radial cross-section.

Flames propagating in mixtures diluted with various inert gases (He, Ar, Ne, N_2) and combinations thereof are now being used to reduce the Lewis number systematically, while maintaining the same equivalence ratio. As the Lewis number decreases, the frequency and amplitude of the pulsations also decrease monotonically. Below a critical Lewis number, the flame instabilities are no longer visible, and the flames propagate in a stable, uniform manner.

Adiabatic, Non-Stretched Flames

Discussions in the preceding sections on the various flame phenomena, such as self-extinguishing flames and flame-balls, have noted the coupled effects of flame stretch and aerodynamic stretch. Such effects can cause the flame temperature to depart from its adiabatic value and, as a consequence, can change the bulk-flame response in terms of propagation rates and extinction limits. Flame stretch is induced by the presence of a nonuniform tangential velocity over a flame surface. Therefore, all practical flames on Earth are also aerodynamically stretched, due to the unidirectional nature of the buoyancy force and the fact that the flame surface is not always normal to this force. Examples are the outwardly propagating spherical flame, the Bunsen flame, and the stagnation flame (Fig. 4(a)). The flat-burner flame (Fig. 4(b)) is non-stretched, but it is not adiabatic because heat loss is intrinsic to its ability to be stabilized over the burner surface.

Since adiabatic, non-stretched flames have not been observed on Earth, their properties cannot be quantified. These flames, however, are of fundamental importance to flame the-

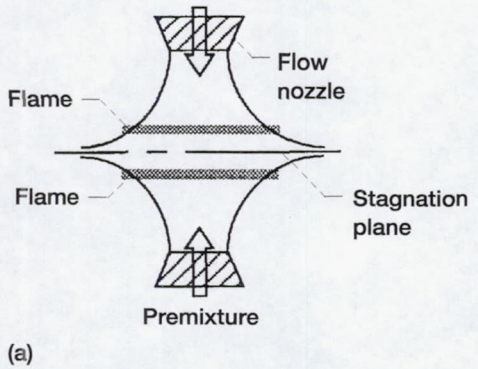

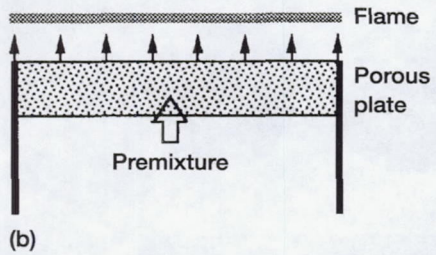

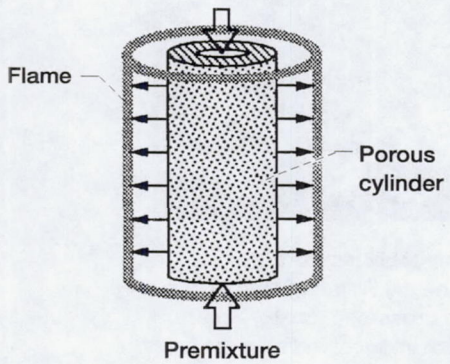

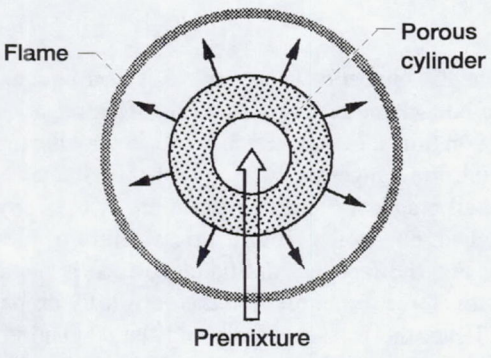

Figure 4.—Various one-dimensional flame configurations. (a) Counterflow flame. (b) Flat flame. (c) Cylindrical flame. (d) Spherical flame.

ory and to our understanding of the flame structure in its basic form. Theoretically, these flames can be produced by ejecting combustibles from cylindrical and spherical porous burners, as shown in Figs. 4(c) and 4(d). Here, stretch is absent because the flame surface is normal to the flow direction. Heat loss can also be effectively eliminated by using sufficiently high flow rates, such that the flame is situated far from the burner surface. The flame is stabilized by flow divergence. However, since cylindrical and spherical symmetries are destroyed in the presence of buoyant flows, these flames can be established only in microgravity environments.

Recent drop-tower experiments have demonstrated the feasibility of a cylindrical flame. Since this flame can have the same burning rate as the corresponding planar configuration, the laminar flame burning rate (per unit flame surface area) can be determined as $m/(2\pi r_f)$, where m is the mass ejection rate from the burner surface (per unit length of cylinder) and r_f is the flame radius. Fig. 5 shows that the experimentally measured burning rates and numerically calculated values compare well for higher non-dimensional surface mass-ejection rates, where the flame is sufficiently far from the burner surface that heat loss is not significant.

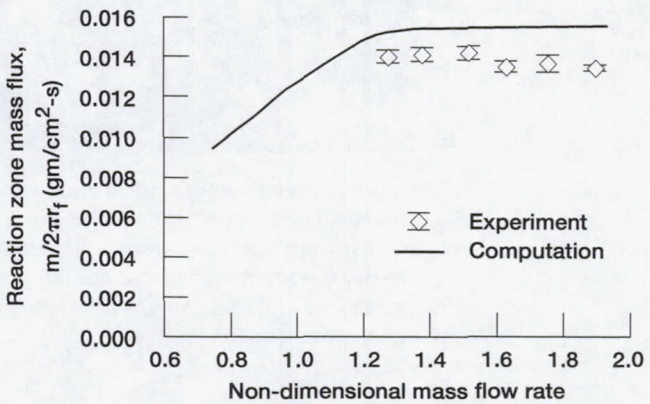

Figure 5.—Computed and experimental reaction-zone mass flux for cylindrical flame in microgravity.

Laminar Diffusion Flame Structure

Gas-jet diffusion flames represent combustion processes found in unwanted fires as well as practical systems. The flame structure is controlled by the complex interaction of many mechanisms (Fig. 6). Because of its geometric simplicity, the gas-jet diffusion flame is often studied as a first step toward understanding complex diffusion-flame processes, especially soot formation and radiative transfer, that are found in practical combustion systems. In normal gravity, buoyancy accelerates

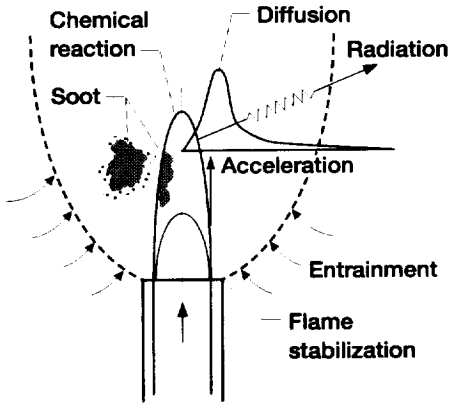

Figure 6.—Schematic of the structure of a laminar gas-jet flame, a complex function of the depicted mechanisms.

the fuel and air flows and may induce turbulence. By studying gas-jet diffusion flames in a microgravity environment, where the effects of buoyancy on flow entrainment and acceleration are negligible, one can simplify the analyses of heat and mass transfer and soot processes.

Burke-Schumann Diffusion Flames

The structure of a gas-jet diffusion flame was first modeled by Burke and Schumann in 1928. Their analytical model assumes that the flame is laminar and enclosed in a chimney supplied with a coaxial flow of oxidizer (Fig. 7). It is thus hypothesized that microgravity (non-buoyant) flames will match the analytical predictions closer than normal-gravity flames, since the analysis assumes that buoyant convection is negligible. Normal-gravity tests that attempt to minimize buoyant convection by low-pressure environments are unable to match the analytical predictions.

Microgravity-test results demonstrate close agreement with Burke-Schumann predictions and show interesting differences from those of conventional flames. Tests conducted in a NASA Lewis drop tower at atmospheric pressure with overventilated hydrocarbon flames in a cylindrical burner showed that the microgravity flames are wider and more rounded at the tip than the normal-gravity flames (Fig. 8 color). For example, the height where the flame reaches its maximum width in normal gravity is low (1/6 of the total height), due to inward buoyant entrainment; but it is significantly higher in microgravity (1/3 of the total height). The luminous flame height is nearly the same at both gravity levels, although the flames are slightly higher in microgravity; the theoretical analysis predicts this difference when axial diffusion is accounted for. Ethane and propane flames reveal an additional buoyant effect; the luminous tip of the flame (the soot shell) is observed to open in microgravity, except at low flow rates. This is due to a combination of reduced oxygen transport to the flame and radiative

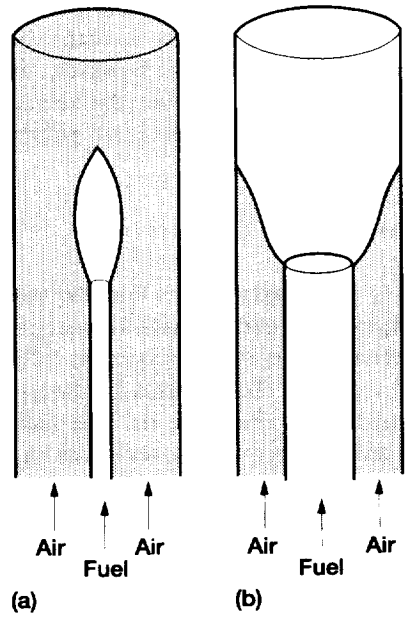

Figure 7.—Cylindrical Burke-Schumann diffusion-flame geometry. (a) Overventilated. (b) Underventilated.

heat loss resulting from a microgravity-enhanced production of soot (because of longer residence times).

Upcoming tests will examine the effect of buoyancy on the flame structure and stability further through velocity, temperature, and chemical-species measurements. An investigation of the state relationships will also be conducted to verify the existence of a "universal" structure for Burke-Schumann diffusion flames in buoyant and non-buoyant environments.

Laminar Fuel Jets

The behavior of a jet of fuel issuing into a quiescent oxidizing atmosphere was investigated in microgravity experiments conducted in the NASA Lewis 5.2-Sec Zero Gravity Facility. The combined effects of the fuel type, fuel flow rate, chamber pressure, and oxygen concentration on the flame structure were measured by cinematography, thermocouples, and radiometers. As also noted for co-flowing jet flames (Burke-Schumann), the observed flames are longer, wider, and often sootier in microgravity than their normal-gravity counterparts (Fig. 9 color). They are dimmer and more reddish, which suggests a lower flame temperature. Some microgravity flames appear to have open tips, as found in Burke-Schumann flames. The microgravity flames exhibit no flickering, even though their normal-gravity counterparts clearly flicker. Whereas the normal-gravity flow field accelerates from jet exit to the tip of the flame, the microgravity flow velocity decreases markedly, causing the observed changes in flame behavior and sooting propensity.

Because the microgravity flames are generally larger and sootier, the thermal radiation from the flame to its surroundings can be appreciably greater in microgravity than in normal gravity. At low-oxygen concentrations, however, microgravity flames are blue and soot-free, whereas the identical normal-gravity flames do not show any significant reduction in soot formation.

Transitional Fuel Jets

With increasing jet velocity or fuel-flow Reynolds number, in either normal gravity or microgravity, laminar gas-jet flames exhibit a transitional stage and may become fully turbulent. The transitional regime is characterized by the appearance of an instability structure at the flame tip. The location where these structures are first observed moves upstream, toward the nozzle, as the jet velocity or Reynolds number is increased. In addition, an enhancement of mixing caused by the instabilities wrinkles the flame and increases its surface area. This increases the total transport per unit length of the flame, thereby shortening the overall normal-gravity flame length.

The laminar-to-turbulent transition process for gas-jet diffusion flames of methane, ethylene, and propane was investigated in the NASA Lewis 2.2-Sec Drop Tower to develop an understanding of the mechanisms that control this process in microgravity. Volumetric flow rates varied from 300 to 500 cc/min in a 0.8-mm-diameter nozzle, providing a cold-jet Reynolds-number range from 1800 to 3200 (based on the nozzle diameter and inlet velocity). Only limited tests were conducted at higher Reynolds numbers, since the transition process in microgravity is essentially complete at Re ~ 3200.

The microgravity flames are laminar for Reynolds numbers up to 2000. The first indication of transition in the microgravity flames was observed at a fuel flow rate of 325 cc/min (Re = 2040). A single disturbance, seen just prior to the end of the 2.2 sec of test time, originates near the flame base and travels downstream, locally distorting the flame front. As the flow rate increases, a greater number of disturbances is observed, but the frequency of generation of the disturbances is not uniform. Up to a flow rate of 450 cc/min (Re = 2800), this characteristic intermittence persists; between the passage of the discrete disturbances, the flame appears undisturbed and laminar. Finally, at a flow rate of 475 cc/min (Re = 3000), a continuous train of disturbances is observed emanating from near the flame base and traveling downstream. The disturbances, which distort the flame front, appear axisymmetric in the lower half of the flame but somewhat asymmetric near the tip.

In general, the characteristic large-scale structures are caused by the instability of the shear layer formed by the fuel-jet injection into quiescent surroundings. As noted, structures with both axisymmetric and asymmetric features are observed. The propagation rate of the axisymmetric structures is higher than that of the asymmetric structures. The flame-height variation with Reynolds number shows that the effective diffusivity for the transitional microgravity flames is smaller than that for the corresponding normal-gravity flames. The increased effective diffusivity for normal-gravity flames is believed to be caused by the preferential generation of small-scale structures due to buoyant acceleration, which increases the local Reynolds number as compared to the microgravity flames.

An important effect of the observed disturbances is their influence on the flame tip. As discussed in the previous section, some laminar flames (*e.g.*, propane) may exhibit open tips in microgravity similar in appearance to underventilated flames. When the intermittent disturbances arrive at the tip of the transitional flame, however, the flame tip tends to close. Between successive disturbances, the tip tends to reopen. When there is a continuous train of disturbance, the tip closing is sustained.

The height of the transitional microgravity flames continues to increase with injection Reynolds number, although at a slower rate compared to the variation in the laminar regime (Fig. 10). For Reynolds numbers greater than 3200, the flame height in normal gravity decreases slightly, indicating that turbulent conditions have been achieved, whereas the flame height in microgravity increases asymptotically. The near-constant normal-gravity flame height as transition to turbulence commences is a result of enhanced turbulent transport, which opposes the tendency to increase flame height by increased jet momentum. The increased microgravity flame height in this transitional range, in contrast, indicates that any enhancement in transport processes due to the disturbances does not overcome the effects of increased jet momentum.

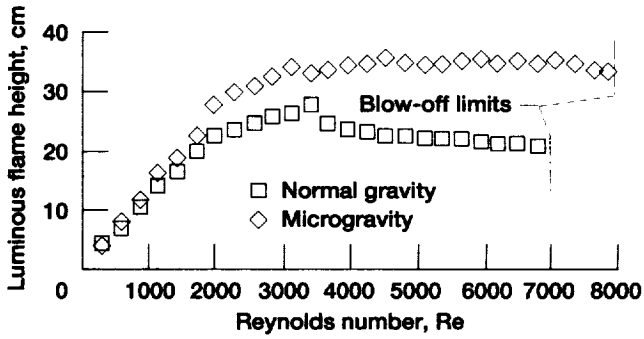

Figure 10.—Measured heights of transitional and turbulent gas-jet flames, for luminous propylene/air flames at 101 kPa in normal gravity and microgravity.

Turbulent Flames/Flame-Vortex Interactions

Turbulent flames exist in high Reynolds number, reacting flows for terrestrial applications, and they contain scales of motion that range down from the size of the device to the

microscopic. Buoyancy effects do not occur in most real devices on Earth because the relatively high speeds make the ratios of turbulent stresses to buoyancy-induced stresses large. The problem in normal gravity is one of observability of the range of scales. In order to conduct experiments, it is desirable to increase size scales to exaggerate minor turbulence effects. When size scales are expanded, buoyancy must be considered because of the large temperature and density gradients across the various turbulent structures. Alternatively, if velocity scales are reduced, buoyancy again interferes because the large-scale turbulent stresses responsible for momentum transport become less than the buoyancy stresses. Consequently, it would be desirable to reduce speeds while real turbulence and observable size scales are retained. This can be done if gravitational effects are reduced through microgravity environments.

Turbulent Diffusion Flames

The transition process in microgravity fuel-jet diffusion flames (described earlier) is characterized by the presence of disturbances that appear intermittently near the flame base and travel downstream. With further increases in the Reynolds number, the disturbances become continuous, and the flame becomes turbulent (Fig. 11 color). In contrast to many laminar flames in microgravity, the turbulent flame has a closed tip. Unlike the normal-gravity turbulent flame, however, the flame height increases asymptotically even in the turbulent regime (although not at the same rate as in the laminar regime, Fig. 10) until the flame is close to blow-off. This indicates that turbulent transport in microgravity is not sufficient to offset the increase in height caused by increased jet momentum.

A current study focuses on the sooting characteristics and radiative transport in turbulent gas-jet diffusion flames. The radiative heat transfer from sooting in turbulent diffusion flames may represent the majority of the theoretical heat release by combustion. Modeling of these flames and their corresponding flow fields is based on a Favre-averaged k-ε-g turbulence model and the laminar flamelet approximation, with modifications to include detailed soot-formation kinetics, radiative heat transfer, and turbulence-radiation interaction. Measurements of the flame-zone temperature and velocity distributions are made in addition to soot volume fractions, since they are all affected by the sooting characteristics. A current model of the turbulent gas-jet diffusion flame can predict the temperature field accurately and the soot volume fractions reasonably well with adjustment of kinetic parameters.

Pulsed microgravity laminar diffusion flames in both gas-jet and co-flowing (Burke-Schumann) configurations are being utilized to study, in the absence of buoyancy, the dynamics of controlled, laminar flame-vortex interactions. Such interactions are commonly used in experiments to understand transport effects in turbulent flames. Pulsing of the flame is achieved by modulating the fuel flow or the air flow. Initial experiments with a pulsed fuel-flow, Burke-Schumann flame have revealed a subharmonic flame response dependent upon the forcing frequency, flow rate, and gravity level. The subharmonic response may be due to vortex merging. Numerical simulations have been successful in predicting the existence of large vortex structures outside the flame sheet, although subharmonic behavior has not yet been predicted.

Pulsed microgravity flames also offer the opportunity to develop universal scaling relations that quantify the effects of flame stretch on combustion, with the complicating effects of buoyancy reduced. Such scaling relations indicate the degree of wrinkling, the probability of flame curvature, and the stretch distribution along the flame as the strength of the vortices vary. In normal-gravity experiments, buoyancy effects stabilize the flame leading edge to a low degree of flame wrinkling, curvature, and stretch.

Three-dimensional flow fields of transitional diffusion flames stabilized on elliptic nozzles are being investigated in a new study. Techniques of passive control (by means of injector geometry variations) and active control (by means of imposed acoustic excitation) of diffusion flames will be evaluated in this study.

Turbulent Premixed-Flame Structure

A fundamental understanding of the coupling between turbulent flames and gravity is important to turbulent-combustion science and applications. Ongoing research attempts to elucidate flame-gravity coupling processes in weakly turbulent, premixed flames (i.e., wrinkled laminar flames) by characterizing the flow fields and flame properties under different gravitational orientations and comparing them to those of microgravity flames. These microgravity experiments are keys to reconciling the differences between flames in normal gravity (+g, flame pointing upward) and reverse gravity (–g, flame pointing downward).

Previous research focused on developing flow visualization for microgravity experiments to determine the mean flame properties. Current research is geared towards developing appropriate diagnostics for measuring scalar and velocity statistics in microgravity. These statistics will enable quantitative and direct comparisons to be made between normal-gravity laboratory results and theoretical predictions.

Conical flames and rod-stabilized V-flames have been used extensively in theoretical and experimental research conducted in the NASA Lewis drop tower and airplane facilities. Under the wide range of flow, mixture, and turbulence conditions investigated, gravity alters the flame flow field and mean flame properties and affects the ignition, stabilization, and blow-off limits. The most significant consequence of buoyancy on +g flames is the generation of flame flickering due to an interaction of hot buoyant products with the ambient air. Without this interaction, flames in –g and microgravity do not flicker. Analysis of the flame-flickering frequencies produces an empirical

relationship that is useful for theoretical prediction of buoyancy-induced flame oscillations. This empirical relationship is a function of Reynolds (Re), Strouhal (St), and Richardson (Ri) numbers as a linear function of St^2/Ri versus $Re^{2/3}$, where St^2/Ri represents the ratio of the fluctuation force to the buoyancy force. The empirical relationship merges all obtained data successfully, including some earlier sub-atmospheric and elevated-gravity (via a centrifuge) results. The divergent trends of the laminar and turbulent conical flame heights show that the properties of +g, −g, and microgravity flames remain fundamentally different even with increasing flow momentum. In +g normal gravity, the flow field generated by the rising products plume is non-divergent and oscillating. In −g, the flow becomes divergent but stable in the region surrounding the flame cone. In microgravity, without buoyancy to alter the flow direction of the hot products, the products form a pocket that grows and expands into the ambient air.

Soot Formation, Aggregation, and Oxidation

From an environmental and economic standpoint, soot is an important combustion intermediary and product. Soot is an aggregate of fine solid particles, comprised of a range of aromatic hydrocarbon species. Soot production is an important pathway for a significant fraction of the fuel in many practical flames; consequently, the soot processes must be defined in order to understand the chemistry and physical transport in these flames. Due to its high radiative emissivity, soot is a major contributor to the radiative heat loss from a flame; and, as a result, soot formation is a strong positive factor in energy extraction for large-scale boilers and furnaces and a negative factor enhancing flame spread in accidental fires. Soot is an intentional by-product in the manufacture of carbon black, an industrial product used in tires, plastics, inks, pigments, magnetic tapes, and carbon-fiber matrices.

Microgravity offers a means to improve our understanding of soot processes because of the unique opportunity to control the flow environment. For example, predictive modeling shows that, due to the lack of buoyant flow, the soot residence time in laminar gas-jet diffusion flames is of the order of 30 times longer in microgravity than in normal gravity. The movement of soot through the flame is also strongly affected by microgravity. In normal-gravity, buoyant flames, soot forms in the hottest regions on the outside of the flame and then moves radially inward toward cooler regions. The soot particles subsequently follow the buoyantly accelerating gas flow until they cross the flame near the flame tip. In microgravity, soot is formed in the coolest regions, and the particles follow a continuously decelerating flow path through zones of ever-increasing temperature.

The longer residence times suggest that broad soot-containing volumes exist inside the microgravity flame. Smoke-height measurements were made for propane and ethylene laminar diffusion flames from jets of 1.6- to 5.9-mm diameter at 50 to 200 kPa (0.5 to 2 atm) pressure in low-gravity tests on the NASA airplane. The smoke height is almost invariant with jet diameter but decreases with chamber pressure. The former result is surprising, since the flame residence time increases with jet diameter. The observed smoke heights at atmospheric pressure are considerably shorter than the buoyant normal-gravity results reported in the literature.

For measurement of soot-particle size, a thermophoretic sampling technique (described in a later section) is used in low-gravity facilities. Microscopic analyses of collected soot show that soot consists of aggregates of generally uniform, near-spherical primary particles. The size of the primary particles is illustrated by data for ethylene and propane diffusion flames from a 1.65-mm i.d. burner for mass flow rates of 1.0 and 1.5 cc/sec (Fig. 12). For all conditions, soot persisted to higher distances above the burner and showed greater average particle diameters in low gravity than in normal gravity. For ethylene, but not propane, the increase in flow rate increased the average primary-particle diameter in low gravity.

TABLE I.— PRIMARY SOOT-PARTICLE MEASUREMENTS AS COLLECTED FROM LAMINAR GAS-JET BURNER

Fuel	Flow Rate (cc/sec)	Gravity Level	Mean Aggregate length (μm)	95 percent Bound (μm)	Actual Min/Max (μm)	Height above burner (mm)	Fractal dimension	Aggregate number analyzed
Ethylene	1.0	1G	0.21	0.10 → 0.42	0.11 → 0.52	10	1.41 ± 0.10	47
Ethylene	1.0	0G	4.71	1.12 → 19.8	1.14 → 18.53	10	1.93 ± 0.34	19
Propane	1.5	1G	0.27	0.14 → 0.51	0.14 → 0.54	30	1.71 ± 0.13	40
Propane	1.5	0G	1.53	0.48 → 4.89	0.50 → 7.27	50	1.57 ± 0.07	39
Burner Diameter 1.65 mm								

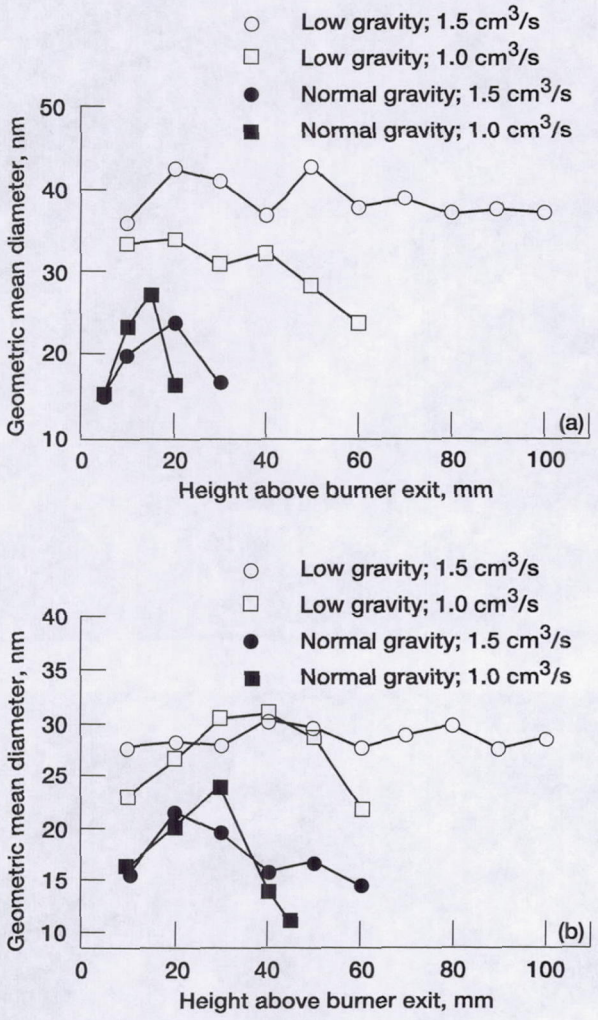

Figure 12.—Effects of gravity on primary soot-particle size for diffusion flames from 1.65-mm-diam burner. (a) Ethylene/air. (b) Propane/air.

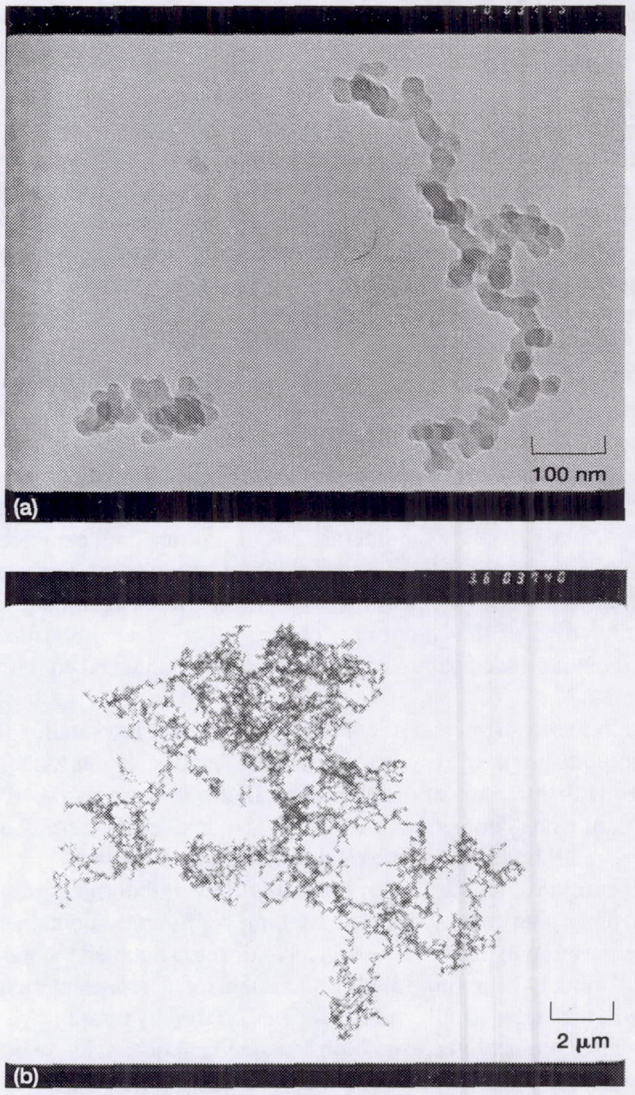

Figure 13.—Photographs of soot-particle aggregates collected 10 mm above a 1.65-mm-diam ethylene burner at 101-kPa total pressure. (a) Normal gravity, 116 000X magnification. (b) Low gravity, 4000X magnification.

Examples of the collected soot aggregates for the cited tests are shown in Fig. 13. The upper photograph shows an aggregate in normal gravity, and the lower one in low gravity (the magnification of the two images are different). Table I summarizes the soot-particle-aggregate measurements for the ethylene and propane flames, each at a selected flow condition in normal gravity and in microgravity. While the soot aggregates are three-dimensional objects, the two-dimensional projections in the photographs may be interpreted in terms of a maximum aggregate length, along with a fractal number. It is clear that the aggregates are much longer in low gravity, suggesting that the increased residence time has promoted a greater amount of particle aggregation than in normal gravity.

Sooting is also being investigated in non-buoyant laminar jet-diffusion flames at reduced pressures. For tests with acetylene flames burning in air at pressures ranging from 13 to 25 kPa, property measurements are made along the axis of the fuel jet, where soot processes in weakly buoyant flames are similar to those in non-buoyant flames. Measurements to be reported include soot volume fractions, thermophoretic soot sampling, temperatures, concentrations of major gas species, and velocities.

Analytical modeling is under development to predict the structure of buoyant and non-buoyant soot-containing jet-diffusion flames. In addition, a large-scale project, *Laminar Soot Processes*, will perform soot measurements on gas-jet diffusion flames in a combustion facility (CM-1) to be flown on Spacelab in 1997.

Droplet and Particle Combustion

Isolated, Pure Fuel Droplet

The combustion of liquid hydrocarbon fuels is not only the major source for transportation and electrical-generation energy in the U.S., but it is also the major source of air pollution. In most applications, the liquid fuel is burned in the form of tiny droplets, in order to provide maximum surface area for a given volume of fuel burned. Therefore, a thorough understanding of the process of fuel-droplet combustion is of practical importance.

From a scientific point of view, isolated, spherically symmetric, single-droplet burning is the simplest example of nonpremixed combustion that involves the participation of a liquid phase (fuel) in the gas-phase diffusion flame. Investigation of the combustion of single, isolated liquid droplets affords the opportunity to study the interactions of physical and chemical processes in an idealized and simplified geometrical configuration. Microgravity facilities offer a unique environment to study some of the important features of droplet combustion without the added complications of buoyancy-induced convection.

In practical sprays, typical droplet diameters are small, and consequently buoyant forces are small. The time scales associated with the combustion of these small droplets are also small, which, when coupled with the small size, makes their study in a normal-gravity environment difficult. Fig. 14 shows a typical (~1 mm) droplet burning in normal gravity and in microgravity. The spherically symmetric burning configuration obtained in microgravity allows researchers to develop detailed theoretical models in a simplified, one-dimensional representation. Also, the larger length and time scales offered by microgravity droplet combustion allows both transient and quasi-steady liquid- and gas-phase and flame-extinction phenomena to be studied in detail.

Past experiments in the NASA Lewis drop towers revealed several previously unknown phenomena related to small droplet combustion in microgravity. These findings include:

(1) a new slow-burning regime,
(2) the influence of the burning rates of hydrocarbon fuels on soot formation,
(3) disruptive burning of initially pure liquid fuel droplets,
(4) a lower limiting-oxygen concentration for droplet combustion in microgravity than in normal gravity,
(5) the importance of the spark-droplet interaction in the ignition of the droplet, and
(6) the identification of product dissolution in the liquid phase of the droplet.

Droplets greater than 1 mm in diameter, which have relatively long combustion time scales, are easier to study; but they can generate significant buoyancy forces. Limited evidence indicates that the burning characteristics are a strong function of droplet size for large droplets in microgravity. Testing conducted on single decane droplets approximately 4 mm in diam-

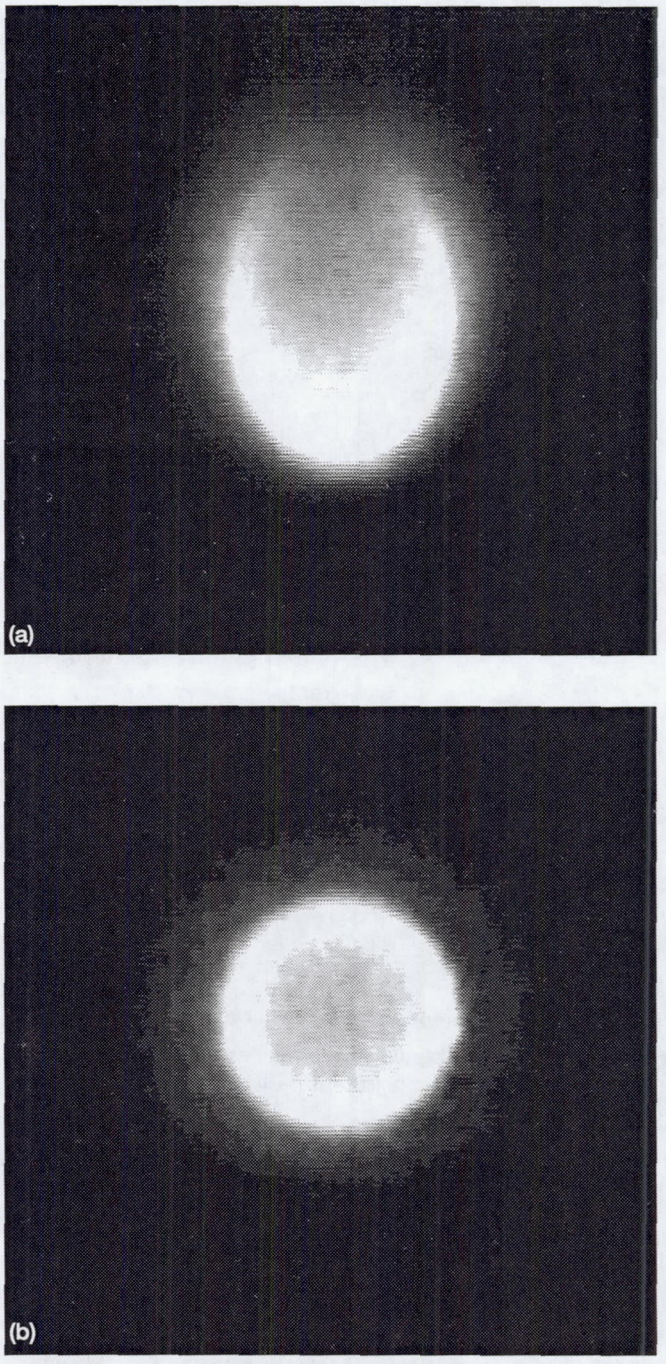

Figure 14.—Combustion of isolated, single droplets of *n*-heptane. (a) Normal gravity: droplet suspended on a fiber. (b) Microgravity: droplet free-floating.

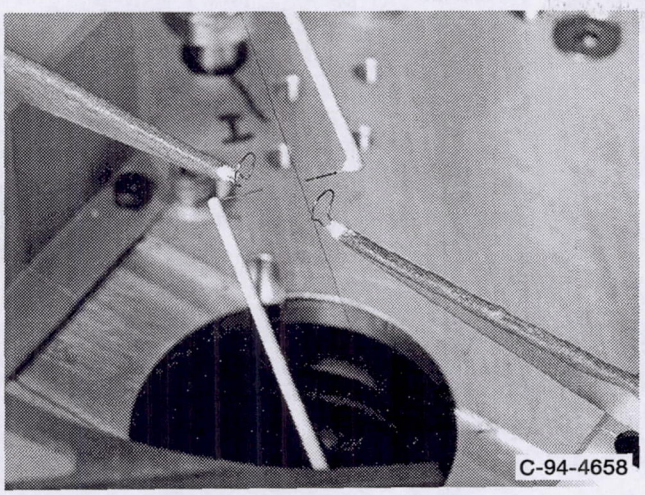

Figure 15.—Opposed-needle droplet-deployment system and hot-wire ignition system used in the microgravity droplet-combustion apparatus.

eter burning in air at 100 kPa in the Japan Microgravity Center 10-sec drop tower showed some unusual results. Immediately after ignition the droplet flame is bright yellow, sooty, and spherical as expected (except for a small non-uniformity due to a minor, residual convective flow). As the burning progresses, the luminosity of the flame decreases, and the flame-standoff ratio (the ratio of the flame diameter to the droplet diameter) is smaller than expected. By the end of the free-fall test, the droplet has not yet burned to completion, but the flame is nearly invisible to the UV camera. It is interesting to note that a smaller (1 to 2 mm initially) decane droplet burned to completion as expected, with a bright yellow, sooty, spherically symmetric flame.

The generation of isolated, near-motionless droplets in a quiescent environment for combustion studies is accomplished by a standardized technique in facilities such as the NASA Lewis drop towers and parabolic-trajectory aircraft. The fuel is injected from two opposing hypodermic needles, which are then separated to a predetermined length to center the injected droplet between the needles and then withdrawn rapidly. Shortly after deployment, the droplet is ignited using two symmetrically placed hot-wire igniters. A back-lighted view of the droplet photographed by a high-speed camera provides the droplet burning-rate history. The flame position is captured by imaging the OH-radical emission from the flame front using a UV-sensitive charge-coupled-device camera. Fig. 15 shows the droplet deployment and ignition subsystems used in these rigs.

Current studies include the combustion of sooting droplets and of emulsion droplets containing metal additives. The latter have the potential for significant reductions in particulate emissions through the nucleation, agglomeration, and possible oxidation of soot particles by the ions produced. Soot formation is believed to affect single fuel-droplet burning rates, causing deviations from the idealized d-squared-law burning theory, depending on the initial droplet size. It is also suspected that low-volatility soot-precursor species could dissolve in the liquid-phase fuel, causing the pure fuel to behave as a multi-component mixture with possible disruptive burning or "micro-explosions" (see following section).

The first flight of the *Droplet Combustion Experiment*, under development for a mission in 1997, will study large n-heptane droplets (1.5 to 5 mm in diameter) burned in a quiescent oxygen-helium environment under varying ambient-pressure conditions. The objective of this experiment is to examine liquid- and gas-phase, steady and unsteady, and flame-extinction phenomena in single-droplet combustion. Varying the pressure and oxygen concentration affects the location of the flame relative to the droplet to place the flame in either a convective-diffusive region (high-oxidizer concentration) or a transient-diffusive region (low-oxidizer concentration). The liquid-phase phenomena consist mainly of transient liquid heating and product dissolution and transport into the liquid phase.

Theoretical models for droplet combustion have been developed successfully to interpret the experimental data, and a variety of asymptotic analyses have been performed. A fully time-dependent, spherically symmetric numerical code with detailed chemical kinetics, capable of simulating ignition, unsteady gas phase combustion, and extinction, is currently available.

Isolated, Multi-Component Droplets

Most practical fuels used in boilers, gas turbines, diesel engines, rockets, and so on, are multi-component mixtures. Typical hydrocarbon fuels consist of several hundreds or thousands of components and show a wide boiling range due to volatility differentials, in contrast to a single-component fuel with a specific boiling point.

As a first step toward understanding multi-component droplet-combustion characteristics, researchers use bi-component fuel mixtures of greatly differing volatilities for the fuel droplets. Again, microgravity provides an ideal environment for the study of bi-component droplet combustion by enabling larger length and time scales to be examined. Two particular phenomena of interest in bi-component droplet combustion are the droplet burning history and the possibility of disruptive burning. The burning history of the bi-component droplet may exhibit three stages because of the dependence on the liquid-phase mass transport. In the initial stage of burning, if liquid-phase mass transport is diffusion-limited, the more volatile component will vaporize and burn preferentially. This results in a liquid-phase boundary layer in the droplet, because liquid-phase mass diffusion is typically slower than droplet regression. With the more volatile component depleted, the second burning stage follows, with the droplet heating to the boiling temperature of the less volatile component. This is followed by the third, quasi-steady burning stage. The phenomenon of dis-

ruptive combustion, or a "microexplosion", occurs when a pocket of more volatile fuel is heated above its homogeneous nucleation temperature for bubble formation. For bi-component droplet combustion, disruptive burning can result if a higher concentration of the more volatile fuel is trapped at the core of a droplet surrounded by a shell of less volatile fuel and if there is sufficient volatility difference between the two fuels.

One of the NASA-supported, bi-component, droplet-combustion investigations, *Fiber-Supported Droplet Combustion*, will burn mixtures of heptane-hexadecane and methanol-dodecanol in oxygen-nitrogen and oxygen-carbon dioxide environments. Fuel droplets are supported by a silicon-carbon fiber and ignited using spark electrodes. Another microgravity, multi-component droplet-combustion study, now underway, focuses on azeotropic mixtures. An azeotrope is a non-ideal mixture that exhibits an extremum in vapor pressure and "volatility reversal" at a particular composition.

Droplet Arrays and Sprays

In practical fuel sprays, droplets do not burn individually but interact with each other during combustion. It is insufficient, then, to base models of fuel-spray combustion entirely on results from single-droplet combustion experiments. Three studies currently underway will extend the results of single-droplet combustion studies to more practical fuel sprays.

Two of these studies deal with droplet arrays. Arrays are a collection of a small number of droplets in a controlled configuration that closely simulates an actual fuel spray but is amenable to detailed analytical treatments. Both studies use fiber-supported droplets where the separation distance of the droplets can easily be controlled.

One study investigates pure fuels in low-pressure environments. For combustion of two-droplet arrays, individual flames surround each droplet early in the flame lifetime. As burning progresses, the flames merge into a single enveloping flame. Late in the flame lifetime, individual flames again surround the droplets as the droplets burn to completion. Similar behavior was observed for the combustion of two-droplet arrays of bi-component fuels, except that the last phase of individual flames is apparently caused by the depletion of the more volatile component. This behavior is analogous to the flame contraction in the burning of a single, bi-component droplet.

The second study investigates arrays of pure fuels and bi-component mixtures in high pressures (above the critical pressure of both fuels), continuing a study of single-droplet combustion of bi-component fuels at high pressures.

A third study examines the combustion of laminar fuel sprays in normal gravity and microgravity. Two spray generation techniques are being used. The first is an electrostatic spray, which allows self-dispersion of the spray due to coulombic repulsion and control of the droplet trajectories. The second is an ultrasonic spray, which allows studies of flame extinction and droplet interaction under low-slip conditions (more amenable to numerical modeling). Two spray configurations are being used, a counterflow geometry and axisymmetric geometry, both in the laminar regime. Limited testing to date in the NASA Lewis 2.2-Sec Drop Tower shows an unexpected influence of buoyancy on the laminar counterflow diffusion flame with an electrostatic spray. In a regime where buoyant effects were expected to be minimal, a laminar counter-diffusion flame was ignited and stabilized first in normal gravity and then exposed to microgravity (the free-fall). Instead of remaining flat, the flame curved in microgravity.

Flammability and Flame Spread Over Liquid Pools

For a liquid pool below its flash point (the minimum temperature to vaporize sufficient fuel to reach the lower flammability concentration), a heat source must provide sufficient energy to preheat and vaporize the necessary fuel for a combustible gas-phase mixture. After ignition, the flame itself provides the energy for the preheating and vaporization necessary for flame spread. To this extent, flame spread over liquid pools is similar to flame spread over solid sheets. The major difference is that internal convective flows will develop in the liquid pool, driven by the heat source through the temperature-induced surface-tension gradients and through buoyancy. Gas-phase motion is governed largely by buoyancy, restricted by the no-slip condition at the gas-liquid interface. Therefore, gravity affects both the liquid- and gas-phase flow fields and influences the supply of oxidizer and heat transfer ahead of the flame. It is not clear *a priori* whether the ignition delay and the flame-spread rate will be faster or slower in microgravity compared to normal gravity, especially if a slow, uniform flow is imposed.

Flame spread over liquids can differ from that over solids in another important way (at least in normal gravity): the flame spread may become pulsating at a certain range of fuel temperatures initially below the flash point. Pulsations develop in which the flame spread goes through a regular cycle of jump (rapid advance), crawl (slow advance or even, for some fuels and environments, a stop or retreat), and jump. The cause and phenomenology of pulsating flame spread are not completely understood, and the role of buoyancy remains especially unclear. It is suggested that the onset of pulsating spread is coincident with the formation of a gas-phase recirculation cell ahead of the spreading flame. At temperatures close to the flash point of the liquid fuel, the recirculation cell is absent, and pulsating spread does not occur. On the other hand, liquid-phase recirculation may also influence the flame pulsations. A series of tests at normal gravity showed that the tray depth has a strong effect on the pulsation frequency, with shallow (2 mm) trays having much higher pulsation rates than 5- or 10-mm-deep trays. Imaging techniques revealed a subsurface vortex formed under the flame leading edge during the crawl portion

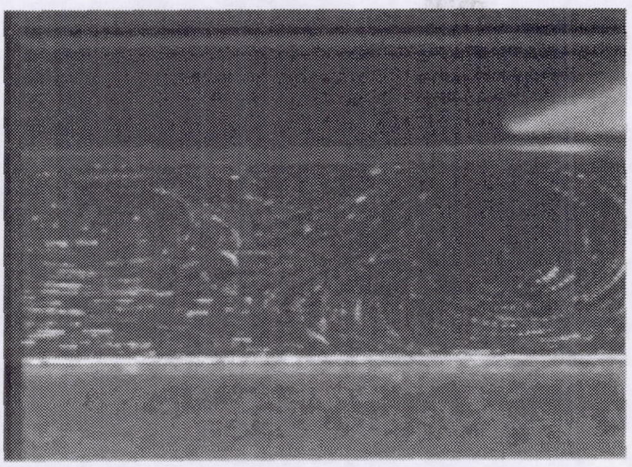

Figure 16.—Particle image velocimetry results showing subsurface vortices in liquid pool ahead of the spreading flame in normal gravity.

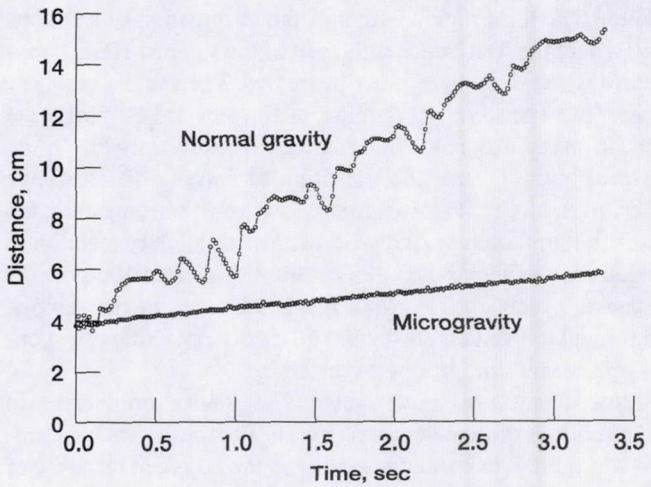

Figure 17.—Experimental data on flame position (half-tray radius) over liquid pool for 1-butanol fuel in normal gravity and microgravity.

of the cycle that carries heat ahead of the flame before the flame jumps (Fig. 16). For shallow trays to as great a depth as 10 mm, this vortex reaches the tray bottom; and it is believed that momentum loss at the bottom changes the pulsation frequency. Experiments at normal gravity with helium instead of nitrogen as the atmospheric diluent showed that for a wide range of temperatures (including temperatures *above* the flash point in air), the flame always pulsates, even with no liquid-phase vortices being formed.

Liquid-pool flame tests with a 10-mm-deep rectangular tray were conducted in the NASA Lewis 5.2-Sec Zero Gravity Facility in 1994. Results of flame-position measurements for 1-butanol fuel are shown in Fig. 17. At conditions where the flame would pulsate at normal gravity, either no ignition or rapid extinction occurred in quiescent microgravity. If air flows of 2 to 10 cm/s opposed to the flame spread were superimposed on the flames, however, ignition and apparently sustained flame spread did occur at the same conditions. Test times were too short, however, to draw a general conclusion.

Numerical modeling of flame spread over liquid pools has also brought significant gains in understanding. A previously developed computer code was modified for use with alcohol fuels, and excellent agreement of experimental results for the flame-spread rate and pulsation frequency was obtained in normal gravity. A key issue examined in the model is the cause of pulsating flame spread. Current development efforts on the code are in the additions of a solid top boundary and forced air flow over the liquid pool, modifications that match the experiment conditions. Techniques to animate the results of the model have been developed, including particle seeding to mimic experimental particle tracking and temperature-derivative fields to match the refractive-index fields.

In order to achieve longer periods of microgravity and allow for more advanced diagnostics, the *Spread Across Liquids* experiment was conducted recently on a sounding rocket (November 1994). This experiment allowed, for the first time, a detailed study of flame spread over liquids in a microgravity environment, using a variety of diagnostics for flame and flow imaging, temperature, and radiation. Preliminary results prior to full analyses show that flame spread is sustained with 10 cm/s opposed air flow and that the flame-spread rate appears to be altered significantly in microgravity.

Smoldering Flame Spread

Smoldering is a non-flaming combustion process that takes place in porous-solid combustible materials, and it is characterized by a heterogeneous surface reaction that propagates within the fuel material. Smoldering is important both as a fundamental combustion mechanism and as a fire precursor, since fires are often triggered by the transition from slow smoldering to rapid flaming. Smoldering transport and reaction processes are complex, and the removal of gravity offers substantial simplifications to their study.

Recent experiments examined smolder-front propagation in normal gravity as a function of the magnitude and direction of forced oxidizer flow. For packed cellulose fuel only very limited effects of gravity can be detected, in part due to the low permeability of the fuel and in part due to the fact that material sedimentation makes it impossible to conduct smolder experiments with upward propagation. These difficulties were surmounted by the use of polyurethane foam for upward-smolder experiments. The tests showed that the propagation of a smolder front from the igniter surface through a foam passes through three regions of differing smolder behavior. The first region is that of variable propagation rate largely dominated by the effects of the igniter. The second region is that of sustained

smolder propagation beyond the region of influence of the igniter. The third region is that of the termination of smoldering, where the front reaches the end of the sample. Here, buoyant transport dominates other processes. The sample typically undergoes transition to flaming in the upward-burning case and, in many instances, in downward burning as well. In the upward-burning case, the transition to flaming occurs above the smolder front; whereas, in the downward-burning case, the transition to flaming usually occurs as a secondary reaction in the char zone above the smolder front. This transition occurs because, as the smolder front reaches the end of the sample, additional oxygen enters the hot char zone, providing the conditions needed for ignition of the char.

Experiments also investigated low-gravity smoldering in NASA Lewis drop towers and aircraft. For these tests, the sample was ignited in normal gravity, and the transient response of the smolder front to the low-gravity environment was observed. Conclusions from these studies are that strong buoyancy effects are evident in those smolder regions equivalent to regions 1 and 2 observed in normal gravity. Transition to low gravity causes the temperature gradients (with respect to time) in the sample to reverse. This effect was seen in both upward propagation and downward propagation. It was impossible, however, to maintain a sustained smolder front under these conditions in airplane tests. The cyclic acceleration forces in the parabolic trajectories would eventually weaken the smolder front to the extent that extinguishment would occur. However, the ability to time the low-gravity parabolas on the airplane flights in concert with smolder-front progress makes it possible to examine the effects of buoyancy throughout the depth of the foam.

Smoldering combustion was also investigated in the *Smoldering Combustion in Microgravity* experiment, a Glovebox experiment on a Shuttle mission. The fuel samples were cylinders (8-cm long by 5-cm diameter) of open-cell polyurethane foam. Each test was conducted in a separate, sealed, transparent container placed inside the Glovebox. The data collection included a video record and thermocouple measurements made at eight locations in the foam. Because the small sample size and the limited igniter power could not compensate for the relatively large heat losses, the smolder reactions self-extinguished in all cases. The extent of smolder propagation observed in the microgravity experiments, however, was greater than that observed in normal gravity with the same hardware.

The next smoldering experiment in space, *Microgravity Smoldering Combustion*, is to be flown on the Shuttle in 1995. Tests will be conducted with cylindrical fuels, 12-cm diameter by 14-cm long, in quiescent and opposed-flow environments.

Flammability and Flame Spread Over Solids

Combustion over solid surfaces provides a direct analogy for several practical applications. The most obvious is that of fire safety, where new information is sought for application to fire prevention and control of materials in both space and terrestrial environments.

Flammability and flame spread over solids in microgravity are most strongly influenced by the gas-phase environment and flow conditions.

Quiescent Environment

Truly quiescent environments are achievable only in microgravity, which eliminates the appreciable buoyant flows always present in normal-gravity flames. Combustion experiments with two thicknesses of thin-paper fuels were conducted under various oxygen concentrations in quiescent microgravity. Results show that, for atmospheres with high oxygen concentrations, the flame-spread rate, V_f, is independent of the gravity level (Fig. 18). This finding is consistent with a thermal theory of flame spread for thin fuels, where the flame-spread rate is controlled by gas-phase heat conduction. For oxygen concentrations below about 30 to 40 percent for the paper fuels, however, V_f is lower in microgravity than in normal gravity. The limiting-oxygen index (LOI, the lowest oxygen concentration in which a flame will self-propagate) is higher in microgravity than in normal gravity (i.e., the flammability range is reduced). Also, the LOI for the two thicknesses of paper do not differ in normal gravity, but they differ in microgravity, with a lower LOI for the single thickness (Fig. 18).

Thermal theory predicts that the flame-spread rates for single-thickness, thin fuels should be twice that of the double-thickness fuel. This behavior is observed in normal gravity and in microgravity except near the LOI, where the ratio of flame-spread rates becomes much larger than two. This near-LOI region is currently being studied, both experimentally and theoretically, to ascertain the mechanisms of flame spread and extinction there. The normal-gravity flame is extinguished by blow-off at low Damkohler number (Da, the ratio of the residence time in the reaction zone to the time required to complete the combustion reaction). In microgravity, however, since the residence time of the reactants is long, extinction must be due to another mechanism.

In order to study thicker solid materials, longer microgravity times than are available in ground-based facilities are necessary. The *Solid Surface Combustion Experiment* (SSCE) has

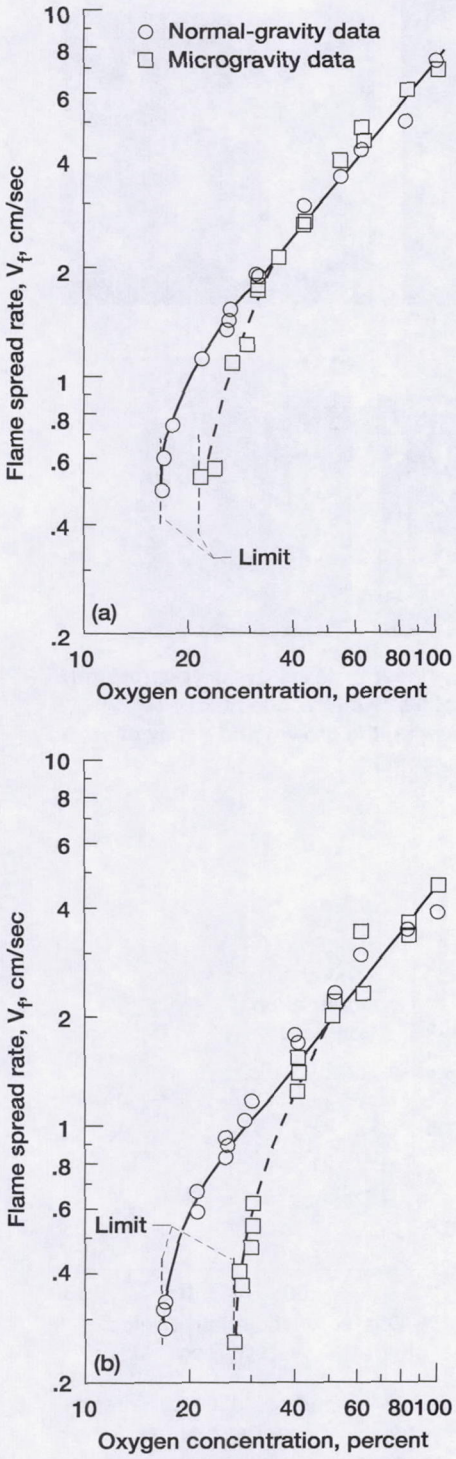

Figure 18.—Experimental data on flame-spread rates for thin-paper fuels in normal gravity and microgravity. (a) Single thickness of fuel. (b) Double thickness of fuel.

flown successfully eight times since 1990. In this experiment, ash-free filter paper or polymethylmethacrylate (PMMA) samples are burned in a quiescent microgravity environment to determine the effects of gravity, oxygen concentration, and pressure on the burning process. Fig. 19 (color) shows a typical flame spreading over thin ash-free paper, taken from one frame of the color motion-picture photography of the SSCE. The flame forms two distinct lobes, each standing well off the fuel surface (invisible as viewed edgewise). The parametric experimental data of flame spread, surface and flame temperatures, and chamber pressure rise provide a set of observations to benchmark flame-spread models over a wide set of conditions. Comparisons of the data to thermally thin combustion models show that radiative heat exchange between the pyrolyzing solid, the gas-phase flame, and the environment must be included to predict the observed trend of increasing flame-spread rate with pressure accurately. Furthermore, while a one-step, steady, fuel-pyrolysis model is adequate for normal-gravity flame spread, an unsteady, multi-step pyrolysis model is needed to represent microgravity flame shape, spread, and extinction. The unique data from the PMMA samples in the last three SSCE flights are now being interpreted to extend the models additionally to thermally thick fuels.

Other microgravity experiments, conducted in a short-duration drop tower, examined the effects of oxygen concentration and atmospheric diluent (CO_2, He, Ar, or N_2) on quiescent flammability. The extinction efficiency of a diluent is measured by the increase in the limiting-oxygen index necessary to support flame spread. Of the diluents tested, carbon dioxide has the highest extinction efficiency (extinguishing ability) because of its strong gas-phase radiative characteristics and its high heat capacity, which promote net heat loss from weak flames near the LOI. Helium is also efficient because of its high thermal diffusivity, which also promotes a high conductive heat loss. Argon, which has the same thermal diffusivity as nitrogen, is least efficient because of its lower heat capacity and thermal conductivity.

A project in progress is studying the interactions between flames spreading over parallel sheets of paper to determine the relative competition between the increased radiative and convective heat exchange against the reduced concentration of oxidizer due to the presence of the second fuel surface. Preliminary testing in a quiescent 30 percent-O_2-He atmosphere found that microgravity flames exhibit a greater interaction than normal-gravity flames for a given separation distance, which was varied from 6.4 to 50 mm. For example, Fig. 20(a) shows four phases of interaction with increasing separation distance. At 10-mm separation, no flame exists between the sheets of paper. At 15 mm, a flame exists, but it is unstable (pulsating). At 30 mm, a stable flame exists that becomes deeply notched as separation increases. At 50 mm, two distinct internal flames propagate between the fuel sheets. The sequence of

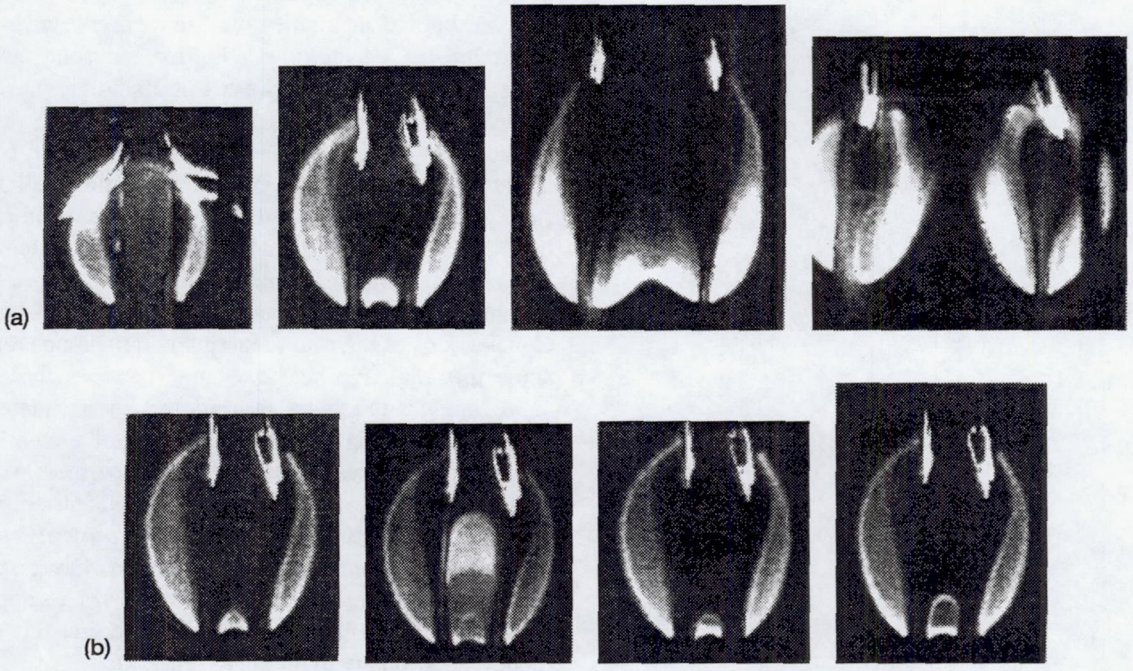

Figure 20.—Edge views of flames propagating over parallel tissue-paper fuels in 30% oxygen/helium, 101-kPa total pressure, microgravity environments. (a) Phases of flame interaction at 10-, 15-, 30-, and 50-mm separation, from left to right. (b) Time sequence, showing the growth and decay of pulsations in the second (15-mm separation) phase.

flame pulsations in the second phase of interaction, which is at the minimum separation distance for any flame propagation, is illustrated by a series of time-related photographs in Fig. 20(b).

Opposed Flow in Microgravity

Drop-tower experiments with thin-paper fuels indicate that low-velocity forced flows, either opposed to or concurrent with the flame spread, have a strong effect on microgravity flammability. This influence may be unique to microgravity, because the low-velocity-flow effect is overwhelmed by that of the buoyancy-induced flow in normal gravity. Fig. 21 (color) shows photographs of flames spreading over paper in air in microgravity with increasing opposed-flow velocities and, for reference, in normal gravity with buoyant flow. At velocities below 5 cm/s (not shown in the figure), the low-gravity flame leading edge is a diffuse blue, and there is a large fuel-rich dark zone between the visible flame and the fuel surface. As opposed-flow velocity is increased, the visible flame is narrower and closer to the fuel surface. Flame temperature apparently increases with flow, as evidenced by brightness (soot production).

A summary of experimental data on paper flame spread as influenced by characteristic relative velocity is shown in Fig. 22 for three atmospheric-oxygen concentrations. The characteristic relative velocity, V_{cr}, is the sum of the flame-

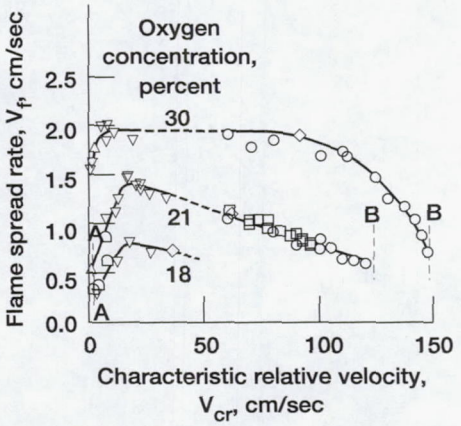

Figure 22.—Experimental flame-spread rates for thin-paper fuels as functions of characteristic relative velocity (flame-spread rate plus forced or induced velocity). The letters A distinguish the quench extinction points (attainable only in microgravity); the letters B distinguish the blow-off extinction points.

spread rate, V_f, and the (generally predominant) forced or buoyancy-induced flow. Again, low-speed flows over these samples, that is, at $V_{cr} < 30$ cm/s, can be obtained only in microgravity. The dependency of V_f on V_{cr} shows a maximum for all three oxygen concentrations, suggesting that different mechanisms control the rate of spread at low and high V_{cr}. The maxima occur in the range of $V_{cr} = 15$ to 20 cm/s, flow rates attainable only in microgravity. At an atmospheric concentration of 30 percent O_2 (and presumable for greater concentrations), V_f is independent of opposed-flow velocity over a wide range of V_{cr}.

The observed preheating and flame lengths also show maxima with opposed-flow rates, with the maxima occurring over the same flow range as for flame-spread-rate maxima. At low opposed-flow velocities, the flame shows an open tip. This implies that this weak flame is underventilated, i.e., not all of the fuel is consumed; and a substantial char remains after extinction even for the very thin fuel used in these experiments.

Numerical models yield flame-spread-rate trends similar to those observed in experiments, whether they include surface radiative loss alone or gas-phase radiation alone. Thus, radiative loss from the fuel surface or flame can serve to quench the flame and may be the extinction mechanism at the LOI in microgravity. There are interesting differences in the flame structure predicted from the two radiative-loss cases; with gas-phase radiation, the flame is smaller, cooler, and closer to the surface, in good agreement with experimental observations. An implicit assumption in the gas-phase radiation calculations is that the gas-to-surface radiative exchange is exactly balanced by the surface loss to the surroundings. Computations with interacting surface and gas-phase radiative transfer may model the experimental results more accurately, but these are difficult to perform due to unknown and variable optical properties of the surface and gas-phase soot particles.

A sounding rocket experiment, *Diffusive and Radiative Transport in Fires*, currently in flight development, is designed to obtain a better definition of the roles of radiative exchange and oxygen mass transport. Black PMMA samples will be burned in very low-speed oxidizer flows at various external radiant-flux levels. New diagnostics will provide color images of the spreading flame and measure the spatial distributions of unreacted fuel, intermediate radicals in the reaction zone, and combustion products.

An experiment under development for spaceflight, *Radiative Ignition and Transition to Spread*, will investigate the three-dimensional time-dependent flame spread initiated from a small, localized ignited area of thin fuel. This is the first systematic study of pre-combustion phenomena in microgravity. The mechanism of the transition from ignition to flame spread controls the extinction limit of flame spread, and it is affected by flame history starting at ignition.

Opposed Flow in Partial Gravity

Results of past tests conducted over a range of accelerations on a centrifuge indicated that the limiting mechanism for flame spreading in opposed flow (at velocities much larger than the flame-spread rate) is the residence time of the reactants relative to the time for completion of the combustion reactions. This mechanism, quantified in a ratio of residence time to chemical-reaction time, the Damkohler number, successfully correlates flame-spread rates over a wide range of oxygen concentrations, opposed-flow velocities, and pressures for normal- and elevated-acceleration levels.

As noted in a previous section, the residence time of the reactants in the quiescent microgravity environment is long, and combustion reactions drive to completion. Hence, radiative heat loss is thought to control the flame-spread rate and extinction limit. Because it does not account for radiative heat losses, the Damkohler number, as formulated, does not correlate flame-spread behavior in either quiescent or low-speed forced-flow microgravity environments.

Improved understanding of the influence of radiation heat loss and residence times on opposed-flow flame spread and extinction may be gained through partial-gravity experiments (environments at finite gravitational accelerations less than normal gravity). Flame-spreading experiments with thin cellulosic fuels were conducted in partial-gravity environments, ranging from 0.05 to 0.6 g, attained in parabolic-trajectory aircraft. Downward-burning data from these tests were compared to the cited results at elevated-gravity accelerations, and they show a continuity of flame-spread behavior from 0.05 to over 4.0 g (Fig. 23). For the lowest oxygen concentrations, flame-spread rates increase as gravity levels decrease below normal gravity. For 18 percent and 21 percent-O_2 atmospheres, however, flame-spread rates show maxima in partial gravity. This behavior is attributed to a transition between the limiting mechanisms of radiative heat loss and insufficient reaction time (low Damkohler number) induced by the change in buoyancy (acceleration level).

Fig. 24 is a further interpretation of the flammability data taken over a range of accelerations. These data are for purely buoyant flow; i.e., the only opposed-flow velocity is that induced by density differences. As local acceleration levels decrease, the opposed-flow buoyant velocities decrease, but the flammability increases (the oxygen-concentration limits are broader). The dotted flammability boundary in Fig. 24 is a prediction of Chen and Cheng. At sufficiently low accelerations, flammability may reverse and decrease to approach the quiescent microgravity LOI of 21 percent in agreement with data presented earlier (Fig. 18). The experimental results have some practical significance in showing that, in downward burning, these materials may be more flammable in Lunar and Martian gravitational environments than on Earth.

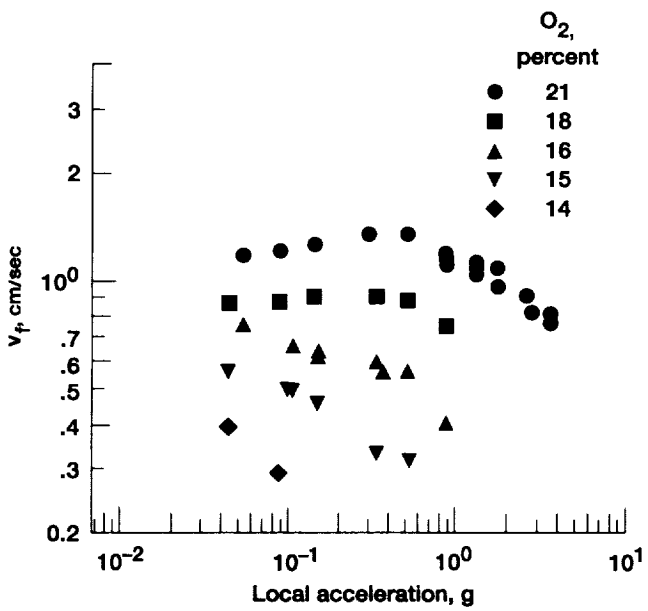

Figure 23.—Experimental downward flame-spread data for thin cellulosic fuels at 101-kPa total pressure over a range of accelerations, including elevated, normal, partial, and low gravity.

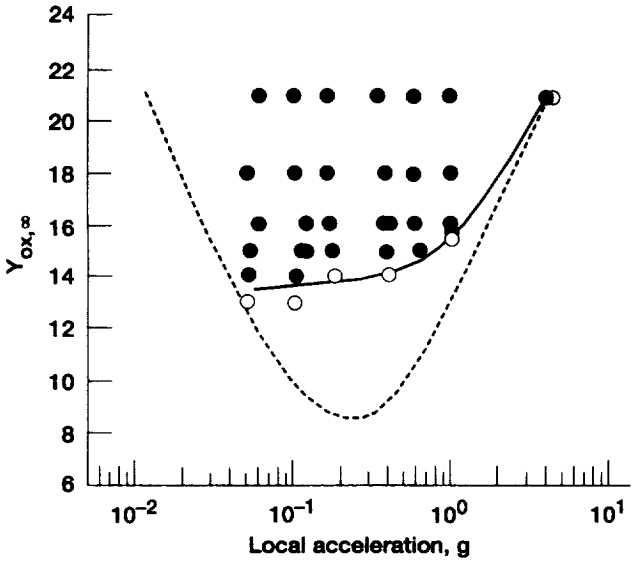

Figure 24.—Experimental flammability map for thin cellulosic fuels at 101-kPa total pressure over a range of local accelerations, with buoyancy-induced flow only. The open symbols are non-ignition points. The dotted curve is a numerical prediction of Chen and Cheng.

Advances in the general correlation of opposed-flow flame-spreading data have been achieved using the partial-gravity data. Traditional correlations of flame spreading compute a

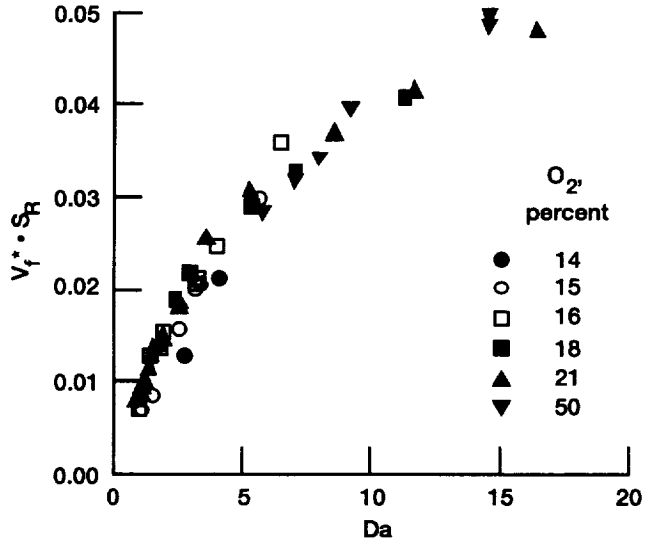

Figure 25.—Dimensionless flame-spread rate correlation for downward burning of thin cellulosic fuels, with the spread rate corrected by a radiation parameter, $S_R = \sigma T_\infty^3/\rho C_p V_r$ The pre-exponential constant in the Damkohler number, Da, is adjusted to make Da = 1 at blow-off extinction.

dimensionless spread velocity by referencing measured values to an ideal based on fast chemical reactions and no heat losses from the flame. These correlations can be improved by the use of an estimate of fuel-surface radiative losses to correct the dimensionless spread velocity. Conceptually, the radiative-loss correction reduces the ideal spread rate in proportion to the fuel-surface radiative emission. Examples of the correlation of a dimensionless spread-rate times the radiation-loss parameter against Damkohler number are shown in Fig. 25 for flame-spread results with varying opposed air flows induced by buoyancy alone in partial- to elevated-gravity environments. This adjusted correlation has the useful attribute of showing a coincidence of blow-off extinction points over a range of conditions from 15 to 21 percent oxygen and 0.16 to 4.25 g.

Concurrent Flow in Microgravity

In normal gravity, flames spreading upward (concurrent with flow direction) over a solid are larger and more energetic than flames spreading downward (opposed to flow direction). Furthermore, the limiting-oxygen index for upward spread is lower than for downward spread. The stabilization point for flames spreading in either configuration occurs at the flame base, where the flame first encounters fresh oxidizer. However, the flame-spread mechanisms are quite different. For downward-spreading flames, the heat transfer ahead of the flame is opposed by the continual stream of fresh, cool oxidizer being drawn into the flame zone. The spread rate is the speed at which this stabilization point creeps down the fuel. In upward-spreading flames, on the other hand, the spread rate (i.e., the rate of

spread of the top of the flame) depends on the overall size of the flame and does not, in general, depend on the rate of spread of the stabilization point. Upward-spreading fires are larger and more hazardous because of the heating potential of the entire flame and thermal plume, which bathe the fuel. The fuel is vaporized more rapidly, heightening the flame and further increasing the rate of heat release. Additionally, upward-spreading fires in normal gravity are accelerating. This unsteadiness causes additional complexity in the modeling effort and in the experimental quantification of this important fire scenario.

Low-gravity experiments are beneficial to the understanding of concurrent-flow flame spread for two reasons. The first reason is to gain information on the fundamental aspects of the problem without the complicating effects of a large buoyant flow. The lower-speed conditions may also inhibit turbulence, simplifying the analysis. The second reason is to acquire realistic experimental data on material flammability behavior to address spacecraft fire-safety concerns. Specifically, a method of correlating the low-gravity flammability of a material to results of normal-gravity testing can identify those materials that pose a fire hazard in space without limiting the variety of materials available for operations on-board spacecraft.

Experiments were performed in the NASA Lewis 5.2-Sec Zero Gravity Facility, where thin rectangular tissue samples were moved through a quiescent chamber to produce a uniform, low-speed concurrent flow past the fuel. Typical flame appearance and temperature profiles are shown in Fig. 26 (color). These drop-tower tests provide an assessment of the effect of different ignition techniques on the approach to a possible steady state.

Analytical models were developed to solve the full Navier-Stokes equations in steady, two-dimensional form, with a one-step, second-order Arrhenius expression to represent the chemical reaction. Model results suggest that a steady state is possible in concurrent-flow flames in microgravity, where the rate of fuel burnout equals the flame-tip spread rate. In the time available in the drop tower (5.2 sec), however, the flames did not reach steady state – they were either growing or shrinking. In Fig. 27, the model results show the effect of radiation on flame shape and temperature. When gas-phase radiation is included, the model leads to shorter, slower-spreading flames that are more in concert with the experimental findings.

A Glovebox experiment, the *Forced Flow Flamespreading Test*, is under development for flight aboard the Russian MIR space station in late 1995 and the Shuttle USML-3 in early 1996. This experiment will provide observations on the effect of low-speed flows and bulk fuel temperature on the ignition, flammability, flame growth, and flame spread of thin solid fuels in a forced-flow microgravity environment. In particular, the experiment will seek observations of the transient and steady-state flame sizes and spread rates, for comparison with modeling results.

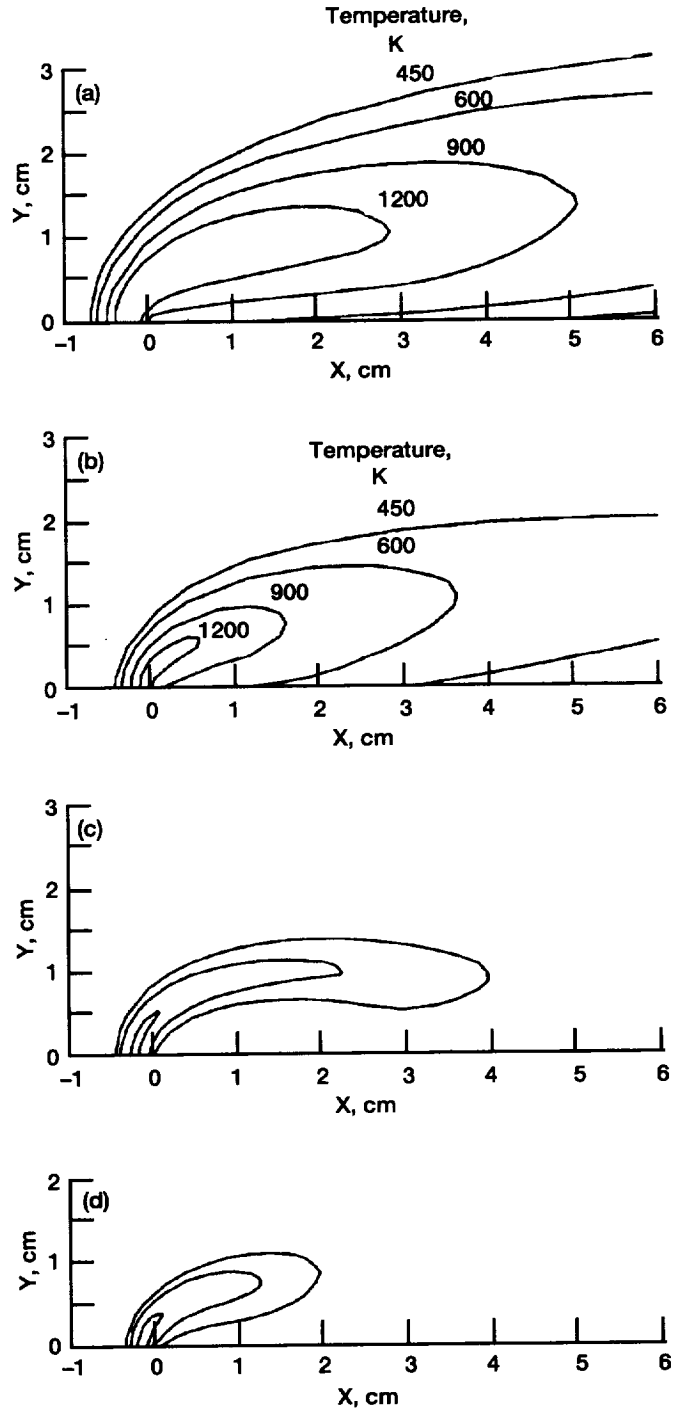

Figure 27.—Calculated contours for flame spread over thin solid fuels in 15% oxygen/nitrogen, 101-kPa total pressure, microgravity environment, with concurrent flow of 6 cm/sec from left to right. Flame-spread rate is 0.42 cm/sec without gas-phase radiation; 0.38 cm/sec with gas phase radiation. The visible flame appearance is shown by fuel consumption-rate contours. (a) Isotherms without gas-phase radiation. (b) Isotherms with gas-phase radiation. (c) Visible flame appearance without gas-phase radiation. (d) Visible flame appearance with gas-phase radiation.

Metal Combustion

Metals generally have high boiling temperatures and heats of combustion. Their oxide products also have high boiling temperatures. Hence, while some metals burn in the vapor phase similar to conventional organic fuels, many metals burn in the solid or liquid phases. For metals burning in the liquid phase (iron for example), the predominant gravity-induced motion is downward, i.e., dripping or sedimentation. This is in contrast to the upward buoyant motion of combustion products in vapor-phase combustion. It is reasonable to expect that the suppression of sedimentation in a microgravity environment will strongly influence the physical characteristics of metal combustion.

To date, experimental studies on metal combustion in microgravity have been conducted only in small-scale, ground-based facilities. Representative tests conducted on metal rods ignited at the bottom, in a 100 percent-O_2 atmosphere over a pressure range from 0.1 to 6.9 MPa, show that the solid regression rate, used as an indication of flame spread, increases with increasing pressure and with decreasing fuel diameter. In this configuration, the melting fuel forms a spherical ball adhering to the unburned metal with an elliptical attachment area. Specific data for iron combustion show that the regression rate is 2 to 3 times more rapid in microgravity than in normal gravity. In addition, certain metals, such as copper, nickel, and stainless steel alloys, that are very difficult to ignite in normal gravity burn completely in microgravity.

Short-duration, low-gravity experiments are underway to determine temperature histories, surface morphology, and combustion-product analyses for metal combustion initiated by non-disturbing radiant heating rather than by the usual promoted ignition.

Combustion Synthesis of Materials

Advanced ceramic and composite materials can offer properties superior to those of conventional materials, such as higher strength, lower weight and improved high-temperature durability. Combustion synthesis, or self-propagating high-temperature synthesis (SHS), invented in Russia in the late 1960's, is an alternative to conventional methods for producing advanced ceramics and composites. The energy efficiency of the SHS process is based on the ability of highly exothermic reactions to be self-sustaining. The reactant mixture, normally in the form of powders, is pressed into a pellet and ignited either at a single point (propagating mode) or overall by heating the whole pellet (simultaneous combustion mode).

One of the main difficulties in combustion synthesis is the control of porosity and the microstructure of the products. The generation of volatile components during the process causes porosity. The residual pores may be filled by a liquid phase, which is the result of the melting of some of the components. SHS reactions generating gaseous, liquid, or combined phases are prone to gravity-induced fluid flows, which may cause non-uniform microstructure and undesirable properties of the product material from the segregation and density gradients. Hence, an improved understanding of the effect of gravity on the combustion synthesis of ceramic matrix-metal infiltrated composites is very important for process and material-property improvement.

A ceramic-aluminum composite system was selected for studying the role of gravity on the liquid phases generated in SHS reactions. The typical ignition temperature for this reaction is in the range of 800 to 900 °C. Aluminum melts at 600 °C. Therefore, there is a strong possibility of gravity-driven flow of the liquid aluminum, causing reactant segregation prior to ignition. Furthermore, since the typical combustion temperature is in the range of 2250 to 2300 °C, the products, consisting of excess liquid aluminum and liquid Al_2O_3 (melting point 2050 °C), will also be subject to gravity-driven flow and segregation in the product phase. Demonstrations of the ceramic-aluminum synthesis in low-gravity airplane tests produced ceramic-metal composites with more uniform distribution of phases and porosity than those produced under normal-gravity conditions.

A similar set of experiments with B_2O_3 as a reactant (melting point 450 °C, boiling point 1860 °C) produced a large volume of high-pressure B_2O_3 gas ahead of the propagating reaction front. This resulted in an expanded or "foamed" ceramic showing volume expansions of the order of 200 percent in normal gravity, 300 percent in low gravity (airplane) and 150 percent in elevated gravity (airplane "pull-up" environment). The addition of Al_2O_3 as a diluent to this reaction reduces the combustion temperature, increasing the degree of porosity and, therefore, the internal surface area of these materials.

Other tests investigated similar reactions that produce higher combustion temperatures, exceeding 2400 °C, and incorporate both aluminum and B_2O_3 as reactants. These reactions produce Al_2O_3-rich whiskers in either normal- or low-gravity conditions. The morphology of the whiskers depends on the gravitational forces. The 10- to 50-mm-long synthesized whiskers are approximately 1 to 5 mm in diameter in normal gravity but approximately 0.1 mm in diameter in low gravity.

These examples indicate that gravitational forces play a dominant role in controlling both the combustion-synthesis reactions and the morphologies of the synthesis products. Current research is geared towards interpreting the differences between normal- and low-gravity processing. In general, gravity will influence the SHS reactions when there is a considerable density difference between reactants, intermediates, or products, when a volatile gas is generated at the reaction front, or when loadings of reinforcing whiskers are high enough. Experimental mechanistic studies have covered investigations

of the key parameters influencing the product morphology and microstructure. These include the reactant density and porosity, initial particle-size distribution, presence of inert diluents in the reactant mixture, initial temperature of the reactants, and method of ignition.

Another approach to improve the understanding of SHS mechanisms is to isolate the various steps involved. To that end, reactant mixtures can be configured in preferred geometries amenable to analysis. For example, aluminum particles clad with an outer layer of nickel are being used to understand the synthesis of NiAl and Ni_3Al. In this case, the lower melting aluminum diffuses radially outward into the nickel layer. Such a process is easier to model and understand than the more standard geometry, in which aluminum melts, flows through the capillaries of a porous Ni/Al pellet, and then diffuses into the nickel particles.

The role of gravity in influencing SHS mechanisms is also being modeled analytically. The goal of an initial analysis is to describe the synthesis of porous condensed materials in which a reactant melts and spreads through the pores of the sample. Both analytical and numerical methods are employed to define uniformly propagating combustion waves, to assess their stability, and to determine behavior in the instability region. The principal physical conclusion from this analysis is that the flow of the melted component can result in non-uniform composition of the product. Unlike models that do not take into account the relative motion of the components, this model demonstrates the dependence of the structure of the product on the mode of propagation of the combustion front and, thus, allows for the evolution to non-uniform structure even if the initial mixture is uniform. The model can derive the pulsating instabilities in the propagating combustion waves that depend on the excess component, refractory or melt, in the initial mixture.

Diagnostic Instrumentation

Significant scientific returns from microgravity combustion-science experiments depend to a great extent on diagnostic systems that can endure the unique and severe operational constraints of microgravity experimentation. Instrumentation in early studies was limited to conventional film-based imaging systems and intrusive temperature and velocity probes, such as thermocouples and hot-wire anemometers.

Advances in diagnostic systems for microgravity experimentation have emphasized optical techniques predominantly. This is because optical measurement techniques are non-perturbing and, in general, well suited to the acquisition of multi-dimensional data fields. The latter quality is very important since a clearer understanding of basic phenomenology, including the verification of fundamental length and time scales and dominating physical mechanisms, is an essential need in microgravity studies. In concert with other aspects of microgravity experimentation, the development of diagnostic instrumentation proceeds from basic requirements of the normal-gravity laboratory through those of ground-based facilities to those of spacecraft accommodations.

Flame Image

Qualitative visualization has long been acknowledged as an important element in the understanding of combustion phenomena. It is an essential aid in the interpretation of single-point temperature, species-concentration, and velocity measurements and in the assessment of the time and length scales of processes occurring in the flow field. In microgravity combustion science, the need for low-light-level visualization is particularly strong, since many phenomena of interest are found near the limits of flammability, ignition, or stability and are subsequently too dim to be visualized by conventional means.

Solid-state, charge-coupled-device (CCD) cameras with microchannel plate intensifiers are being used to image flames that are below the sensitivity range of conventional detectors or photographic films. The intensifier, in essence, amplifies the incoming light, thereby increasing the detector sensitivity by as much as four orders of magnitude. This increased sensitivity permits the use of narrow-bandwidth spectral filters to isolate emissions from species or to mask the effect of more luminous regions, such as black-body radiation from soot. The use of the intensified array camera in low-gravity airplane tests revealed heretofore unseen flame structures in premixed hydrogen/air combustion and the nature of weakly luminous flames spreading over paper and plastic fuels.

Infrared-imaging cameras have recently become available for the near- and mid-infrared wavelength bands. The cameras permit the visualization of weak flames in the presence of emissions from hot combustion products such as water, carbon dioxide, and soot. For example, infrared images of burning plastic were obtained in low-gravity airplane experiments to identify the spatial extent of fuel and product spread. Likewise, infrared images of liquid-surface temperatures were obtained in a microgravity sounding-rocket experiment.

A more thorough characterization of combustion in the infrared spectrum may enable, in certain cases, the determination of major species concentrations and temperature. An imaging spectrometer capable of resolving water and carbon dioxide emission bands has been designed and is being constructed. This instrument, in conjunction with analysis software, will provide both spatially- and spectrally-resolved images.

Knowledge of the position of the flame reaction zone is important for comparison to computer models, but imaging of the natural flame luminosity gives only a spatially-integrated view of the entire flame. Non-intrusive measurements of species, such as the OH radical, are desirable for their ability to image the reaction zone. Detection of CH radicals using a

solid-state titanium:sapphire laser was demonstrated in the laboratory. Such a device minimizes the problems of dyes and corrosive gases associated with other laser sources, although the latter have other applications. Imaging of single-droplet combustion using species deliberately seeded in the fuel and a small pulsed nitrogen-dye laser system was demonstrated in low-gravity aircraft tests.

Refractive Index

The determination of refractive-index fields has long been used for both qualitative visualization and quantitative measurements of temperature distributions of combustion reactions or species-concentration distributions of non-reacting flows. Interferometric methods are often used for this purpose, but they are not ideally suited for microgravity combustion-science applications, principally because of their strict requirements for mechanical stability. In contrast, deflectometric methods (i.e., methods that measure the bending of light rays due to non-uniformities in refractive index) are considerably less complex, more tolerant of mechanical and thermal fluctuations, and adaptable to large fields of view.

The system that has been developed at the NASA Lewis Research Center is based on the use of continuously graded color filters. A collimated, broad-band light source is used to illuminate the test section. After passing through the combustion field of interest, the decollimated output is focused onto a filter possessing a spatially dependent color-transmission function. Changes in the refractive-index distribution due to changes in temperature or species concentrations cause the incoming light rays to bend, thus altering the position in which they pass through the color filter. The distribution of hues manifest in the qualitative appearance of the resulting images affords great detail, owing to the ability of the eye to resolve subtle differences in color. The continuous nature of the "rainbow" filter also provides improved spatial resolution relative to conventional knife-edge methods. A simple image-digitizing and processing system has been developed to quantify the color attributes of the observed image and, hence, the ray deflections that produced it. Once quantified, these ray deflections can, in turn, be related to the aforementioned physical quantities of interest. This approach has been demonstrated to provide a measurement sensitivity that is comparable to that achievable using interferometric techniques. Systems of this type have been used in the laboratory to measure refractive-index distributions in heated liquid pools and in axially symmetric jet-diffusion flames (Fig. 28 color). They have also been constructed for use in the NASA Lewis drop towers, aircraft, and sounding rockets.

Soot Volume Fraction

For decades, soot volume fractions in combustion applications were determined through optical extinction methods. Current techniques benefit from the use of coherent, monochromatic sources (lasers). These sources offer advantages of well defined spectral characteristics, critical to the resolution of the spectrally dependent properties of carbonaceous soot, and precise optical-beam manipulation. Two methods under development for microgravity combustion-science applications at NASA Lewis are those of extinction tomography and laser-induced incandescence.

The application of the principles of tomography to two-dimensional optical-extinction measurements can replace conventional, time-consuming sequential point imaging that is unsuitable for short-term microgravity tests. In a single scan, extinction tomography provides a full-field absorbance at video framing rates. Fig. 29 shows examples of soot volume-fraction maps obtained through this method. The contour surfaces of soot volume fraction in the upper sketches are projected to form two-dimensional maps of soot volume fraction in the lower sketches. For the laminar acetylene/nitrogen jet-diffusion flames in microgravity, the soot volume fractions are higher and extend farther spatially, compared to those in normal gravity. Soot particles escape from the tip of the flame in microgravity, but they are confined to the non-luminous flame in normal gravity.

Laser-induced incandescence (LII) uses an intense source energy to heat soot to temperatures far above the background. For sub-microsecond laser pulses, consideration of relative magnitudes shows that the energy-addition rate greatly exceeds the loss rate from thermal conduction, vaporization, or radiation. Laser intensities of 10^7 W/cm^2 or greater rapidly heat soot particles to the vaporization temperature, roughly 4000 K. In accordance with the Planck radiation law, the particle thermal emission at these elevated temperatures increases and shifts to the blue compared to non-heated soot and flame gases. The resultant blue-shifted emission from the laser-heated soot is predicted theoretically to be a function of soot volume fraction, and measurements show that the LII signal is linearly proportional to the soot volume fraction. Absolute calibration of the technique is made by *in situ* comparison of the LII signal to a system with a known soot volume fraction. Point measurements use a photomultiplier tube with spectral and temporal discrimination against natural flame luminosity. One- and two-dimensional measurements use a gated intensified-array camera.

Knowledge of the soot volume fraction and spatial distribution is central to several types of combustion phenomena. Formation of a soot shell around isolated burning droplets controls the radiative heat transfer from the flame back to the droplet and the burning rate of the fuel droplet. As an illustration, Fig. 30 is a temporal sequence of images from a burning fuel droplet of decane, where each image is separated by 300 msec. The first image, Fig. 30(a), is natural flame luminosity obtained ~280 msec after ignition, while Figs. 30(b) to (f) are LII images. The ruler superimposed on Figs. 30(e) and 30(f) was placed in the LII object plane prior to combustion. The optical fiber bead that supports the droplet appears as a small white spot due to glare.

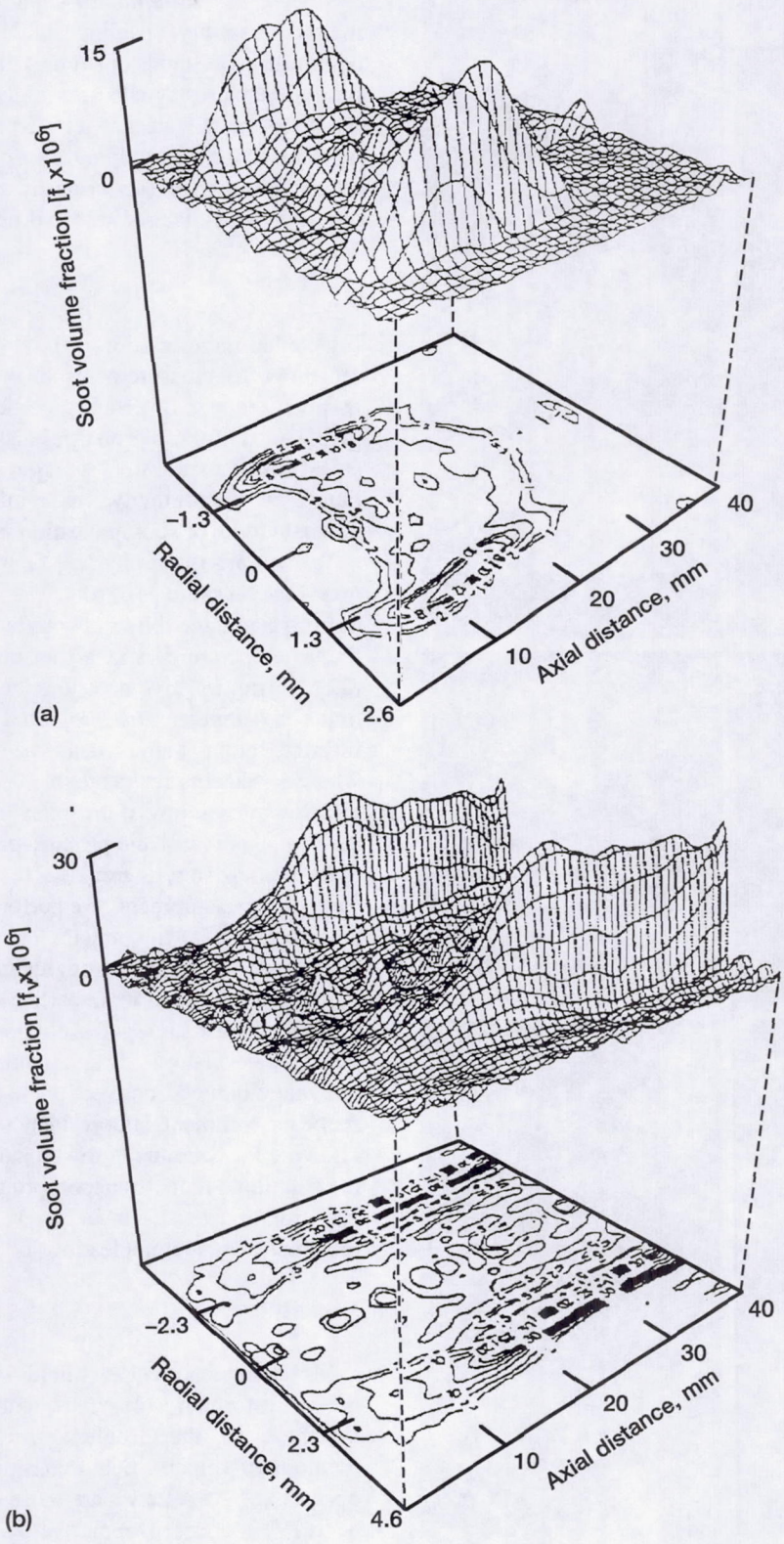

Figure 29.—Soot volume-fraction contours obtained by extinction tomography for 50% acetylene/nitrogen jet diffusion flames in air. (a) Normal gravity. (b) Microgravity.

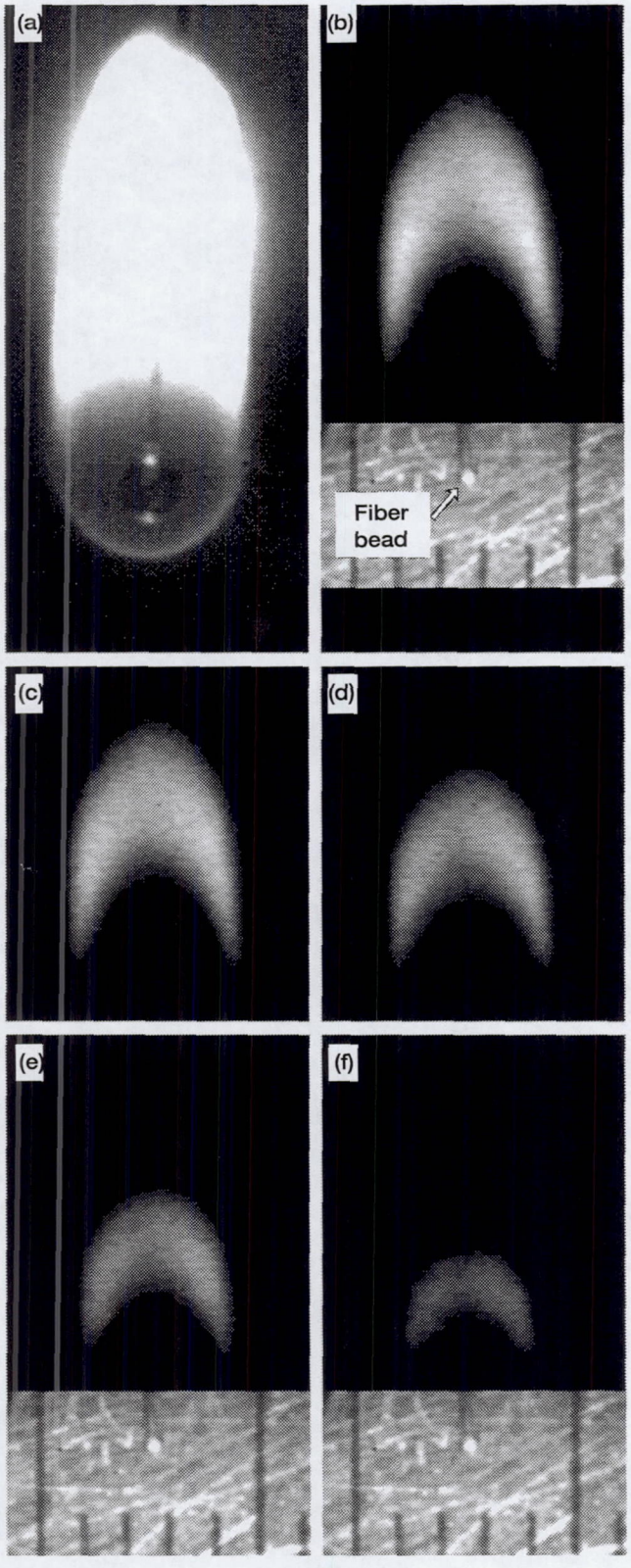

Figure 30.—Images of a burning droplet of decane. (a) 280 sec after ignition, by natural luminosity. (b) to (f) Subsequent flames, in time-related sequences, 300 ms apart, by laser-induced incandescence (LII).

Since LII is not a line-of-sight technique, it possesses geometric versatility enabling studies involving heterogeneous combustion of liquids or solids. LII also has high temporal resolution because signals are induced by a single laser pulse. Even in steady-state gas-jet diffusion flames, LII provides a measure of the soot volume fraction, independent of unknown contributions from scattering by soot aggregates and absorption by polycyclic aromatic hydrocarbons.

Soot Size

Detailed interpretation of laser-induced incandescence and other optical measurements of soot depends upon both the number and size of primary particles composing soot aggregates. Each of these properties also affects the radiative emission from flames, often a major energy-loss mechanism for flames in microgravity. Such information also aids in the understanding of soot nucleation and aggregation processes.

To measure these physical features of soot accurately, one must recover samples of soot. The technique of thermophoretic sampling utilizes the temperature difference between soot at flame temperatures and a transmission electron microscopy (TEM) grid, to drive soot to adhere to the grid. In this technique, a sampling grid supported by a thin probe is rapidly inserted into a flame via air-actuated pneumatic cylinders, where it remains resident for 10 to 500 msec. Transmission electron microscopy of the recovered grids is used to visualize the soot aggregates and primary particles and quantify the primary-particle size, aggregate size, and fractal character. These sampling measurements are performed in both normal gravity and microgravity to compare and contrast differences in soot primary-particle size and aggregate dimensions.

Fig. 13, presented in an earlier section, shows TEM micrographs of soot aggregates obtained from ethylene diffusion flames in normal gravity and in microgravity. In the absence of buoyancy-induced convection to remove the soot from the flame environment, soot residence times are greatly extended, allowing for continued growth and aggregation processes. For the simplified flame-transport processes in microgravity, interpretation of data such as in Fig. 13 can serve as input to model the kinetics of soot nucleation and growth processes in flames.

Velocity

Measurement of velocity fields in flows with combustion can provide information on such quantities as residence time, mixing rates, and the turbulent structure of the flow field. Two methods of velocity-field determination under current development at NASA Lewis are those of particle-image velocimetry (PIV) and laser Doppler velocimetry (LDV).

PIV measures velocity fields by seeding the flow with particles and then illuminating the flow using a light sheet a few hundred micrometers thick and several centimeters wide. When the flow field is imaged normal to the light sheet, the

position of the particles as a function of time may be recorded using either film or a CCD camera. These images may then be computer analyzed using the particle-displacement-tracking algorithms developed at NASA Lewis to calculate velocity vectors across the field of view.

Because of the low velocities of the non-buoyant flows studied in microgravity, it is challenging to develop an entrainment method for the seed particles in the flow field. In the low-flow environment, cyclonic seeders that inject gas orthogonal to the flow out of the burner tend not to entrain particles. Therefore, a turbulent chamber with an inlet parallel to the axis of the burner has proven to be the most useful method of entraining particles. The seed chamber used at NASA Lewis has a gas-inlet diameter of 0.1 mm. For a propane-burner diameter of 1.65 mm, for example, the non-buoyant mass flow rates require an exit velocity of 30 cm/s to achieve a Reynolds number of 2000 for self-stirring turbulent flow. If the seeding particles flow well, the result is a system that dispenses particles at a constant rate over long periods of time.

LDV measures velocity fields by interpretation of scattered-light signals from small seed particles entrained in the flow field. The velocity of the seed particles causes this scattered light to be Doppler-shifted; by measuring the frequency of this shift, it is possible to determine the velocity of the particles. Since the technique can determine the velocity in approximately 100 μsec per particle, implementation of line or area scans on time scales that are small in comparison to the temporal evolution of the flow field is possible. In addition, the ability to perform extremely rapid, single-point velocity measurements makes it possible to measure velocity fluctuations and construct a temporal turbulence spectrum.

Current operating LDV systems are large and consume relatively large amounts of power, which is a result of the coherent laser sources and sensitive photodetectors required to perform these measurements. Recent advances in solid-state laser diode and avalanche-photodiode detector technologies offer LDV systems that are quite compact and require only a few watts of electrical power. Optical transmitter/receiver modules of this type are currently being tested in the laboratory, and provisions are being made for their employment in the various microgravity facilities. One of these devices is illustrated in Fig. 31.

Advanced LDV systems are the types commonly referred to as dual Doppler, heterodyne, or fringe anemometers. This arrangement is predicated on the heterodyning of the scattered signal from two probe beams, the intersection of which defines the optical measurement volume. The dual-beam arrangement results in a detected signal whose frequency is proportional to

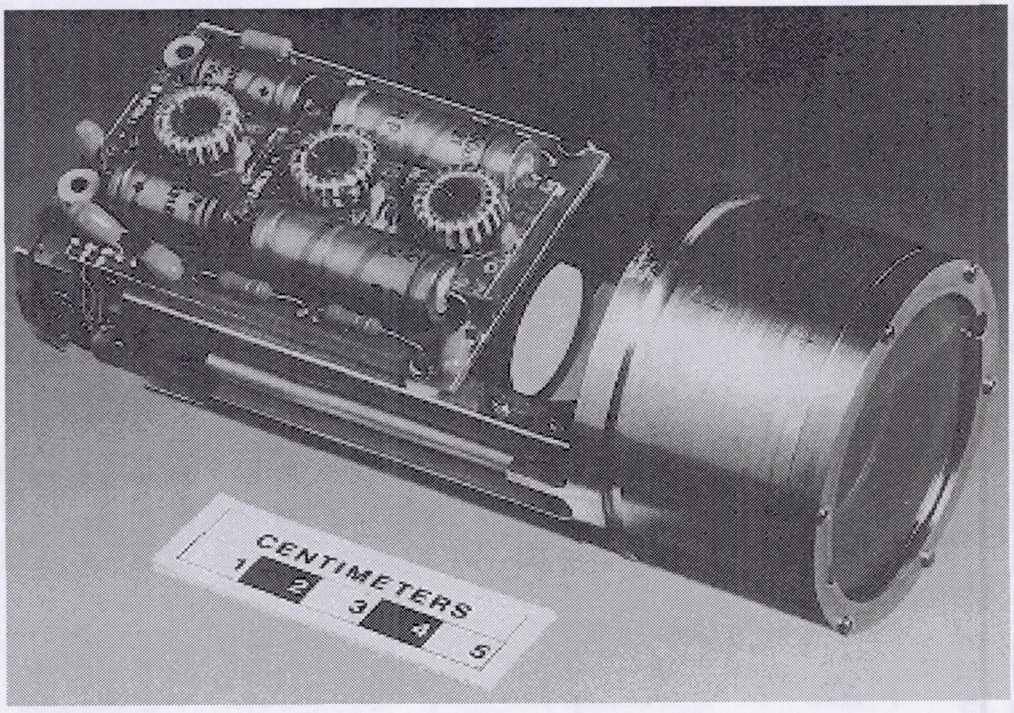

Figure 31.—Compact laser Doppler velocimeter (LDV) unit.

the particle velocity, simplifying what would otherwise be the requirement for measuring a shift that is extremely small relative to the optical frequency of the probe beams. The transverse dimension of the measurement volume for laser diodes operating in the range of 780 nm is of the order of 100 μm. This is somewhat larger than that provided by more conventional LDV optics. Fringe spacings at the beam intersection region are 3 to 4 μm, thus requiring the seed particles to be smaller than this dimension. Work is currently in progress to develop seeding systems that are not predicated on packed or fluidized beds, since arrangements of this type are problematic for implementation under microgravity conditions.

Dedicated signal processing (DSP) methods are used to manipulate the high-rate data, with near-real-time estimation, display, and archiving of the Doppler-burst frequencies. Advances in DSP capabilities have resulted in signal processors of increased sophistication, enabling data acquisition and frequency estimation to be performed at higher rates and to greater accuracy.

Temperature

Conventional methods for the determination of temperatures, such as thermocouples and broad-band point radiometers, are being augmented by non-intrusive optical methods of greater versatility. These techniques fall into three distinct classes: emission measurements, implicit methods, and spectral methods.

Emission pyrometry represents an advance over broad-band, point radiometric measurements. One-dimensional line measurements have been implemented by introducing thin (15 μm) silicon carbide fibers into the flame front. These fibers provide several advantageous features, such as well characterized emissivity and precise spatial location of the measurement volume. Their small size provides rapid temporal response, while minimally perturbing the phenomena under study. An array of fibers can be constructed to yield two-dimensional temperature data; the fibers are imaged using conventional CCD cameras or staring infrared arrays, depending on the temperature range and other spectral interferences that may be present. Imaging pyrometry can also be performed on naturally occurring soot particles. In a system under development for a Shuttle experiment, a two-wavelength ratio measurement in the visible spectrum is used to simplify assumptions about the spectral dependence of the emissivity from soot.

Implicit measurements of temperature are based on gas density or refractive index. Gas density uses elastic Rayleigh scattering. Under isobaric conditions, the proportional relationship of the scattered intensity to the local gas-phase temperature can be exploited to infer temperature. Relatively strong Rayleigh scattering cross-sections enable multi-dimensional imaging experiments to be performed using a planar illumination geometry. Refractive-index measurements are currently made by rainbow schlieren (continuous-color filtering), described in a previous section. The line-of-sight nature of this technique relegates quantitative application to systems possessing simple symmetric geometries.

Spectral methods encompass a number of approaches. In one such application, a tunable, pulsed titanium:sapphire laser is used to determine temperature via laser-induced fluorescence (LIF). LIF is utilized in this context by scanning the laser over several rotational transitions originating from different rotational levels having temperature-dependent populations. Rotational-temperature measurements are also being implemented in the form of a line-of-sight absorption technique. In this case, a near-IR solid-state laser diode is rapidly scanned over a pair of absorption lines exhibiting well-characterized temperature dependence. Liquid-phase thermometry also uses fluorescence of a dopant introduced into the liquid. Ultraviolet light from a small nitrogen laser is used to excite the ground-state molecules of the dopant to their excited state. These excited-state molecules may react with a partner molecule to form an *excited* state com*plex* (exciplex). The exciplex fluorescence is red-shifted relative to that of the dopant monomer. Under controlled conditions, one can calibrate the ratio of fluorescence intensities to ascertain the dependence on temperature.

Chemical Species

Chemical-species determination in microgravity flames is a necessary part of understanding the complex interactions between chemical reaction, heat transfer, and mass transfer. These measurements present some interesting challenges. Chemical-species identification is usually accomplished by physical sampling, which may not accurately represent the sampled system and generally provides no spatial or temporal information. Spectroscopic methods are superior for combustion research. Mass spectrometry and gas chromatography have been used in ground-based studies, and compact versions of these devices are available or under development for use in flight experiments. Most spectroscopic measurements are based on infrared absorption. A portable laser-diode absorption spectrometer has been developed for NASA Lewis under the Small Business Innovative Research program. The principal limitation of the very sensitive spectrometer is the need for a different laser source for each species. Fourier Transform Infrared (FTIR) spectroscopy is capable of multi-species sampling, but the current generation of instruments is not readily applied to microgravity platforms.

For identification of oxidizer species, other techniques under development use absorption spectroscopy with ultraviolet and diode-laser light sources. Raman spectroscopy can supplement this information and yield temperature measurements as well. Locating the fuel and oxidizer in the flame is feasible using planar imaging techniques. Fuel location can be imaged by adding a fluorescent-tracer species, whose volatility and burning characteristics are matched to the fuel. Oxygen location can be imaged directly by self-fluorescence, using the same ultraviolet light sources used for absorption.

Spacecraft Fire Safety

Although current spacecraft fire protection may be adequate, the application of microgravity combustion knowledge to fire safety merits considerable attention in order to optimize components and operations in current spacecraft and to acquire improved and innovative techniques for the future long-duration International Space Station Alpha (ISSA).

Current Spacecraft Practices and Policies

The strategy of spacecraft fire safety is influenced by the type of mission. For short-duration missions, the Shuttle for example, prevention is the primary emphasis. If a fire event of any consequence occurs, the mission can be terminated and the spacecraft returned to Earth for ground inspection, cleanup, and repairs, as necessary.

For long-duration, near-permanent missions, the ISSA for example, prevention is still emphasized, but its enforcement becomes more difficult. A greater quantity of waivered materials and wastes may accumulate, and there is a higher probability of breakdowns and ignitions. The secondary protection of detection and suppression becomes more important. While the emergency rescue of the crew is feasible, risk-mitigation planning aims to limit the worst-case scenario to that of minimum damage threatening neither the crew nor the mission integrity. In contrast to the short-duration-mission recovery option, ISSA operations, including "post-incident" inspection, cleanup, and repair activities, must be performed in orbit, using available stores.

Automated fire detection in spacecraft is by means of smoke detectors using the principles of ionization-current interruption (the Shuttle) or light-beam obscuration and scattering (the ISSA). The selection of the light-beam (photoelectric) type for the ISSA is because of size and energy-consumption advantages rather than performance superiority. Normal-gravity smoke-chamber tests have established detector sensitivities and response times, but corresponding performance in microgravity has never been demonstrated.

Primary fire suppression in the Shuttle is by means of Halon 1301 fire extinguishers. Although the manufacture of Halon 1301, a stratospheric ozone-layer depleter, is now prohibited by international protocol, existing suppression systems may be retained. Halon 1301 is a very efficient extinguishant for many types of incipient and flaming fires, and its possible toxic and corrosive by-products can be removed during post-mission ground cleanup. The Shuttle fire extinguishers are supplemented by a fixed, remotely operated system for suppression during critical periods, such as reentry, when the mobility of the crew is limited.

For the ISSA, carbon dioxide is proposed as the agent to avoid the availability and cleanup difficulties of Halon 1301. To conserve mass and power, no central fixed system is planned. Portable fire extinguishers, along with breathing masks, will be available at accessible locations in each module. Certain operating systems and experiments may very likely require the installation of fixed individual suppression bottles for remotely operated extinguishment. The spatial and cost penalties of this added protection may be charged to the "payload" users.

Issues and Needs

The key opportunities for further microgravity combustion studies relevant to spacecraft fire safety are:

(1) the correlation of material flammability in microgravity to results of normal-gravity testing for practical, realistic acceptance criteria,

(2) the evaluation of early-warning techniques for fire precursors based on their detectable characteristics,

(3) the development of centralized and multiple-sensor systems for efficient and optimized fire detection,

(4) the determination of the effectiveness, response time, and physical dispersion of extinguishers,

(5) the evaluation of continuous monitoring of atmospheric contaminants for fire warning and environmental control,

(6) the establishment of quantitative risk assessments and numerical fire-field models to predict fire-precursor scenarios, ventilation patterns, optimum detection and suppression locations, and escape routes, and

(7) the development of techniques for post-fire cleanup of combustion and extinguishment products from the atmosphere and surfaces.

Status of Projects

A project evaluating the NASA material flammability-test methods provided two important recommendations. First, the NASA upward-flammability test may be made more sensitive and more representative of precursor fire conditions by preheating the samples. Second, the heat-release test methods may be adopted as alternatives to the NASA pass-fail flame-spread test. Heat-release data provide commonality with recognized aircraft standards for material acceptance, and heat release is a material characteristic often predictable from thermal and transport properties. The most important deficiency in material-flammability assessments, however, is the lack of microgravity flammability data, no matter how limited, for correlation to normal-gravity test results.

A probabilistic risk-assessment modeling and ground-based experiment provided several important results. First, statistical risk methods established the probabilities of scenarios consistent with Shuttle experience, i.e., electrical-wiring overloads. Second, analytical models calculated heat release, mass-burning rate, and smoke and gas evolution for the defined scenarios and more generalized conditions. Third, data from short-term (2.2-sec) microgravity and reference normal-gravity experi-

ments provided preliminary information on the consequences of the scenarios. Results established that overloaded wire insulations readily ignite and pyrolyze in microgravity, but the physical behavior of the pyrolyzing insulation and the soot and gaseous-product evolution differs from that in normal gravity.

Two new spacecraft fire-safety projects were recently initiated. The *Wire Insulation Flammability* experiment was conducted June 1992 on a Shuttle Glovebox accommodation to measure the flame-spread rates of polyethylene wire insulations with directional air flows. The wire samples were preheated electrically and then ignited at one end by an external hot-wire coil. Several interesting observations and conclusions came from the experiment, which have relevance to wire overloads as potential spacecraft fire scenarios. The spreading flame stabilizes around a spherical or ellipsoidal globule of molten insulation adhering to the wire (Fig. 32 color). Air-flow direction affects the microgravity flame-spread rate and particle evolution. The flame-spread rate is about 2-times greater with air flow concurrent to the flame spread than with air flow opposed. On the other hand, the rate is about 1.5-times greater in downward-flow normal-gravity than in concurrent-flow microgravity conditions. The mean soot-particle diameter is greater in microgravity than in normal gravity, by a factor of two for concurrent flow and three for opposed flow.

The second project is a test of spacecraft smoke detectors in the *Comparative Soot Diagnostics* experiment, which is scheduled for a Glovebox accommodation on the Shuttle in early 1996. The overall experiment will measure the near-field soot-particle generation and agglomeration from representative fuels, including an overheated space-rated wire and ignited flight-data paper. Two smoke detectors (a Shuttle model and an ISSA prototype) will be mounted in a downstream duct to determine the sensitivity and response time of the sensors with respect to the progress of the model fires and their smoke emissions. Spacecraft smoke detectors have never before been evaluated in microgravity, and the lack of correspondence between normal-gravity and microgravity soot evolution and morphology makes it impossible to predict the response and alarm set-point of detectors for efficient and optimum employment in spacecraft service.

Program Participation

Ground-Based and Spaceflight Opportunities

NASA provides financial and facility support to Principal Investigators (P.I.) in the field of microgravity combustion science. Initial proposals for definition studies and subsequent pro-gress are evaluated by the peer-review process, which addres-ses the following types of questions:

(1) Is there a clear need for microgravity experimentation, particularly space-based experimentation?

(2) Is the effort likely to result in a significant advancement to the state of understanding?

(3) Is the scientific problem being examined of sufficient intrinsic interest or practical application?

(4) Is the conceptual design and technology required to conduct the experiment sufficiently developed to ensure a high probability of success?

Principal Investigators collaborate with a NASA technical monitor to conduct the necessary research associated with the initial proposals. Preliminary testing in the NASA Lewis ground-based facilities (drop towers and aircraft) is strongly encouraged in the "definition-study" phase. If it is believed that, following the definition study, spaceflight experiments are justified, the P.I. proposes a Shuttle flight experiment through a competitive solicitation (described below). If the P.I. wins a project award through this solicitation, the project becomes a flight candidate. Soon thereafter, the P.I. presents her or his detailed objectives, test requirements, and a conceptual design to another independent peer-review panel of scientists and engineers, who assess the likelihood of the proposed flight experiment to meet its objectives. If this "Science Concept Review" is successful, NASA assigns a team of engineers and scientists to the multi-year development of space-flight hardware to meet the specifications of the P.I.. NASA continues to support the P.I. throughout this development period in conducting further research, providing consultation, and guiding the design and safety reviews prior to space flight. The nominal time frame from flight-experiment candidacy to spaceflight manifest is about six years. This time can be shortened by the use of existing hardware or facilities (described in Appendix A). The P.I. continues to monitor the experiment during spaceflight, performs the subsequent analyses, and publishes the results (an obligation) in archival journals.

The above scenario is typical for space-based experiments. NASA also supports theoretical and diagnostics research, as well as microgravity experiments that can be completed in the ground-based test phase in drop towers or aircraft.

NASA Research Announcements

Proposals for either definition study or flight-experiment candidacy are solicited via a NASA Research Announcement (NRA). The first NRA focusing on microgravity combustion science was issued in late 1989. It resulted in 13 definition-study awards and 6 flight-experiment-candidacy awards out of 65 proposals. The second microgravity combustion NRA was released in 1993, and it resulted in 33 definition and 6 flight-experiment-candidate studies out of 99 proposals. The plan now is to issue an NRA for microgravity combustion science every two years.

Finally, NASA offers financial support to graduate students through its Graduate Student Research Program and post-doctorate fellowships through the National Research Council. More information about the details of these programs and the process of proposal submission, progress reviews, and space-flight project selection is available by writing to the Microgravity Combustion Branch, MS 500-115, NASA Lewis Research Center, 21000 Brookpark Road, Cleveland, Ohio 44135.

Concluding Remarks and a View of the Future

Advancement in combustion-science knowledge is commonly achieved via inference, since the specific quantities of interest, *e.g.*, various forces, transport rates and chemical-species concentrations, are rarely measured directly. Parametric experiments in which the initial pressure, oxygen concentration, diluent type, material thickness, flow rates, and geometries are varied seek to improve the level of understanding of controlling mechanisms, chemical kinetics, and fluid dynamics of flame systems. Microgravity offers an alternative means both to uncover underlying physics and to test the robustness of our understanding. Today, the capability of performing combustion experiments that eliminate the influence of gravity exists, albeit with unique impediments and complexities. These microgravity experiments produce surprising, interesting, and sometimes unexplained observations with high frequency, revealing that our intuition and knowledge of combustion processes are less extensive than often assumed.

The predominant feature of microgravity combustion is that, for laboratory-scale flames, buoyancy-induced flows are nearly eliminated. A new range of velocities between those associated with diffusive and buoyant convective transport (1 to 30 cm/sec in present laboratory-scale experiments) is made available for study by imposing a known flow in microgravity or by subjecting the system to partial gravity. Several interacting transport processes have been identified repeatedly and form common themes to be accounted for in microgravity flame models and simulations, for example, diffusional transport of oxygen and products over large spatial scales, radiative heat transfer even in small-sized flames, and hot-gas expansion.

Present combustion-science textbooks contain zero-gravity theories that are founded historically on normal-gravity experiments; examples include isolated droplet burning, Burke-Schumann gas-jet flames, auto-ignition, flammability and stability, laminar burning velocities of premixed gases, and the less-developed treatises on flame spread over condensed-phase materials. The microgravity environment now offers the means for a straightforward comparison between theory and experiment. Further motivation to perform combustion experiments in space is in the necessity to maintain and improve fire safety aboard human-crewed spacecraft. Many findings from microgravity combustion research are of direct relevance to the NASA material-flammability and toxicological-screening test procedures and to the identification of fire signatures, i.e., heat release, smoke production, flame visibility and radiation.

Considerable progress is being achieved in improving the capabilities of the microgravity combustion-science program. For example, a broad range of non-intrusive instruments has been devised and developed to meet the restrictions of volume, weight, and power, and the high vibratory and shock loads imposed in all microgravity facilities, from drop towers to the Shuttle. Substantial progress has also been made in expediting the development of space experiments and in reducing the long period, measured in years, between the initial concept and the eventual data return. A major factor in the improvement will be in the increased reuse of flight-qualified designs and hardware. Further experience in the management of the overall microgravity combustion-science program will also yield benefits in efficiency, with heightened cooperation and familiarity of concepts among the researchers and the NASA design, payload-integration, and safety panels.

The microgravity combustion-science program is expected to continue its strong growth in the near future, quantified by the number of investigations NASA will support. Open competitions promoted by NASA Research Announcements at two-year intervals, with selection via peer review, will be the only mechanism for researchers to be awarded funds for investigations in microgravity combustion science. Expansion of opportunities for graduate students and post-doctorate fellowships is planned. Exploitation of international collaborations, such as those involving the use of the MIR space station and the International Space Station Alpha, is also expected.

In the future, further expansion of scientific studies is expected into areas of current terrestrial research interest, such as turbulent combustion, soot processes, spray combustion, and flame-based synthesis of high-value materials. A greater portion of the NASA scientific research support will be justified by its practical benefit or relevance. The progress in microgravity combustion science will be expected to have a major impact on our society.

Appendix A:
Research Facilities and Accomodations

Ground-Based Facilities

A variety of ground-based microgravity or low-gravity facilities is available to researchers. Each has specific capabilities and characteristics that must be considered by an investigator when selecting the one best suited to a particular type of experiment.

The majority of combustion studies to date have been conducted in either of two free-fall drop towers at the NASA Lewis Research Center. The 2.2-Sec Drop Tower, as the name implies, provides 2.2 sec of microgravity test time for experiment packages with up to 150 kg of hardware mass. A schematic diagram of this drop tower is shown in Fig. 33. The drop chamber is 27-m high (the actual drop height is 24 m) with a cross-section of 1.5 by 2.75 m. The experiment package is enclosed in a drag shield (Fig. 34), which has a high ratio of mass to frontal area, hence a low drag coefficient. The drag shield/experiment assembly is hoisted to the top of the building and suspended there by a highly stressed wire that is attached to the release system. A drop is initiated when the wire is notched, causing it to fail. As the drag shield/experiment assembly falls, the experiment package is free to move within the drag-shield enclosure, and the drag forces are negligible. Residual acceleration is estimated to be of the order of 10^{-5} g. The assembly is decelerated at the bottom by compression of an air bag, limiting the deceleration loads to peak levels ranging from 15 to 25 g. Though the microgravity time is limited to 2.2 sec, the facility offers advantages of rapid turnaround time between experiments and low-cost operations. It is often used for proof-of-concept or preliminary experimentation.

The 5.2-Sec Zero Gravity Facility (Fig. 35) offers expanded experiment and diagnostic capabilities compared to those available in the 2.2-Sec Drop Tower. The facility is a 6.1-m-diameter steel-walled vacuum chamber, 145-m deep, that provides the 132-m drop distance required for 5.18 sec of free fall, during which residual accelerations as low as 10^{-6} g can be achieved. Experiment packages with up to 450 kg in total mass are mounted in a one-meter-diameter carrier (Fig. 36). Prior to each test, the free-fall chamber is evacuated to a final pressure of about 1 Pa (10^{-2} torr) to eliminate air drag. The experiment drop is initiated by shearing a bolt in the release mechanism that suspends the experiment and carrier. The carrier falls in the vacuum chamber, and it is decelerated at the chamber bottom by impact into a 6.1-m deep container containing small pellets of expanded polystyrene.

Specially modified jet aircraft flying parabolic (Keplerian) trajectories can provide significant increases in low-gravity experiment time compared to drop towers, with a penalty of higher gravity levels. For an experiment fixed to the body of an aircraft, accelerations in the range of 10^{-2} g can be obtained for up to 20 seconds. During one flight sequence, numerous parabolic trajectories are possible. While the aircraft trajectories do not offer true microgravity, they do provide researchers with advantages over drop-tower testing. Aircraft facilities permit operator interactions, allowing researchers to monitor their experiments in real-time and to reconfigure them between trajectories. Aircraft also allow researchers to utilize a wide variety of diagnostic equipment, since delicate equipment is not exposed to the severe shock loadings experienced in drop towers.

The NASA Lewis Research Center DC-9 is NASA's newest low-gravity aircraft. (Prior experimentation was performed on the NASA Lewis Learjet and the NASA Johnson KC-135A.) The interior layout of the airplane offers an open cabin area of approximately 15.8 by 2.78 m for experiment placement (Fig. 37). The large cabin volume also permits the free-floating of experiments to reduce residual accelerations to the level of 10^{-3} g for time periods of 5 to 10 sec, depending on the experiment size. The DC-9 can perform up to 30 trajectories per flight. Intermediate acceleration levels of less than 0.1 to 0.5 of normal gravity (partial gravity) can also be achieved in this aircraft by modified trajectories.

Sounding rockets bridge the gap between ground-based and spaceflight facilities. A variety of sounding-rocket carriers that can attain altitudes of 30 to 1200 km are available for science payloads. These flights achieve acceleration environments of the order of 10^{-4} g for 5 to 15 minutes or longer. Payloads may vary in length, but their diameter is generally limited to 44 cm, although some rockets accommodate packages up to 56 cm in diameter. For payload recovery, parachute systems impose landing loads equivalent to 30 to 50 g.

Most sounding-rocket experiments operate autonomously. Because the sounding rocket flight lasts on the order of minutes, it is possible to uplink commands for operation and control and to downlink data, all in real-time. This capability can provide much flexibility in the design and operation of the experiment.

Space Accommodations

While the ground-based facilities of drop towers and aircraft are essential for microgravity experiments in combustion science, the longer-duration microgravity laboratories of the U.S. Space Shuttle and the future International Space Station Alpha (ISSA) greatly expand the capabilities for investigations. The Shuttle flight duration for science missions is 7 to 13 days. In Shuttle operations, the drag and gravity-gradient forces limit the background acceleration to a level of around 10^{-4} g. In the

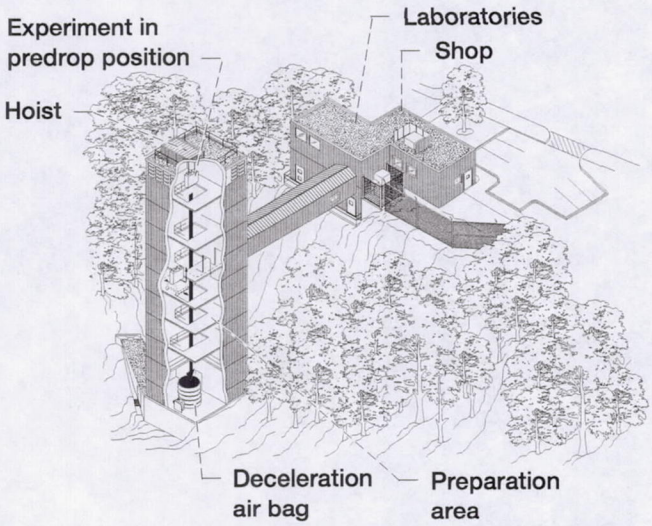

Figure 33.—Sketch of the NASA Lewis Research Center 2.2-Sec Drop Tower.

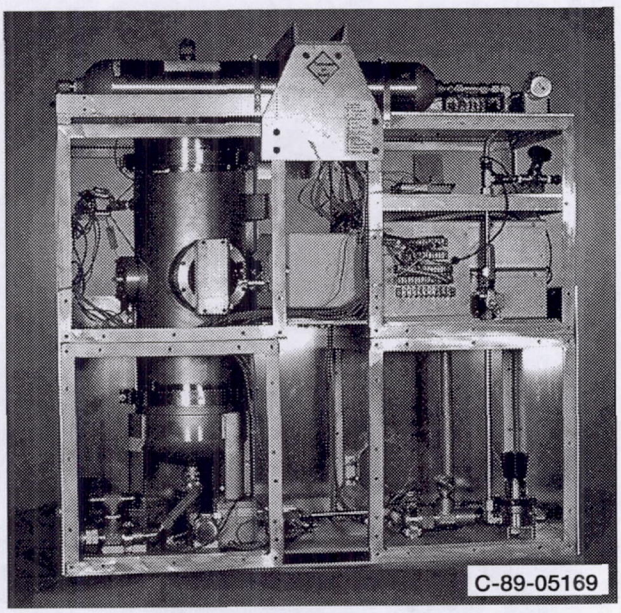

Figure 34.—Photograph of typical experiment package (combustion tunnel) for use in the 2.2-Sec Drop Tower.

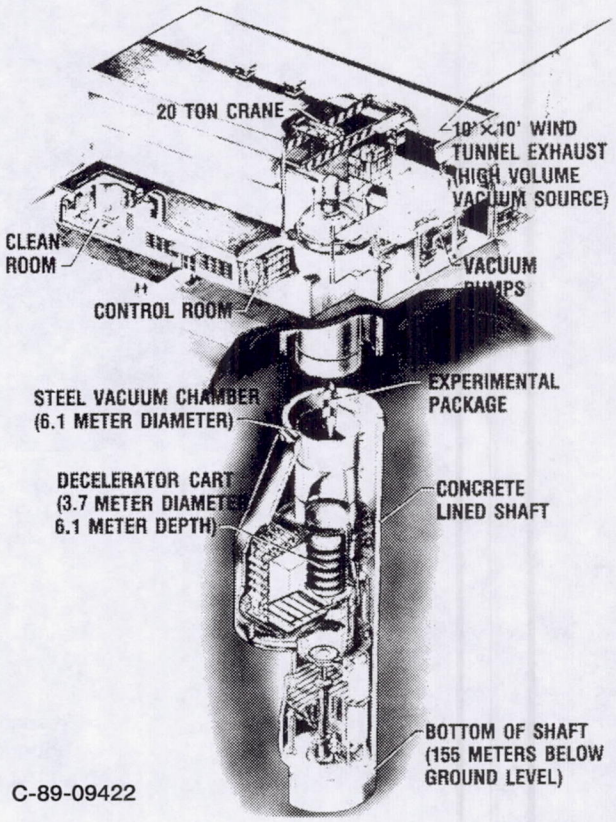

Figure 35.—Sketch of the NASA Lewis Research Center 5.2-Sec Zero Gravity Facility.

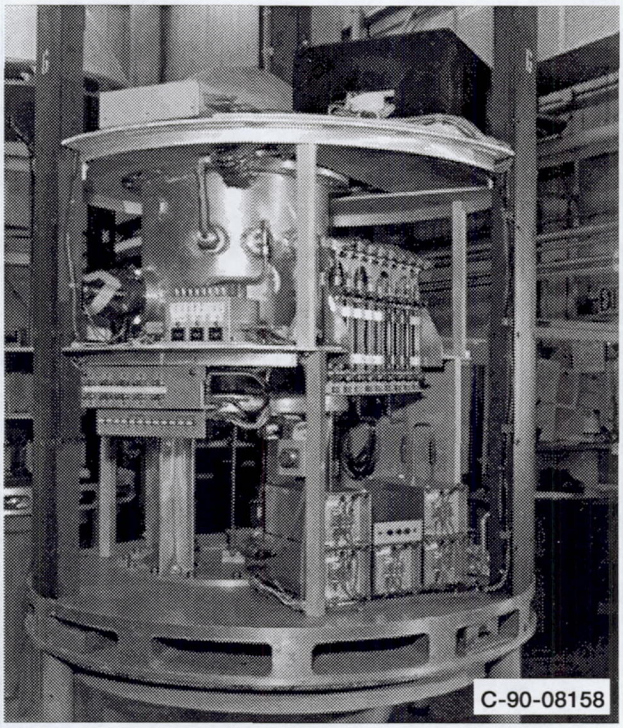

Figure 36.—Photograph of typical experiment vehicle (combustion chamber) for use in the Zero Gravity Facility.

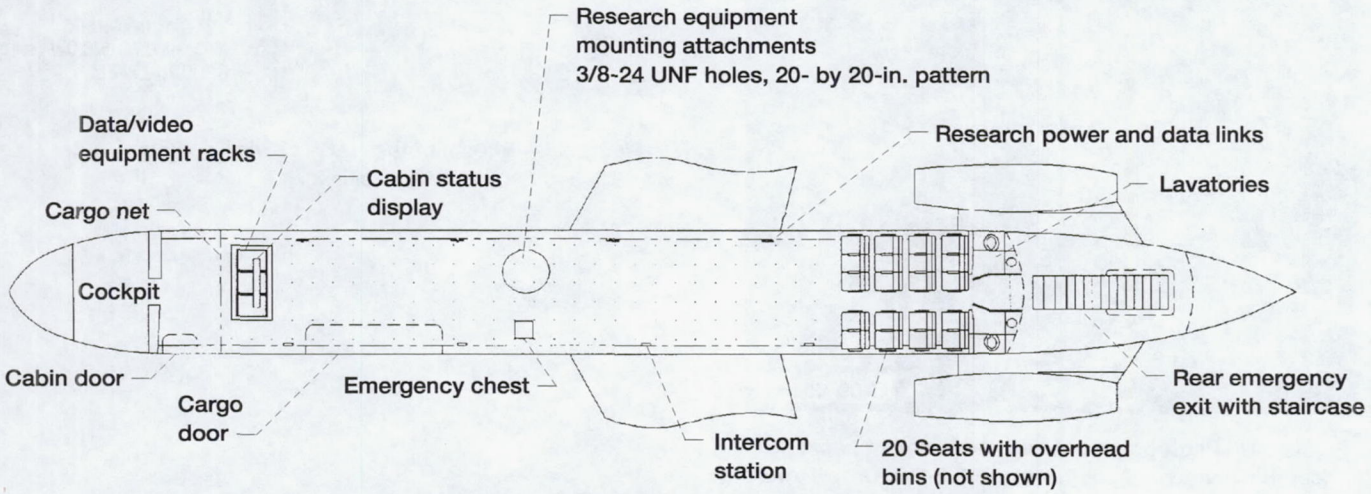

Figure 37.—Plan view of NASA Lewis Research Center DC-9 Airplane Facility.

future, the ISSA will provide a similar quality microgravity environment with test durations of months.

Table II describes the carriers, or space accommodations, available for experiments in combustion science. Existing experiment payloads are shown in the top rows. The *Solid Surface Combustion Experiment* is an example of hardware dedicated to the requirements of a single investigator, yet versatile in its accommodation to the Shuttle payload bay or mid-deck lockers. A few dedicated experiments, for example, *Microgravity Smoldering Combustion* and *Transitional Gas Jet Diffusion*, are in development in Getaway Special carriers (GASCAN). These are standardized accommodations used as ballast in the Shuttle payload bay, sharing available space with major payloads. The combustion-science experiments will have small, sealed chambers and a flow system. Each chamber is presently instrumented for measurement of interior pressure, temperatures, radiometry, and video recording through a chamber window. The carriers have self-contained power and data acquisition and storage. The GASCAN experiments are not accessible to the crew, and they must be automated and software controlled. Table II also shows one proposed experiment for the Shuttle mid-deck, the *Droplet Combustion Experiment*. The droplet deployment, ignition, and many of the controls in this experiment to study the combustion of free-floated droplets and arrays are automated, but the crew can be involved in selected test procedures and observations.

Multi-user hardware is a logical means for achieving efficient and flexible utilization of space-based facilities for microgravity combustion research. Use of common subsystems in hardware development avoids the high cost of repeatedly developing flight-qualified hardware and extends the useful life of such hardware. The Combustion Module, CM–1, is a multi-user facility now in construction for an initial assignment on a Shuttle laboratory mission (Spacelab) in 1997 (Table II). The CM–1 components are housed in two adjoining racks. The single rack, shown on the left in Fig. 38, contains the fluid-supply package, to store and meter fuels, oxidizers, and diluents, and the video-recording equipment. The double rack has the experimental combustion chamber, power supplies, experiment processor, diagnostics, and exhaust system. The flexibility required to perform multiple experiments (initially two for the CM–1) is provided by mounting each set of experiment-specific hardware on a structure that can be interchanged and remounted within the double rack during the orbital operations.

The future facility, COMB–M1, also described in Table II, is basically an advancement of CM–1 to transfer it from Spacelab to the ISSA. The long duration of a Space Station mission will permit extensive apparatus and diagnostic adjustments or reconfigurations, so that a highly productive combustion laboratory will be available to serve the needs of a diverse scientific community. COMB–M1 is to have five subsystems (diagnostics, fluids, avionics, mechanical/structure, and data acquisition and control), mounted in two racks for the experiment and the power supply/data management systems.

Finally, the Glovebox facility, presently flying on the Shuttle and Spacelab but planned for the ISSA, provides a sealed working volume in which small-scale experiments may be conducted. The Glovebox provides connections for experiment power, video, and multiple-view still photography and for gas cleanup and filtration systems. Clever design of experiment packages offers the opportunity to conduct multiple-point tests through the protected manipulation by the crew member. Three combustion experiments (*Candle Flames*, *Wire Insulation Flammability*, and *Polyurethane Foam Smoldering*) were conducted successfully in a Glovebox on a Shuttle mission in July 1992, and more experiments are planned.

TABLE II.— SUMMARY OF CURRENT AND DEVELOPMENTAL SPACEFLIGHT ACCOMMODATIONS FOR MICROGRAVITY COMBUSTION SCIENCE

Name/ Carriers/ Dates Flown	Chamber Characteristics	Specialized Sub-systems	Imaging Systems	Other diagnostics
Solid surface Combustion Expt/ Shuttle Middeck; Spacelab SMIDEX 10/90-12/96	39 1; 2 windows; 2 atm; up to 50% O2	Hot Wire Ignition; Trap Door Extinguishment;	2 perpendicular, 16 mm cine cameras	6 Thermocouples (T/C's); Pressure transducer (P)
Microgravity Smoldering Combustion/GASCan/1996	2 @ 20 1 each; 2.8 atm	Blowdown air flow system;	1 Standard Color Video Camera w/1 recorder	12 T/C's; 1 P
Droplet Combustion Experiment/ Spacelab SMIDEX; possibly also in MCF 4/97	70 1; 4 windows including stereoscopic view port for crew; 1.5 atm; up to 50% O2	Computer-controlled droplet dispensing & deployment; multiple liquid fuel reservoirs; premixed gas bottle farm w/ Vacuum Vent from chamber	80 f/sec cine camera; std color video; UV intensified array video camera perpendicular to cine camera	5 T/C's; 1 P
Transitional Gas Jet Diffusion Flames/ GASCan/1996	50 1; no windows;1 atm; air	Hot wire ignition; vortex generating mechanism	2 standard (std) color video cameras and recorders	3 radiometers; 8 T/C's; 1 P
CM–1/Spacelab 4/97	78 1; 6 windows; 30% O2	Premixed gas bottle farm plus Vacuum Vent; digitization of image data	Std color video; UV intensified array video camera; near-IR intensified array video camera	Soot sampling; 2-wavelength soot pyrometry; 2D soot volume fraction; 2 radiometers
COMB–M1/Space Station/On-orbit 3/99	78 1; 6 windows; 0.5-3 atm; TBD	Fluid Supply System and Exhaust gas Clean-up/Vacuum Vent	Same as CM–1 plus high-frame rate video	Same as CM–1 plus Rainbow Schlieren Deflectometry
Glovebox Facility/Spacelab; Middeck; MIR 6/92 → ongoing	30 1; 1 window; open to cabin atmosphere, so about 1 atm/air at 1 atm	Exhaust gas clean-up; low-speed air flow through chamber; gloveports to enable expt operations by the crew	2 std color and 2 std B/W video systems	Polutant level monitoring

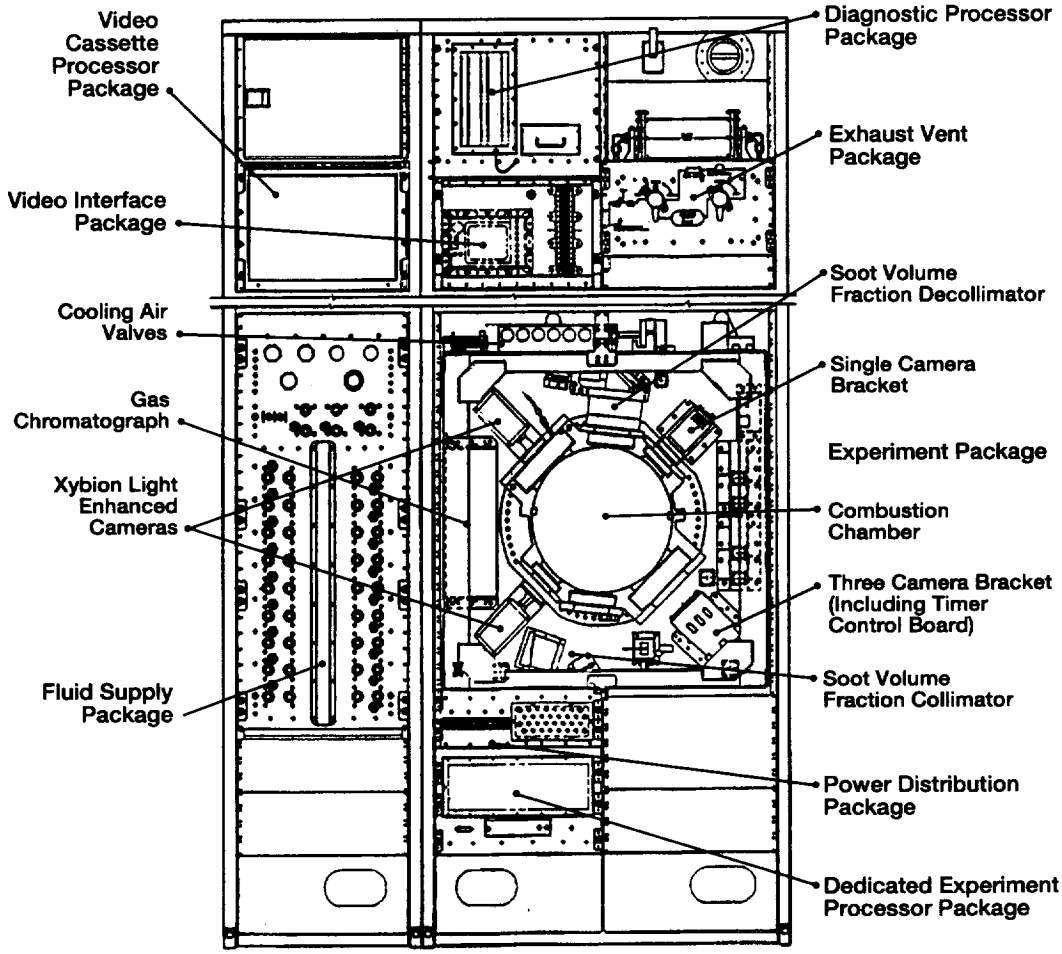

Figure 38.—Sketch of the multi-user Combustion Module, CM-1, now under construction to accommodate two experiments for Spacelab in 1997.

Appendix B
List of Funded Participants

Currently funded participants and their projects under the NASA Microgravity Combustion Science Research Announcement are listed according to subject categories that correspond to the major sections of this review. Each project is listed once, although some of the projects clearly overlap several of the categories.

Candle Flames

Daniel L. Dietrich
NASA Lewis Research Center
Cleveland OH
Candle Flames in Microgravity

Premixed Gas Combustion

John D. Buckmaster
University of Illinois
Urbana IL
Modeling of Microgravity Combustion Experiments

Kazhikathra Kailasanath
Naval Research Laboratory
Washington DC
Unsteady Numerical Simulations of the Stability and Dynamics of Flames in Microgravity

Chung K. Law
Princeton University
Princeton NJ
Studies of Flame Structure in Microgravity

Suresh Menon
Georgia Institute of Technology
Atlanta GA
Premixed Turbulent Flame Propagation in Microgravity

Paul D. Ronney
University of Southern California
Los Angeles CA
The Structure of Flame-Balls at Low Lewis Number (SOFBALL)

M.D. Smooke
Yale University
New Haven CT
Numerical Modeling of Flame-Balls in Fuel-Air Mixtures

Laminar Diffusion Flame Structure

M. Yousef Bahadori
Science Applications International Corp.
Torrance CA
Effects of Buoyancy on Transition/Turbulent Gas Jet Diffusion Flames

L.D. Chen
University of Iowa
Iowa City, IA
Buoyancy Effects on the Structure and Stability of Burke-Schumann

Diffusion Flames

Fokion N. Egolfopoulos
University of Southern California
Los Angeles CA
Aerodynamic, Unsteady, Kinetic, and Heat Loss Effects on the Dynamics and Structure of Weakly Burning Flames in Microgravity

Frank Fendell
TRW, Inc.
Redondo Beach CA
Unsteady Diffusion Flames: Ignition, Travel, and Burnout

Simone Hochgreb
Massachusetts Institute of Technology
Cambridge MA
Chemical Inhibitor Effects on Diffusion Flames in Microgravity

Moshe Matalon
Northwestern University
Evanston IL
Structure and Dynamics of Diffusion Flames in Microgravity

Turbulent Flames/Flame-Vortex Interactions

Ajay K. Agrawal
University of Oklahoma
Norman OK
Effects of Energy Release on Near Field Flow Structure of Gas Jets

Robert K. Cheng
Lawrence Berkeley Laboratory
Berkeley CA
Gravitational Effects on Premixed Turbulent Flames: Microgravity Flame Structures

James F. Driscoll
University of Michigan
Ann Arbor MI
Flame Vortex Interactions Imaged in Microgravity

Said Elghobashi
University of California at Irvine
Irvine CA
Effects of Gravity on Sheared and Nonsheared Turbulent Non-premixed Flames

Jean R. Hertzberg
University of Colorado
Boulder CO
Three-Dimensional Flow in a Microgravity Diffusion Flame

Soot Formation, Aggregation, and Oxidation

Mun Young Choi
University of Illinois at Chicago
Chicago, IL
The Effects of Sooting in Reduced Gravity Droplet Combustion

Gerard M. Faeth
University of Michigan
Ann Arbor MI
Investigation of Laminar Jet Diffusion Flames in Microgravity: A Paradigm for Soot Processes in Turbulent Flames (LSP)

Droplet and Particle Combustion

C. Thomas Avedisian
Cornell University
Ithaca NY
Multicomponent Droplet Combustion in Microgravity: Soot Formation, Emulsions, Metal-Based Additives, and the Effect of Initial Droplet Diameter

Daniel L. Dietrich
NASA Lewis Research Center
Cleveland OH
Combustion of Interacting Droplet Arrays in a Microgravity Environment

Alessandro Gomez
Yale University
New Haven CT
Spray Combustion at Normal and Reduced Gravity in Counterflow and Co-flow Configurations

J. Thomas McKinnon
Colorado School of Mines
Golden CO
Combustion of PTFE: The Effect of Gravity on Ultrafine Particles Generation

Benjamin D. Shaw
University of California at Davis
Davis CA
Combustion of Two-Component Miscible Droplets in Reduced Gravity

Forman A. Williams
University of California at San Diego
La Jolla CA
Scientific Support for a Space Shuttle Droplet Burning Experiment

Forman A. Williams
University of California at San Diego
La Jolla CA
High-Pressure Combustion of Binary Fuel Sprays

Jiann C. Yang
National Institute of Standards and Technology
Gaithersburg MD
Combustion of a Polymer (PMMA) Sphere in Microgravity

Flammability and Flame Spread Over Liquid Pools

Howard D. Ross
NASA Lewis Research Center
Cleveland OH
Flame Spread Across Liquids (SAL)

Smoldering Flame Spread

A. Carlos Fernandez-Pello
University of California at Berkeley
Berkeley CA
Fundamental Study of Smoldering Combustion in Microgravity (MSC)

Flammability and Flame Spread Over Solids

Robert A. Altenkirch
Mississippi State University
Mississippi State MS
Scientific Support for an Orbiter Middeck Experiment on Solid Surface Combustion (SSCE)

Robert A. Altenkirch
Mississippi State University
Mississippi State MS
Low-Velocity Opposed-Flow Flame Spread in a Transport-Controlled Microgravity Environment (DARTFire)

Robert A. Altenkirch
Mississippi State University
Mississippi State MS
Reflight of the Solid Surface Combustion Experiment with Emphasis on Flame Radiation Near Extinction

Takashi Kashiwagi
National Institute of Standards and Technology
Gaithersburg MD
Ignition and the Subsequent Transition to Flame Spread in Microgravity

Paul D. Ronney
University of Southern California
Los Angeles CA
Flow and Ambient Atmosphere Effects on Flame Spread at Microgravity

James S. T'ien
Case Western Reserve University
Cleveland OH
Combustion of Solid Fuel in Very Flow Speed Oxygen Streams

David Urban
NASA Lewis Research Center
Cleveland OH
Interaction Between Flames on Parallel Solid Surfaces

Indrek S. Wichman
Michigan State University
East Lansing MI
Studies of Wind-Aided Flame Spread Over Thin Cellulosic Fuels in Microgravity

Metal Combustion

Melvyn C. Branch
University of Colorado
Boulder CO
Ignition and Combustion of Bulk Metals in a Microgravity Environment

Edward L. Dreizen
AeroChem Research Laboratories, Inc.
Princeton NJ
Internal and Surface Phenomena in Heterogeneous Metal Combustion

Combustion Synthesis of Materials

Bernard J. Matkowsky
Northwestern University
Evanston IL
Filtration Combustion for Microgravity Applications: (1) Smoldering, (2) Combustion Synthesis of Advanced Materials

John J. Moore
Colorado School of Mines
Golden CO
A Fundamental Study of the Combustion Synthesis of Ceramic-Metal Composite Materials Under Microgravity Conditions

Arvind Varma
University of Notre Dame
Notre Dame IN
Gasless Combustion Synthesis from Elements Under Microgravity: A Study of Structure Formation Processes

Diagnostic Instrumentation

William D. Bachelo
Aerometrics, Inc.
Sunnyvale CA
Development of Advanced Diagnostics for Characterization of Burning Droplets in Microgravity

Jerry C. Ku
Wayne State University
Detroit MI
Soot and Radiation Measurements in Microgravity Turbulent Jet Diffusion Flames

Joel A. Silver
Southwest Sciences, Inc.
Santa Fe NM
Quantitative Measurement of Molecular Oxygen in Microgravity Combustion

Michael Winter
United Technologies Research Center
East Hartford CT
Laser Diagnostics for Fundamental Microgravity Droplet Combustion Studies

Appendix C
Selected Bibliography

Candle Flames

Dietrich, D.L.; Ross, H.D.: and T'ien J.S.: Candle Flames in Microgravity: Space Shuttle Results. *Fall Tech. Meeting of the Eastern States Sec.*, The Combustion Inst., Paper 91, Oct. 1993.

Dietrich, D.L.; Ross, H.D.; and T'ien, J.S.: The Burning of a Candle in Reduced Gravity: Space Shuttle and Drop Tower Results. AIAA 94-0429, Jan. 1994.

Ross, H.D.; Dietrich, D.L.; and T'ien, J.S.: Candle Flames in Microgravity: USML-1 Results - 1 Year Later. Ramachandran, N.; Frazier, D.O.; Lehoczky, S.L.; and Baugher, C.L., eds.: *Joint Launch + One Year Science Review of USML-1 and USMP-1 with the Microgravity Measurement Group*. NASA Conf. Publ. 3272, Vol. II, May 1994, pp. 541-568.

Premixed Gas Combustion

Abbud-Madrid, A.; and Ronney, P.D.: Premixed Flame Propagation in an Optically-Thick Gas. *AIAA Jour.*, Vol. 31, 1993, pp. 2179-2181.

Buckmaster, J.; Gessman, R.; and Ronney, P.: The Three-Dimensional Dynamics of Flame-Balls. *The Twenty-Fourth Symp. (International) on Combustion*, The Combustion Inst., Pittsburgh, 1992, pp. 29-36.

Buckmaster, J.; Ronney, P.; and Smooke, M.: Flame Balls-Past, Present and Future. AIAA 93-0712, Jan. 1993.

Buckmaster, J.; Smooke, M.; and Giovangigli, V.: Analytical and Numerical Modeling of Flame-Balls in Hydrogen-Air Mixtures. *Combustion and Flame*, Vol. 94, 1993, pp. 113-124.

Dunsky, C. M.: Microgravity Observations of Premixed Laminar Flame Dynamics. *The Twenty-Fourth Symp. (International) on Combustion*, The Combustion Inst., Pittsburgh, 1992, pp. 177-187.

Kailasanath, K.: Laminar Flames in Premixed Gases. *Numerical Approaches to Combustion Modeling*, Prog. Astro. Aero., Vol. 135, AIAA, Washington, 1991, pp. 225-256.

Kailasanath, K.; Ganguly, K.; and Patnaik, G.: Dynamics of Flames Near the Rich-Flammability Limit of Hydrogen-Air Mixtures. Kuhl, A.L.; Leyer, J.-C.; Borison, A.A.; and Sirignano, W.A., eds.: *Dynamics of Gaseous Combustion*, Prog. Astro. Aero., Vol. 151, AIAA, 1993, Washington, pp. 247-262.

Lozinski, D.; and Buckmaster, J.: Absolute Flammability Limits and Flame-Balls. *Combustion and Flame*, Vol. 97, 1994, pp. 301-316.

Patnaik, G.; and Kailasanath, K.: Effect of Gravity on the Stability and Structure of Lean Hydrogen-Air Flames. *The Twenty-Third Symp. (International) on Combustion*, The Combustion Inst., Pittsburgh, 1991, pp. 1641-1647.

Patnaik, G.; Kailasanath, K.; and Oran, E.S.: Effect of Gravity on Flame Instabilities in Premixed Gases. *AIAA Jour.*, Vol. 29, 1991, pp. 2141-2148.

Pearlman, H.G.; and Ronney, P.D.: Self-Organized Spiral and Circular Waves in Premixed Gas Flames. *Jour. of Chemical Physics*, Vol. 101, 1994, pp. 2632-2633.

Pearlman, H.G.; and Ronney, P.D.: Near-Limit Behavior of High- Lewis Number Premixed Flames in Tubes at Normal and Low Gravity. *Physics of Fluids*, Vol. 6, 1994, pp. 4009-4018.

Ronney, P.D.: Laser Versus Conventional Ignition of Flames. *Optical Eng.*, Vol. 33, 1994, pp. 510-521.

Ronney, P.D.; Whaling, K.N.; Abbud-Madrid, A.; Gatto, J.L.; and Pisowicz, V.L.: Stationary Premixed Flames in Spherical and Cylindrical Geometries. *AIAA Jour.*, Vol. 32, 1994, pp. 569-577.

Ronney, P.D.; and Yakhot, V.: Flame Broadening Effects on Premixed Turbulent Flame Speed. *Comb. Sci. Technol.*, Vol. 86, 1992, pp. 31-43.

Shy, S.S.; Ronney, P.D.; Buckley, S.G.; and Yakhot, V.: Experimental Simulation of Premixed Turbulent Combustion Using Aqueous Autocatalytic Reactions. *The Twenty-Fourth Symp. (International) on Combustion*, The Combustion Inst., Pittsburgh, 1992, pp. 543-551.

Sloane, T.M.; and Ronney, P.D.: A Comparison of Ignition Phenomena Modeled with Detailed and Simplified Kinetics. *Comb. Sci. Technol.*, Vol. 88, 1993, pp. 1-13.

Laminar Diffusion Flame Structure

Atreya, A.; Agrawal, S.; Sacksteder, K.; and Baum, H.R.: Observations of Methane and Ethylene Diffusion Flames Stabilized Around a Blowing Porous Sphere Under Microgravity Conditions. AIAA 94-0572, Jan. 1994.

Bahadori, M.Y.; Stocker, D.P.; and Sotos, R.G.: Effects of Oxygen Concentration on Radiation from Microgravity Laminar Propane Diffusion Flames. *Joint Tech. Meeting of the Central and Eastern States Secs.*, The Combustion Inst., Paper 1, March 1992, pp. 41-45.

Bahadori, M.Y.; Stocker, D.P.; Vaughan, D.F.; Zhou, L.; and Edelman, R.B.: Effects of Buoyancy on Laminar, Transitional, and Turbulent Gas Jet Diffusion Flames. Williams, F.A.; Oppenheim, A.K.; Olfe, D.B.; and Lapp, M.: eds., *Modern Developments in Energy, Combustion, and Spectroscopy*, Pergamon Press, Oxford, 1993, pp. 49-66.

Buckmaster, J.: The Structure and Stability of Laminar Flames. *Annual Review of Fluid Mechanics*, Vol. 25, 1993, pp. 21-53.

Hegde, U.; and Bahadori, M.Y.: An Analytical Model for Gravitational Effects on Burke-Schumann Flames. *Fall Meeting of the Western States Sec.*, The Combustion Inst., Oct. 1992.

Hegde, U.; and Bahadori, M.Y.: Gravitational Influences on the Behavior of Confined Diffusion Flames. AIAA 92-0334, Jan. 1992.
Patnaik, G.; and Kailasanath, K.: Numerical Simulations of the Extinguishment of Downward Propagating Flames. *The Twenty-Fourth Symp. (International) on Combustion*, The Combustion Inst., Pittsburgh, 1992, pp. 189-195.
Patnaik, G.; and Kailasanath, K.: Simulation of Multidimensional Burner-Stabilized Flames. AIAA 93-0241, Jan. 1993.
Pickett, K.; Atreya, A.; Agrawal, S.; and Sacksteder, K.R.: Radiation from Unsteady Spherical Diffusion Flames in Microgravity. AIAA 95-0148, Jan. 1995.
Stocker, D.P.: The Effect of Reduced Gravity on the Shape of Laminar Burke-Schumann Diffusion Flames. *Spring Tech. Meeting of the Central States Sec.*, The Combustion Inst., Paper 15, April 1991.
Stocker, D.P.: Diluent Effects on Laminar Burke-Schumann Diffusion Flames in Microgravity. *Spring Tech. Meeting of the Central States Sec.*, The Combustion Inst., Paper 16, April 1991.
Stocker, D.P.: Size and Shape of Laminar Burke-Schumann Diffusion Flames in Microgravity. *Spring Tech. Meeting of the Central States Sec.*, The Combustion Inst., Paper 42, May 1992.
Stocker, D.P.; Sheu, J.C.; and Chen, L.-D.: Preliminary Observations of the Effect of Microgravity on a Pulsed Jet Diffusion Flame. *Fall Meeting of the Western States Sec.*, The Combustion Inst., Oct. 1993.
Wu, F.; and Fendell, F.: Unsteady Planar Diffusion Flames: Ignition, Travel, Burnout. AIAA 95-0147, Jan. 1995.

Turbulent Flames/Flame-Vortex Interactions

Bedat, B.; Kostiuk, L.W.; and Cheng, R.K.: Characterization of Acoustic Effects on Flame Structures by a Beam Deflection Technique. *Fall Meeting of the Western States Sec.*, The Combustion Inst., Paper No. 93-066, Oct. 1993.
Ku, J.C.; Tong, L.; Sun, J.; Greenberg, P.S.; and Griffin, D.W.: Soot Formation and Radiation in Turbulent Jet Diffusion Flames Under Normal and Reduced Gravity Conditions. Ross, H.D., ed.: *Second International Microgravity Combustion Workshop*, NASA Conf. Publ. 10113, 1993, pp. 121-133.
Zhou, L.; Hegde, U.; and Bahadori, M.Y.: Experimental Observations of Turbulent Gas Jet Diffusion Flames in Microgravity. *Joint Tech. Meeting of the Central and Eastern States Secs.*, The Combustion Inst., Paper 67, March 1992, pp. 362-366.

Soot Formation, Aggregation, and Oxidation

Choi, M.Y.; Dryer, F.L.; Green, G.J.; and Sangiovanni, J.J.: Soot Agglomeration in Isolated, Free Droplet Combustion. AIAA 93-0823, Jan. 1993.
Koylu, U.O.; and Faeth, G.M.: Optical Properties of Soot Emissions in Buoyant Laminar Diffusion Flames. *Jour. Heat Trans.*, Vol. 116, 1994, pp. 971-979.
Lin, K.-C.; and Faeth, G.M.: Hydrodynamic Suppression of Soot Emissions in Laminar Diffusion Flames. AIAA 95-0375, Jan. 1995.
Mortazavi, S.; Sunderland, P.B.; Jurng, J.; Koylu, U.O.; and Faeth, G.M.: Structure of Soot-Containing Laminar Jet Diffusion Flames. AIAA 93-0708, Jan. 1993.
Paul, M.R.; Issacci, F.; Apostolakis, G.E.; and Catton, I.: The Morphological Description of Particles Generated from Overheated Wire Insulations in Microgravity and Terrestrial Environments. Sadhal, S.S.; and Hashemi, A., eds.: *Heat Transfer in Microgravity Systems-1993*, ASME HTD Vol. 235, 1993, pp. 59-66.
Paul, M.; Issacci, F.; Catton, I.; and Apostolakis, G.: Elemental Description of Smoke Particles. AIAA 94-0433, Jan. 1994.
Sunderland, P.B.; Mortazavi, S.; Faeth, G.M.; and Urban, D.L.: Laminar Smoke Points of Nonbuoyant Jet Diffusion Flames. *Combustion and Flame*, Vol. 96, 1994, pp. 97-103.

Droplet and Particle Combustion

Card, J.M.: Asymptotic Analysis for the Burning of n-Heptane Droplets Using a Four-Step Reduced Mechanism. *Combustion and Flame*, Vol. 93, 1993, pp. 375-390.
Card, J.M.; and Williams, F.A.: Asymptotic Analysis with Reduced Chemistry for the Burning of n-Heptane Droplets. *Combustion and Flame*, Vol. 91, 1992, pp. 187-199.
Card, J.M.; and Williams, F.A.: Asymptotic Analysis of the Structure and Extinction of Spherically Symmetrical n-Heptane Diffusion Flames. *Comb. Sci. Technol.*, Vol. 84, 1992, pp. 91-119.
Cho, S.Y.; Yetter, R.A.; and Dryer, F.L.: A Computer Model for One-Dimensional Mass and Energy Transport in and around Chemically Reacting Particles, Including Complex Gas-Phase Chemistry, Multi-Component Molecular Diffusion, Surface Evaporation and Heterogeneous Reaction. *Jour. of Computational Physics*, Vol. 102, 1992, pp. 160-179.
Choi, M.Y.; Cho, S.Y.; Dryer, F.L.; and Haggard, J.B., Jr.: Some Further Observations on Droplet Combustion Characteristics: NASA LeRC-Princeton Results. Gatos, H.C.; and Regal, L.L., eds.: *Proc. IKI/AIAA Microgravity Sci. Symp.*, Moscow, May 1991, pp. 294-304.
Choi, M.Y.; Cho, S.Y.; Dryer, F.L.; and Haggard, J.B., Jr.: Computational/Experimental Basis for Conducting Alkane Droplet Combustion Experiments on Space-Based Platforms. H.J. Rath, ed.: *Microgravity Fluid Mechanics, Proc. of the IUTAM Congr.*, Springer-Verlag, Berlin, 1992, pp. 337-353.
Choi, M.Y.; Dryer, F.A.; Card, J.M.; Williams, F.A.; Haggard, J.B., Jr.; and Borowski, B.A.: Microgravity Combustion of Isolated n-Decane and n-Heptane Droplets. AIAA 92-0242, Jan. 1992.

Curtis, E.C.; and Farrell, P.V.: A Numerical Study of High Pressure Droplet Vaporization. *Combustion and Flame*, Vol. 90, 1992, pp. 85-102.
Dryer, F.L.: Computation/Experimental Studies of Isolated, Single Component Droplet Combustion. Ross, H.D., ed.: *Second International Microgravity Combustion Workshop*, NASA Conf. Publ. 10113, 1993, pp. 291-296.
Gomez, A.: The Electrospray: Fundamentals and Applications. Kelleher, M.D., *et al.*, eds., *Experimental Heat Transfer, Fluid Mechanics and Thermodynamics*, Vol. 1, Elsevier, 1993, p. 270.
Gomez, A.; and Chen, G.: Charge-Induced Secondary Atomization of Droplets in Diffusion Flames of Electrostatic Sprays. *Comb. Sci. Technol.*, Vol. 96, 1994, pp. 47-59.
Gomez, A.; and Tang, K.: Charge and Fission of Droplets in Electrostatic Sprays. *Physics of Fluids*, Vol. 6, 1994, pp. 404-414.
Hartfield, J.P.; and Farrell, P.V.: Droplet Evaporation in a High-Pressure Gas. *Jour. Heat Trans.*, Vol. 115, 1993, pp. 699-706.
Hegde, U.; Ross, H.D.; and Facca, L.T.: Longitudinal Mode Instabilities of Particle Cloud Combustors in a Reduced Gravity Environment. *Comb. Sci. Technol.*, Vol. 94, 1994, pp. 279-294.
Jackson, G.S.; and Avedisian, C.T.: Experiments on the Effect of Initial Diameter in Spherically Symmetric Droplet Combustion of Sooting Fuels. AIAA 93-0130, Jan. 1993.
Jackson, G.S.; Avedisian, C.T.; and Yang, J.C.: Observations of Soot During Droplet Combustion at Low Gravity-Heptane and Heptane/Monochloroalkane Mixtures. *Inter. Jour. of Heat and Mass Trans.*, Vol. 35, 1992, pp. 2017-2033.
Mikami, M.; Kono, M.; Sato, J.; Dietrich, D.; and Williams, F.A.: Combustion of Miscible Binary-Fuel Droplets at High Pressure Under Microgravity. *Comb. Sci. Technol.*, Vol. 90, 1993, pp. 111-123.
Takei, M.; Kobayashi, H.; and Niioka, T.: Ignition Experiment of a Blended-Fuel Droplet in a Microgravity Field. *Microgravity Sci. Technol.*, Vol VI (3), Sept. 1993, pp. 184-187.
Tang, K.; and Gomez, A.: On the Structure of an Electrostatic Spray of Monodisperse Droplets. *Physics of Fluids*, Vol. 6, 1994, pp. 2317–2332.
Williams, F.A.: Studies of Droplet Burning and Extinction. Ross, H.D., ed.: *Second International Microgravity Combustion Workshop*, NASA Conf. Publ. 10113, Feb. 1993, pp. 283-290.
Zhang, B.L.; Card, J.M.; and Williams, F.A.: Application of Rate-Ratio Asymptotics to the Prediction of Extinction for Methanol Droplet Combustion. *Spring Tech. Meeting of the Western States Sec.*, The Combustion Inst., March 1994.

Flammability and Flame Spread Over Liquid Pools

Miller, F.J.; and Ross, H.D.: Further Observations of Flame Spread Over Laboratory-Scale Alcohol Pools. *The Twenty-Fourth Symp. (International) on Combustion*, The Combustion Inst., Pittsburgh, 1992, pp. 1703-1711.
Schiller, D.N.; Ross, H.D.; and Sirignano, W.A.: Computational Predictions of Flame Spread Over Alcohol Pools. AIAA 93-0825, Jan. 1993.

Smoldering Flame Spread

Stocker, D.P.; Olson, S.L.; Torero, J.L.; and Fernandez-Pello, A.C.: Microgravity Smoldering Combustion on the USML-1 Shuttle Mission. Avedisian, C.T., ed.: *Heat Transfer in Microgravity*, ASME HTD, Vol. 269, 1993, pp. 99-110.
Stocker, D.P.; Olson, S.L.; Torero, J.L.; and Fernandez-Pello, A.C.: Microgravity Smoldering Combustion on the USML-1 Space Shuttle Mission. Ramachandran, N.; Frazier, D.O.; Lehoczky, S.L.; and Baugher, C.L., eds.: *Joint Launch + One Year Science Review of USML-1 and USMP-1 with the Microgravity Measurement Group*. NASA Conf. Publ. 3272, Vol. II, May 1994, pp. 609-629.
Torero, J.L.; Fernandez-Pello, A.C.; and Urban, D.: Experimental Observation of the Effect of Gravity Changes on Smoldering Combustion. *AIAA Jour.*, Vol. 32, 1994, pp. 991-996.

Flammability and Flame Spread Over Solids

Altenkirch, R.A.; Sacksteder, K.; Bhattacharjee, S.; Rama chandra, P.A.; Tang, L.; and Wolverton, M.K.: The Solid Surface Combustion Experiment Aboard the USML-1 Mission. Ramachandran, N.; Frazier, D.O.; Lehoczky, S.L.; and Baugher, C.L., eds.: *Joint Launch + One Year Science Review of USML-1 and USMP-1 with the Microgravity Measurement Group*. NASA Conf. Publ. 3272, Vol. I, May 1994, pp. 83-101.
Bhattacharjee, S.; and Altenkirch, R.A.: A Comparison of Theoretical and Experimental Results in Flame Spread Over Thin Condensed Fuels in a Quiescent, Microgravity Environment. *The Twenty-Fourth Symp. (International) on Combustion*, The Combustion Inst., Pitts burgh, 1992, pp. 1669-1676.
Bhattacharjee, S.; Altenkirch, R.A.; and Sacksteder, K.: Implications of Spread Rate and Temperature Measurements in Flame Spread Over a Thin Fuel in a Quiescent, Microgravity Space-Based Environment. *Comb. Sci. Technol.*, Vol. 91, 1993, pp. 225-242.
Bonneau, L.; Joulain, P.; Most, J.M.; and Fernandez-Pello, A.C.: Flat Plate Diffusion Flame Combustion in Microgravity. AIAA 93-0826, Jan. 1993.
Bullard, D.B.; Tang, L.; Altenkirch, R.A.; and Bhattacharjee, S.: Unsteady Flame Spread over Solid Fuels in Microgravity. *Adv. Space Res.*, Vol. 13 (7), 1993, pp. 171-184.
Chen, C.H.; and Cheng, M.C.: Gas-Phase Radiative Effects on Downward Flame Spread in Low Gravity. AIAA 94-0576, Jan. 1994.

Ferkul, P.V.: A Model of Concurrent Flow Flame Spread Over a Thin Solid Fuel. NASA Contr. Report 191111, April 1992.
Ferkul, P.V.; and T'ien, J.S.: Numerical Computation of Low-Speed Concurrent Flow Flame Spread in Mixed Buoyant and Forced Flow. AIAA 93-0827, Jan. 1993.
Ferkul, P.V.; and T'ien, J.S.: A Model of Low-Speed Concurrent Flow Flame Spread Over a Thin Fuel. *Comb. Sci. Technol.*, Vol. 99, 1994, pp. 345-370.
Grayson, G.D.; Sacksteder, K.R.; Ferkul, P.V.; and T'ien, J.S.: Flame Spreading Over a Thin Solid in Low Speed Concurrent Flow-Drop Tower Experimental Results and Comparison with Theory. *Microgravity Sci. Technol.*, Vol. VII (2), July 1994, pp. 187-195.
Greenberg, P.S.; Sacksteder, K.R.; and Kashiwagi, T.: Wire Insulation Flammability Experiment: USML-1 1 Year Post Mission Summary. Ramachandran, N.; Frazier, D.O.; Lehoczky, S.L.; and Baugher, C.L., eds.: *Joint Launch + One Year Science Review of USML-1 and USMP-1 with the Microgravity Measurement Group.* NASA Conf. Publ. 3272, Vol. II, May 1994, pp. 631-655.
Jiang, C.-B.; and T'ien, J.S.: Numerical Computations of Flame Spread Over a Thin Solid in Forced Concurrent Flow with Gas-Phase Radiation. *Fall Tech. Meeting of the Eastern States Sec.*, The Combustion Inst., Dec. 1994, pp. 222-225.
Jiang, C.-B.; T'ien, J.S.; and Ferkul, P.V.: Numerical Computation of Buoyant Upward Flame Spread and Extinction Over a Thin Solid in Reduced Gravity. *Tech. Meeting of the Central States Sec.*, The Combustion Inst., Paper 12, June 1994.
Kushida, G.; Baum, H.R.; Kashiwagi, T.; and di Blasi, C.: Heat and Mass Transfer from Thermally Degrading Thin Cellulosic Materials in a Microgravity Environment. *Jour. Heat Trans.*, Vol. 114, 1992, pp. 494-502.
Nakabe, K.; McGrattan, K.B.; Kashiwagi, T.; Baum, H.R.; Yamashita, H.; and Kushida, G.: Ignition and Transition to Flame Spread Over a Thermally Thin Cellulosic Sheet in a Microgravity Environment. *Combustion and Flame*, Vol. 98, 1994, pp. 361-374.
Ohlemiller, T.; and Shields, J.: One- and Two-Sided Burning of Thermally Thin Materials. *Fire and Materials*, Vol. 17, 1993, pp. 103-110.
Olson, S.L.; and Hegde, U.: Imposed Radiation Effects on Flame Spread Over Black PMMA in Low Gravity. *Fall Tech. Meeting of the Eastern States Sec.*, The Combustion Inst., Paper 78, Dec. 1994, pp. 348-351.
Ramachandra, P.A.; Altenkirch, R.A.; Bhattacharjee, S.; Sack steder, K.; and Wolverton, M.K.: The Behavior of Flames Spreading Over Thin Solids in Microgravity. *Combustion and Flame*, Vol. 100, 1995, pp. 71-84.
Sacksteder, K.R.; and T'ien, J.S.: Downward Diffusion Flame Spread and Extinction in Variable Gravitational Fields: Lunar and Martian Simulation. AIAA 93-0828, Jan. 1993.
Sacksteder, K.R.; and T'ien, J.S.: A New Formulation of Damkohler Number for Studying Opposed Flow Flame Spread and Extinction. AIAA 95-0150, Jan. 1995.
Sacksteder, K.R.; and T'ien, J.S.: Buoyant Downward Diffusion Flame Spread and Extinction in Partial-Gravity Accelerations. *The Twenty-Fifth Symp. (International) on Combustion*, The Combustion Institute, Pittsburgh, 1995.
Tang, L.; Altenkirch, R.A.; Ramachandra, P.; Wolverton, M.K.; Bhattacharjee, S.; and Sacksteder, K.: Unsteady Flame Spread Over Thin Solid Fuels in Quiescent Environments. *Joint Tech. Meeting of the Central and Eastern States Secs.*, The Combustion Inst., Paper 117, March 1992. pp. 606-610.
West, J.; Bhattacharjee, S.; and Altenkirch, R.A.: A Comparison of the Roles Played by Natural and Forced Convection in Opposed-Flow Flame Spreading. *Comb. Sci. Technol.*, Vol. 83, 1992, pp. 233-244.
West, J.; Bhattacharjee, S.; and Altenkirch, R.A.: Surface Radiation Effects on Flame Spread Over Thermally Thick Fuels in an Opposing Flow. *Jour. Heat Trans.*, Vol. 116, 1994, pp. 646-651.
Yang, C.-T.; Goldmeer, J.S.; Urban, D.L.; and T'ien, J.S.: Combustion of a Solid Cylinder in Low-Speed Flows. *Fall Tech. Meeting of the Eastern States Sec.*, The Combustion Inst., Paper 1, Dec. 1994, pp. 47-50.
Zhou, L.; and Fernandez-Pello, A.C.: Solid Fuel Combustion in a Forced, Turbulent Flat Plate Flow: The Effect of Buoyancy. *The Twenty-Fourth Symp. (International) on Combustion*, The Combustion Inst., Pittsburgh, 1992, pp. 1721-1728.

Metal Combustion

Abbud-Madrid, A.; Branch, M.C.; Feiereisen, T.J.; and Daily, J.W.: Ignition of Bulk Metals by a Continuous Radiation Source in a Pure Oxygen Atmosphere. Janoff, D.D.; and Stoltzfus, J.M., eds.: *Flammability and Sensitivity of Materials in Oxygen-Enriched Atmos pheres*, ASTM STP 1197, ASTM, Philadelphia, 1993, pp. 211-222.
Abbud-Madrid, A.; Fiechtner, G.J.; Branch, M.C.; and Daily, J.W.: Ignition and Combustion Characteristics of Pure Bulk Metals: Normal Gravity Test Results. AIAA 94-0574, Jan. 1994.
Dreizen, E.L.: Stages in Al Particle Combustion in Air. *Fall Tech. Meeting of the Eastern States Sec.*, The Combustion Inst., Paper 2, Dec. 1994, pp. 51-54.
Feiereisen, T.J.; Branch, M.C.; Abbud-Madrid, A.; and Daily, J.W.: Gravity and Pressure Effects on the Steady-State Temperatures of Heated Metal Specimens in a Pure Oxygen Atmosphere. Janoff, D.D.; and Stoltzfus, J.M., eds.: *Flammability and Sensitivity of Materials in Oxygen-Enriched Atmospheres*, ASTM STP 1197, ASTM, Philadelphia, 1993, pp. 196-210.
Steinberg, T.A.; Wilson, D.B.; and Benz, F.: The Burning of Metals and Alloys in Microgravity. *Combustion and Flame*, Vol. 88, 1992, pp. 309-320.

Combustion Synthesis of Materials

Aldushin, A.P.; Matkowsky, B.J.; Shkadinsky, K.G.; Shkadinskaya, G.V.; and Volpert, V.A.: Combustion of Porous Samples with Melting and Flow of Reactants. *Comb. Sci. Technol.*, Vol. 99, 1994, pp. 313-343.

Barmatz, M.; Yiin, T.Y.; Moore, J.J.; and Feng, H.J.: Microwave-Induced Combustion Synthesis of Ceramic and Ceramic-Metal Composites. *Conference on Composites*, Amer. Ceramics Soc., Cocoa Beach FL, Jan. 1995.

Feng, H.J.; Hunter, K.R.; and Moore, J.J.: Combustion Synthesis of Ceramic and Metal-Matrix Composites. *Jour. Mater. Synth. Proc.*, Vol. 2 (2), 1994, pp. 71-86.

Feng, H.J.; and Moore, J.J.: Combustion Synthesis of High Performance Ceramic-Metal Composites. Upadhya, K., ed.: *High Performance Metal and Ceramic Matrix Composites*, The Metallurgical Soc., Warrendale, PA, 1994, pp. 157-174.

Feng, H.J.; Moore, J.J.; and Wirth, D.G.: Combustion Synthesis of Expanded, Foamed Composite Materials. Ravi, V. A.; and Srivatsan, T.S., eds.: *Processing and Manufacture of Advanced Materials for High Temperature Applications II*, The Metallurgical Soc., Warrendale, PA, 1993, pp. 243-251.

Hunter, K.R.; and Moore, J.J.: The Effect of Gravity on the Combustion Synthesis Processing of Advanced Materials. Schiffman, R.A.; and Andrews, F.B., eds.: *Sixth Int. Symp. on Experimental Methods for Microgravity Mater. Sci.*, The Metallurgical Soc., Warrendale, PA, 1994, pp. 125-131.

Lantz, C.; Teft, P.; Moore, J.J.; and Readey, D.W.: Self Propagating Reactive Synthesis of Ceramics in a Microgravity Environments. Schiffman, R.A.; and Patielli, C., eds.: *Seventh Int. Symp. on Exper. Methods for Microgravity Mater. Sci.*, The Metallurgical Soc., Warrendale, PA, Feb. 1995.

Moore, J.J.: An Examination of the Thermochemistry of Combustion Synthesis Reactions. Ravi, R.A.; Srivatsan, T.S.; and Moore, J.J., eds.: *Processing and Fabrication of Advanced Materials III*, The Metallurgical Soc., Warrendale, PA, 1994, pp. 817-831.

Moore, J.J.; Readey, D.W.; Feng, H.J.; Monroe, K.; and Mishra, B.: The Combustion Synthesis of Advanced Materials. *Jour. of Metals*, Vol. 46 (11), 1994, pp. 72-78.

Perkins, N.R.; Moore, J.J., Readey, D.W.: The Synergistic Effects of Coupling Combustion Synthesis with Vapor Phase Transport in the Synthesis of Advanced Materials. Moore, J.J.; Froes, F.H.; and Lavernia, E., eds.: *Advanced Synthesis of Engineered Structural Materials*, ASM Inter., Warrendale, PA, 1992, pp. 59-65.

Whitehead, S.B.; and Moore, J.J.: In-Situ Synthesis of Macroporous Ceramic Composite Materials. *Symp. on Advances in Porous Materials*, MRS Annual Meeting, Boston, Paper No. W1-7.4, Nov. 1994.

Diagnostic Instrumentation

Buchele, D.R.; and Griffin, D.W.: A Compact Color Schlieren Optical System. *Applied Optics*, Vol. 32, 1993, pp. 4218-4222.

Felske, J.P.; and Ku, J.C.: A Technique for Determining the Spectral Refractive Indices, Size, and Number Density of Smoke Particles from Light Scattering and Spectral Extinction Measurements in Flames. *Combustion and Flame*, Vol. 91, 1992, pp. 1-20.

Griffin, D.W.; and Greenberg, P.S.: Selected Microgravity Combustion Diagnostic Techniques. Ross, H.D., ed.: *Second International Microgravity Combustion Workshop*, NASA CP-10113, 1993, pp. 141-147.

Klimek, R.B.; and Paulick, M.J.: Color Image Processing and Object Tracking Workstation. NASA Tech. Memo. 105561, April 1992.

Lock, J.A.; Seasholtz, R.G.; and John, W.T.: Rayleigh-Brillouin Scattering to Determine One-Dimensional Temperatures and Number Density Profiles in a Gas Flow Field. *Applied Optics*, Vol. 31, 1992, pp. 2839-2841.

Otugen, M.V.; Annen, K.D.; and Seasholtz, R.G.: Gas Temperature Measurements Using the Dual-Line Detection Rayleigh Scattering Technique. *AIAA Jour.*, Vol. 31, 1993, pp. 2098-2103.

Pline, A.D.; Wernet, M.P.; and Hsieh, K.-C.: Ground-based PIV and Numerical Flow Visualization Results from the Surface Tension Driven Convection Experiment. Trolinger, J.D.; and Lal, R.B., eds: *Crystal Growth in Space and Related Optcal Diagnostics. SPIE Proc.*, Vol. 1557, July 1991, pp. 222-234.

Rubinstein, R.; and Greenberg, P.S.: Rapid Inversion of Angular Deflection Data for Certain Axisymmetric Refractive Index Distributions. *Applied Optics*, Vol. 33, 1993, pp. 1141-1144.

Seasholtz, R.G.: 2-D Velocity and Temperature Measurements in High Speed Flows Based on Spectrally Resolved Rayleigh Scattering. *New Trends in Instrumentation for Hypersonic Research*, Kluwer Academic Publishers, Netherlands (NASA Tech. Memo. 105784), 1992.

Seasholtz, R.G.; Zupanc, F.J.; and Schneider, S.J.: Spectrally Resolved Rayleigh Scattering Diagnostic for Hydrogen-Oxygen Rocket Plume Studies. *Jour. Propul. Power*, Vol. 8, 1992, pp. 935-942.

Silver, J.A.; and Kane, D.J.: Combustion Diagnostics for Microgravity Research Using Near-IR Diode Lasers. Southwest Sciences, Inc., Final Report for NASA Contract NAS3-25981, 1993.

Stanton, A.C.; Bomse, D.S.; Oh, D.B.; and Silver, J.A.: Combustion Diagnostics for Microgravity Research Using Near-IR Laser Diodes. Southwest Sciences, Inc., Final Report for NASA Contract NAS3-25815, 1993.

Weiland, K.J.: Intensified Array Camera Imaging of Solid Surface Combustion Aboard the NASA Learjet. *AIAA Jour.*, Vol. 31, 1993, pp. 786-788.
Weiland, K.J.: Visualization and Imaging Methods for Flames in Microgravity. Ross, H.D., ed.: *Second International Microgravity Combustion Workshop*, NASA Conf. Publ. 10113, Feb. 1993, pp. 99-104.
Wernet, M.P.: Particle Displacement Tracking Applied to Air Flows. *Proc. Fourth Inter. Conf. on Laser Anemometry and Applications*, Cleveland OH, Aug. 1991.
Winter, M.: Laser Diagnostics for Microgravity Droplet Studies. AIAA 94-0431, Jan. 1994.
Wong, W.K.: Spatial and Spectral Sensor for Microgravity Combustion Experiments. Sensor Systems Group, Inc., Final Report for NASA Contract NAS3-26545, 1993.

Spacecraft Fire Safety

Apostolakis, G.E.; Catton, I.; Issacci, F.; Jones, S.; Paul, M.; Paulos, T.: and Paxton, K.: Experimental Needs for Spacecraft Risk Assessment. Kashiwagi, T. ed.: *Fire Safety Science-Proc. of the Fourth Inter. Symp.*, Inter. Assoc. for Fire Safety Science, Boston, 1994, pp. 949-960.
Apostolakis, G.E.; Catton, I.; Paulos, T.: Paxton, K.; and Jones, S.: Findings of a Review of Spacecraft Fire Safety Needs. NASA Contr. Report 189181 (UCLA ENG 92-19), July 1992.
Friedman, R.: Fire Safety Practices and Needs in Human-Crew Spacecraft. *Jour. of Applied Fire Science*, Vol. 2 (3), 1992-1993, pp. 243-259.
Friedman, R.: Risks and Issues in Fire Safety on the Space Station. NASA Tech. Memo. 106430, March 1994.
Friedman, R.; and Urban, D.L.: Contributions of Microgravity Test Results to the Design of Spacecraft Fire-Safety Systems. AIAA 93-1152, Feb. 1993.
Judd, M.D.: Practical Problems Related to Flammability and Combustion in Space. Kaldeich, B., ed.: *Proc. First European Symp. on Fluids in Space*, ESP SP-352, June 1992, pp. 145-161.
Ohlemiller, T.J.: An Assessment of the NASA Flammability Screening Test and Related Aspects of Material Flammability. NASA Contr. Report 189226 (NISTIR 4882), Aug. 1992.
Paulos, T.; Issacci, F.; Catton, I.; and Apostolakis, G.E.: Estimation of the Frequency of Electrical Overload Events in Space Station Freedom. *Proc. Probabilistic Safety and Management Conf. (PSAM II)*, Session 099, March 1994, pp. 15-20.
Paulos, T.; Paxton, K.; Jones, S.; Issacci, F.; Catton, I.; and Apostolakis, G.: Risk-Based Spacecraft Fire Safety Experiments. AIAA 93-1153, Feb. 1993.
Paxton, K.R.; Issacci, F.; Apostolakis, G.; and Catton, I.: A Methodology for Quantifying Fire Risk On-Board Spacecraft. *Proc. Probabilistic Safety and Management Conf. (PSAM II)*, Session 102, March 1994, pp. 9-14.
Paxton, K.R.; Jones, S.T.; Paulos, T.; Issacci, F.; Apostolakis, G.E.; and Catton, I.: Smoke and Flammability of Wires in Microgravity. Sadhal, S.S.; and Hashemi, A., eds.: *Heat Transfer in Microgravity Systems-1993*, ASME HTD Vol. 235, 1993, pp. 43-48.
Shipp, M.P.; Andrews, S.; Burry, P.E.; and Ferdell, P.J.: A Preliminary Experimental Investigation of Fire Behavior in Microgravity. Rygh, K.; and Flidh, J., eds.: *Columbus Parabolic Fire Experiment Report Phase One*, ESTEC Report COL-TN-ESA 003, Sept. 1992.
Shipp, M.; and Spearpoint, M.: The Detection of Fires in Microgravity. Kashiwagi, T. ed.: *Fire Safety Science–Proc. of the Fourth Inter. Symp.*, Inter. Assoc for Fire Safety Science, Boston, 1994, pp. 739-750.

General and Facilities

Graham, S.J.; and Rhome, R.C.: Achievements in Microgravity: Ten Years of Microgravity Research. AIAA 94-0344, Jan. 1994.
Law, C.K.; and Faeth, G.M.: Opportunities and Challenges of Combustion in Microgravity. *Prog. Energy Comb. Sci.*, Vol. 20, 1994, pp. 65-113.
Microgravity Combustion Group: Microgravity Combustion Science: Progress, Plans, and Opportunities. NASA Tech. Memo. 105410, April 1992.
Ross, H.D., ed.: Second International Microgravity Combustion Workshop. NASA Conf. Publ. 10113, Feb. 1993.
Ross, H.D.: Neither Up Nor Down: A Perspective on Combustion Science in Microgravity. *Fall Tech. Meeting of the Eastern States Sec.*, The Combustion Inst., Invited Paper, Oct. 1993.
Stocker, D.P.; Greenberg, P.S.; and Ross, H.D.: Small-Scale Combustion Experiments on the USML-1 Shuttle Mission. *Spring Tech. Meeting of the Central States Sec.*, The Combustion Inst., May 1992.
Yaniec, J.S.: User's Guide for NASA Lewis Research Center DC-9 Reduced-Gravity Aircraft Program. NASA Tech. Memo. 106755, Jan. 1995.

Additional References, Accepted and to Appear Soon (All Subjects)

Apostolakis, G.E.; Catton, I.; Issacci, F.; Jones, S.; Paul, M.; Paulos, T.: and Paxton, K.: Risk-Based Spacecraft Fire-Safety Experiments. *Reliability Eng. and System Safety.*
Buckmaster, J.; and Agarwal, A.: Unsteady Spherical Flames in Dusty Gases. *Comb. Sci. Technol.*
Buckmaster, J.; and Jackson, T.: The Effects of Radiation on the Thermal-Diffusive Stability Boundaries of Premixed Flames. *Comb. Sci. Technol.*
Greenberg, P.S.; Klimek, R.B.; and Buchele, D.: Quantitative Rainbow Schlieren Deflectometry. *Applied Optics.*

Hunter, K.R.; and Moore, J.J.: Effect of Gravity on the Combustion Synthesis of Ceramics and Ceramic-Metal Composites. *Jour. of Mat. Synth. Proc.*

-Kostiuk, L.W.; and Cheng, R.K.: The Imaging of Premixed Flames in Microgravity. *Experiments in Fluids.*

Ku, J.C.; Griffin, D.W.; Greenberg, P.S.; and Roma, J.: Buoyancy Induced Differences in Soot Morphology. *Combustion and Flame.*

McGrattan, K.B.; Kashiwagi, T.; Baum, H.R.; and Olson, S.L.: Effects of Ignition and Wind on the Transition to Flame Spread in a Microgravity Environment. *Combustion and Flame.*

Moore, J.J.: Self Propagating Reactive Synthesis of Advanced Materials. Keynote Lecture, *Proc. of 1994 Powder Metallurgy World Congress*, European Powder Metal Assoc., Paris, June 6-9, 1994.

Moore, J.J.; and Feng, H.J.: Combustion Synthesis of Advanced Materials: Part I, Reaction Parameters. *Prog. in Materials Sci.*

Moore, J.J.; and Feng, H. J.: Combustion Synthesis of Advanced Materials: Part II, Classification, Applications and Modeling. *Prog. in Materials Sci.*

Patnaik, G.; and Kailasanath, K.: Numerical Simulations of Burner-Stabilized Hydrogen-Air Flames in Microgravity. *Combustion and Flame.*

Ronney, P.D.: Some Open Issues in Premixed Turbulent Combustion. Buckmaster, J.D.; and Takeno, T., eds., *Mathematical Modeling in Combustion and its Interaction with Numerical Computation*, Springer-Verlag, 1995.

Schult, D.A.; Matkowsky, B.J.; Volpert, V.A.; and Fernandez-Pello, A. C.: Ignition and Extinction of Forced Opposed Flow Smolder Waves. *Combustion and Flame.*

Silver, J.A.; Kane, D.J.; and Greenberg, P.S.: Quantitative Species Measurements in Microgravity Flames Using Near-IR Diode Lasers. *Applied Optics.*

Vander Wal, R.L.; and Weiland, K.J.: Laser-Induced Incandescence: Development and Characterization Towards a Measurement of Soot Volume Fraction. *Jour. of Applied Physics B.*

Vander Wal, R.L.; and Dietrich, D.L.: Laser-Induced Incandescence Applied to Droplet Combustion. *Applied Optics.*

Zhu, J.Y.; and Ronney, P.D.: Simulation of Front Propagation at Large Non-Dimensional Flow Disturbance Intensities. *Comb. Sci. Technol.*

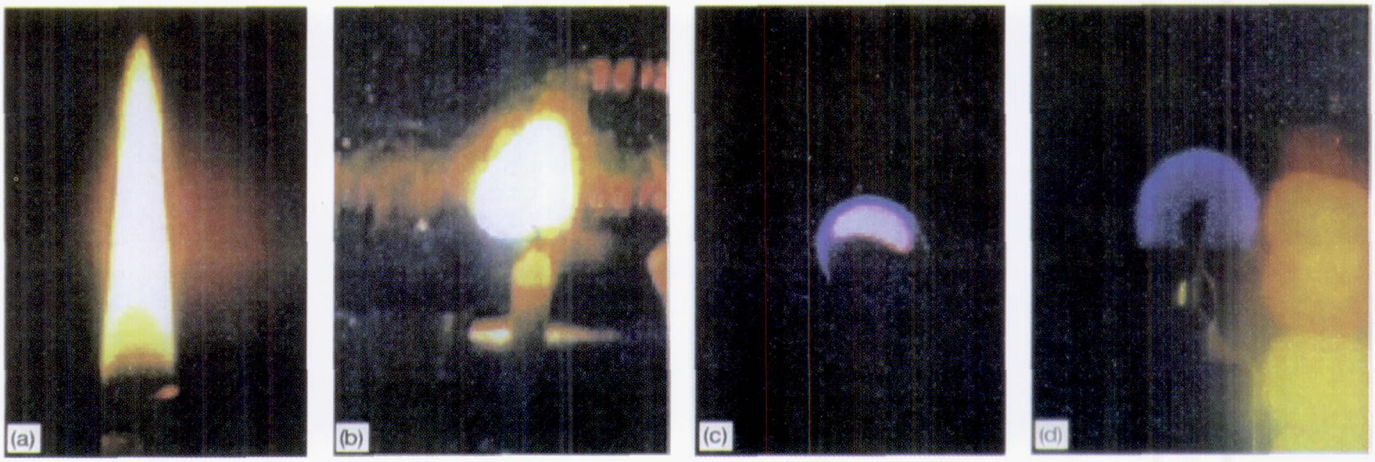

Figure 1.—The candle flame in differing acceleration (gravity) levels. (a) Normal gravity. (b) Low gravity (0.02 g) in airplane. (c) Microgravity ($<10^{-4}$ g) in drop tower. (d) Microgravity ($<10^{-5}$ g) in shuttle.

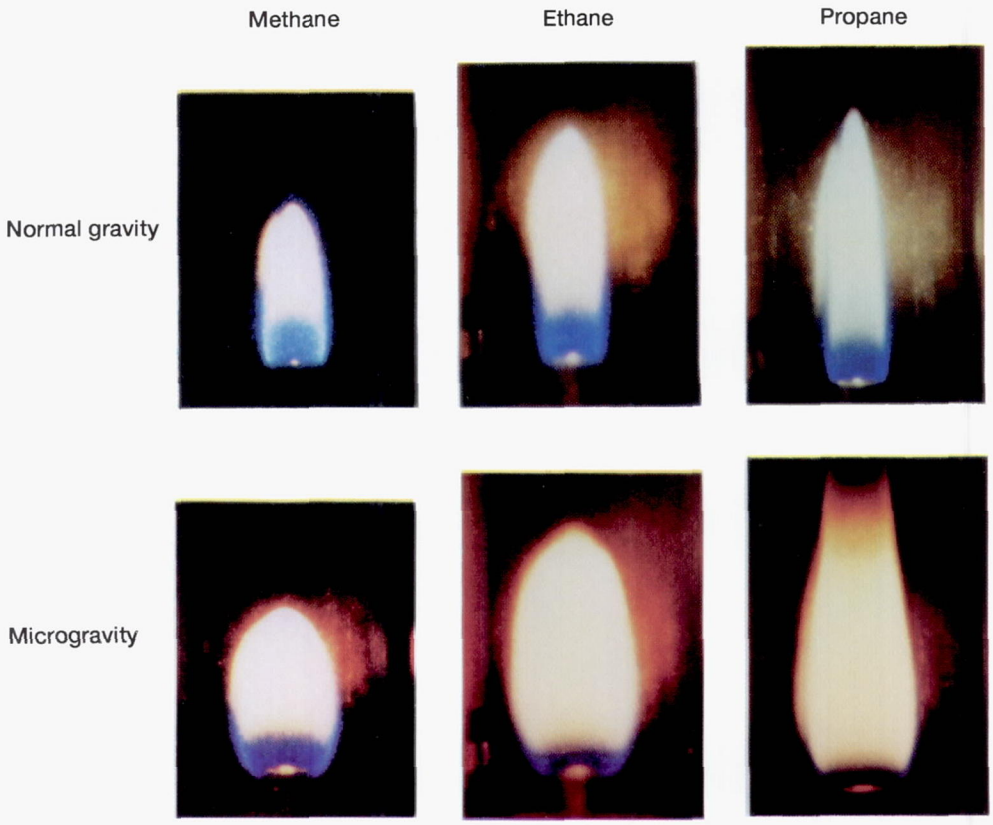

Figure 8. —Photographs of cylindrical Burke-Schumann diffusion-flame shapes for three fuels in normal gravity and microgravity. Common conditions are outer-tube radius, 2.33 cm; inner-tube radius, 0.28 cm; fuel/air velocity ratio, 1.37; and oxygen consumption rate, approximately 2.5 cm^3/sec.

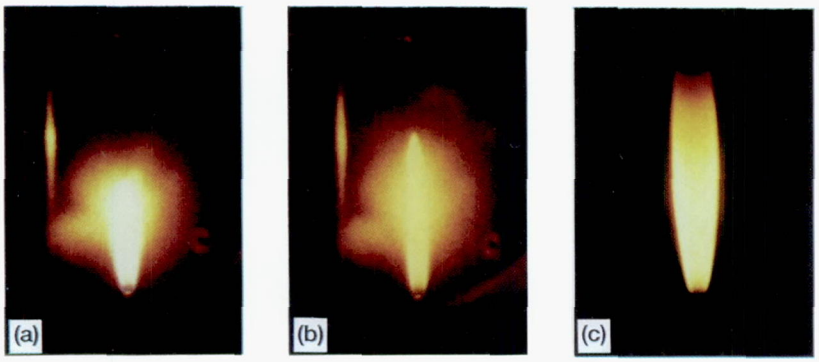

Figure 9.—Photographs of laminar propane/air gas-jet flames from a 1.65-mm nozzle, 1.5 cm^3/sec fuel flow, 101 kPa total pressure. Normal-gravity flames show extremes due to flicker. (a) Normal gravity, minimum flame height. (b) Normal gravity, maximum flame height. (c) Microgravity.

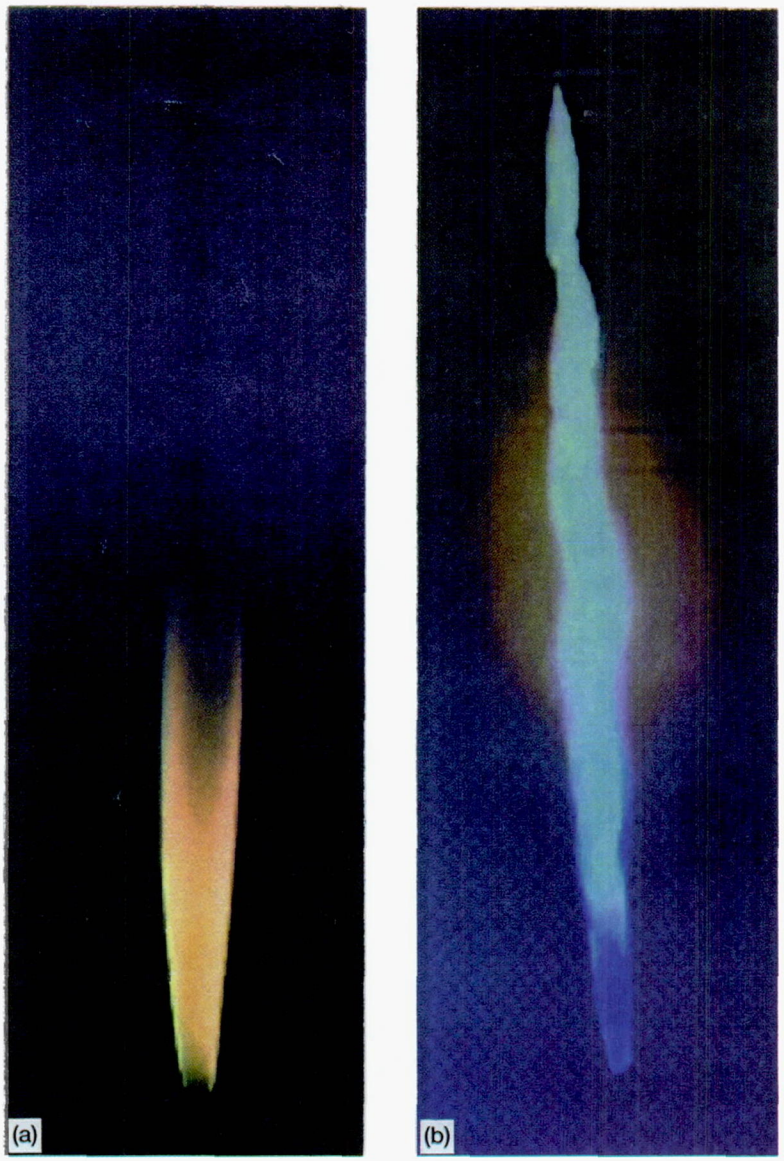

Figure 11.—Photographs of propane/air gas-jet flames in microgravity. (a) Laminar flame at fuel flow-rate of 200 cm^3/sec. (b) Developed turbulent flame at fuel flow-rate of 500 cm^3/sec.

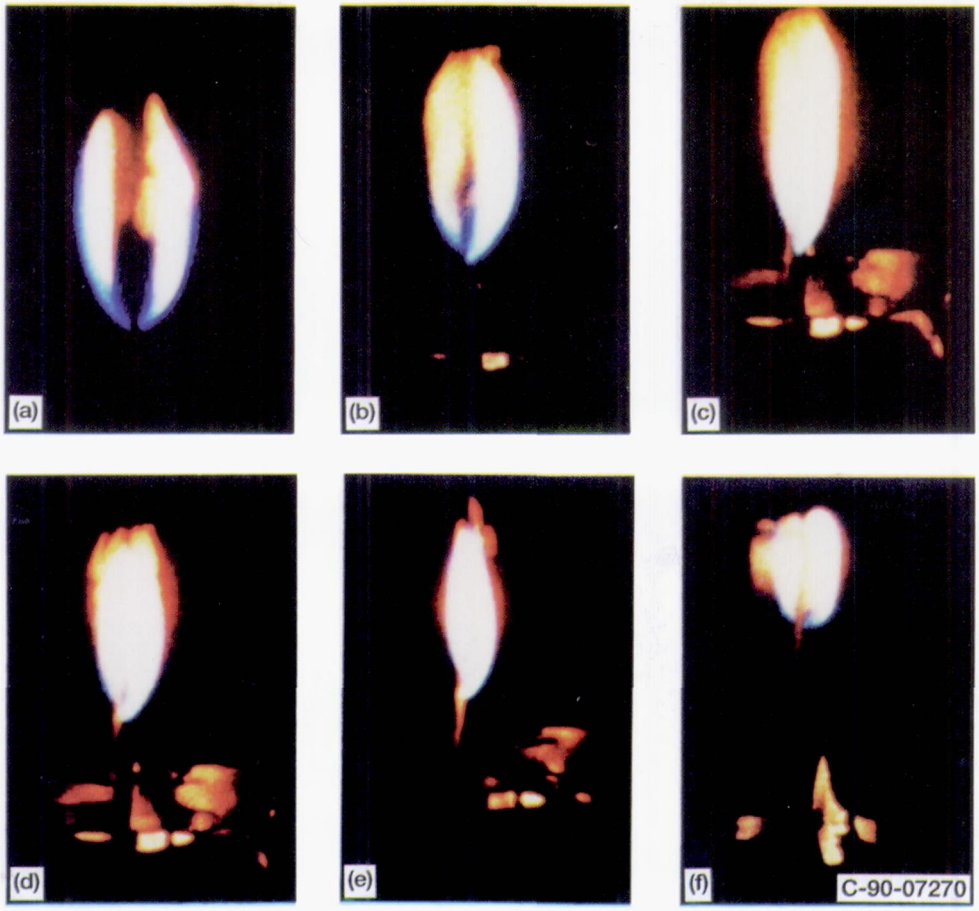

Figure 21.—Edge views of flames spreading over thin-paper fuels in microgravity, with opposed flow velocities as noted. (a) 5 cm/sec. (b) 10 cm/sec. (c) 15 cm/sec. (d) 20 cm/sec. (e) 30 cm/sec. (f) Buoyancy-induced flow in normal gravity.

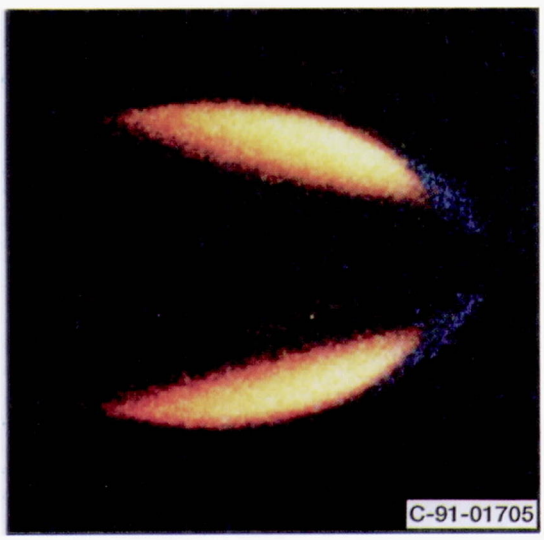

Figure 19.—Edge view of flame advancing from left to right over ash-free filter-paper fuel in 50% oxygen/ nitrogen, 150-kPa total pressure, microgravity environment, from the Solid Surface Combustion Experiment.

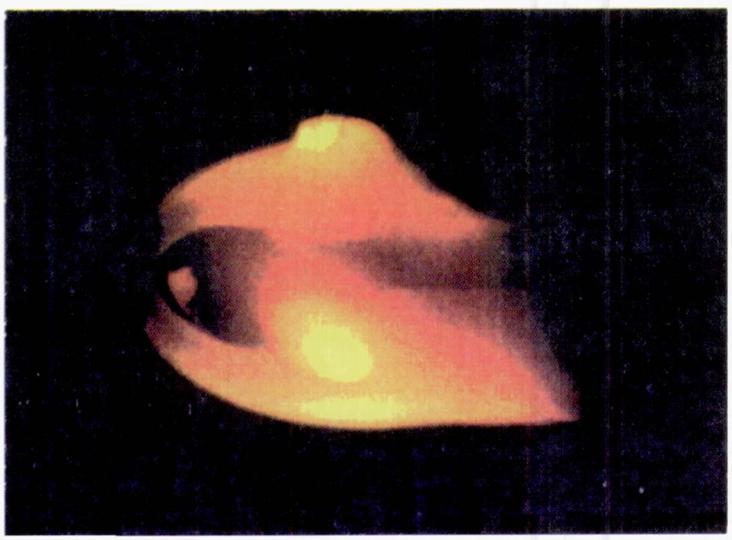

Figure 32.—Photograph of burning polyethylene wire insulation in microgravity, from the Wire Insulation Flammability experiment. Flame spread and concurrent air flow are from left to right. Note the globules of molten insulation both adhering to the wire and drifting away.

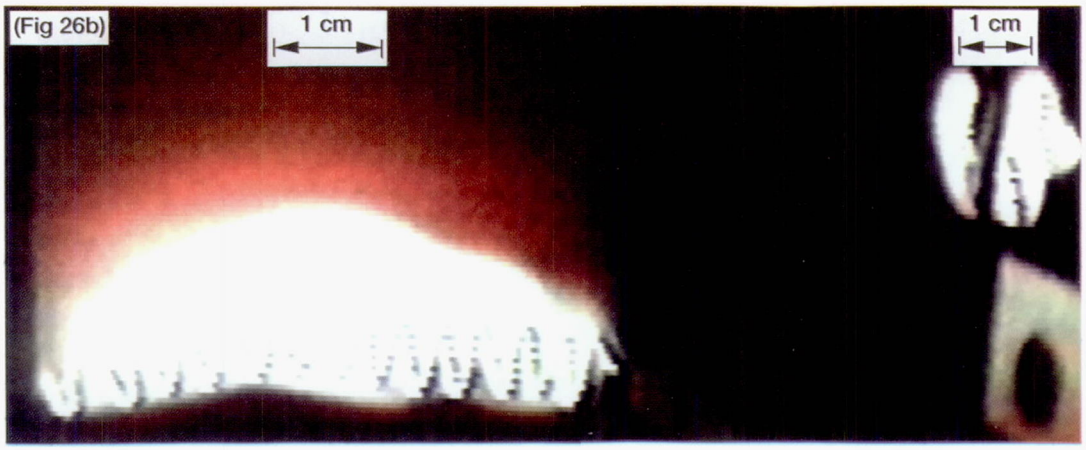

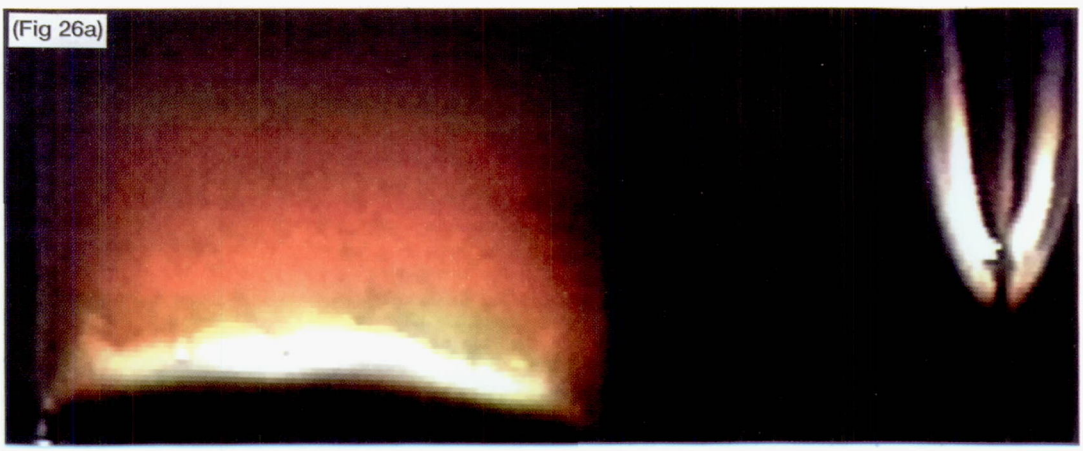

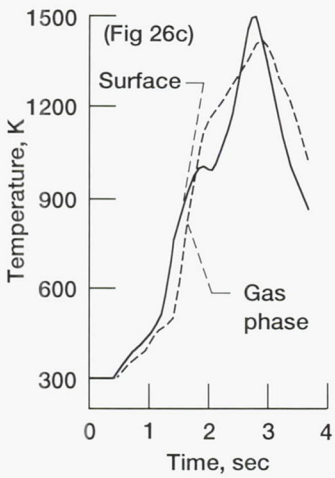

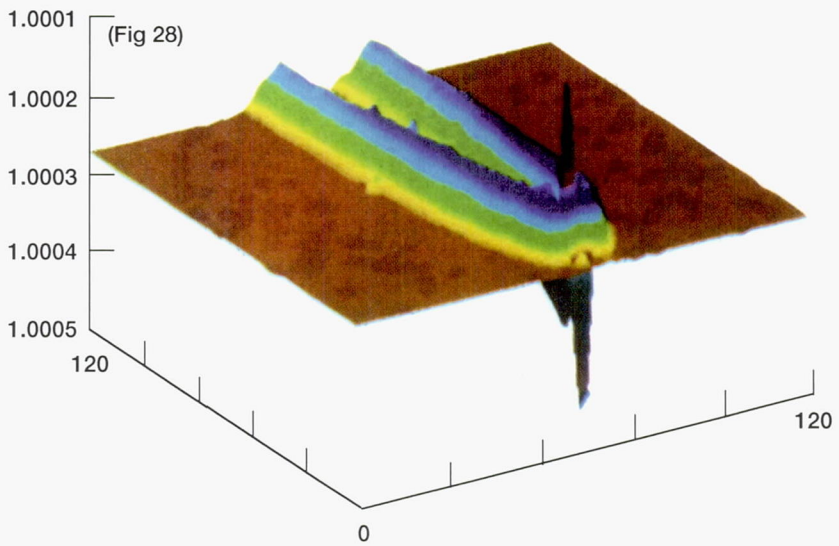

Figure 28.—Refractive-index contours obtained by rainbow schlieren for partially premixed methane/air flame.

Figure 26.—Flame appearance and temperature measurements for flame over tissue-paper fuels in 18% oxygen/nitrogen, 101-kPa total pressure, microgravity environments with 10 cm/sec concurrent flow. (a) Side and edge views at ignition (time = 0). (b) Side and edge views at end of experiment (time = 3.7 sec). (c) Temperature histories at fuel surface and in gas phase 1 cm above surface.

REPORT DOCUMENTATION PAGE

Form Approved
OMB No. 0704-0188

1. AGENCY USE ONLY (*Leave blank*)	2. REPORT DATE	3. REPORT TYPE AND DATES COVERED
	April 1995	Technical Memorandum

4. TITLE AND SUBTITLE
Microgravity Combustion Science: 1995 Program Update

5. FUNDING NUMBERS
WU-962-22-00

6. AUTHOR(S)
The Microgravity CombustionBranch;
Howard D. Ross, Suleyman A. Gokoglu, and Robert Friedman, editors

7. PERFORMING ORGANIZATION NAME(S) AND ADDRESS(ES)
National Aeronautics and Space Administration
Lewis Research Center
Cleveland, Ohio 44135-3191

8. PERFORMING ORGANIZATION REPORT NUMBER
E-9456

9. SPONSORING/MONITORING AGENCY NAME(S) AND ADDRESS(ES)
National Aeronautics and Space Administration
Washington, D.C. 20546-0001

10. SPONSORING/MONITORING AGENCY REPORT NUMBER
NASA TM-106858

11. SUPPLEMENTARY NOTES
Prepared for the 3rd International Microgravity Workshop sponsored by NASA Lewis Research Center. Responsible person, Howard D. Ross, organization code 6711, (216) 433-2562.

12a. DISTRIBUTION/AVAILABILITY STATEMENT
Unclassified - Unlimited
Subject Category 23

This publication is available from the NASA Center for Aerospace Information, (301) 621-0390.

12b. DISTRIBUTION CODE

13. ABSTRACT (*Maximum 200 words*)

Microgravity greatly benefits the study of fundamental combustion processes. In this environment, buoyancy-induced flow is nearly eliminated, weak or normally obscured forces and flows can be isolated, gravitational settling or sedimentation is nearly eliminated, and temporal and spatial scales can be expanded. This document reviews the state of knowledge in microgravity combustion science with the emphasis on NASA-sponsored developments in the current period of 1992 to early 1995. The subjects cover basic research in gaseous premixed and diffusion-flame systems, flame structure and sooting, liquid droplets and pools, and solid-surface ignition and flame spread. They also cover applied research in combustion synthesis of ceramic-metal composites, advanced diagnostic instrumentation, and on-orbit fire safety. The review promotes continuing research by describing the opportunities for Principal Investigator participation through the NASA Research Announcement program and the available NASA Lewis Research Center ground-based facilities and spaceflight accommodations. This review is compiled by the members and associates of the NASA Lewis Microgravity Combustion Branch, and it serves as an update of two previous overview reports.

14. SUBJECT TERMS
Combustion; Diffusion flames; Flame propagation; Flames; Measuring instruments; Metal fuels; Premixed flames; Reduced gravity; Soot; Synthesis (chemistry); Weightlessness

15. NUMBER OF PAGES
55

16. PRICE CODE
A04

17. SECURITY CLASSIFICATION OF REPORT	18. SECURITY CLASSIFICATION OF THIS PAGE	19. SECURITY CLASSIFICATION OF ABSTRACT	20. LIMITATION OF ABSTRACT
Unclassified	Unclassified	Unclassified	